

DECLARATION OF TRACEY J. OLANYK

I, Tracey J. Olanyk, declare as follows:

1. I am over the age of majority and make this declaration of my own personal knowledge.
2. I am the Associate University Librarian of the University of Pittsburgh Resource Acquisition and Discovery Department, located at 7500 Thomas Blvd, Pittsburgh, PA 15608. I have held the position as Associate University Librarian for Resource Acquisitions and Discovery since July 1, 2023. In 1997 I held the position of Library Specialist in the Microforms and Serials Department.
3. Based on my understanding of standard policy at the time, the University libraries had subscriptions to and regularly receive periodicals into their collections. Upon receipt of a periodical issue, the staff member responsible for processing newly received periodical issues would stamp the publication with the received date. The Library's normal business practice was to receive new items and make them available to the public within a few days of when they were received, and certainly within one week.
4. According to the dates stamped on the individual volumes and my understanding of standard policy at the time, the following periodicals and articles were received by the University of Pittsburgh libraries:
 - a. ***Power Engineering***, Volume 113, Issue 6, dated June 1, 2009 and containing the article "A Variety of Hg Capture Solutions Are Available" by Steve Blankinship was received by the University of Pittsburgh Libraries on June 22, 2009 and was made available to the public within a few days of receipt, and certainly within one week. The University of Pittsburgh Libraries had a subscription to the print version of the *Power Engineering* periodical from 1950 to 2018. A copy of the first few pages of the periodical issue, including the page having the "date received" stamp, as it is maintained in the Library's collection, plus the article in question, is attached as Exhibit A.

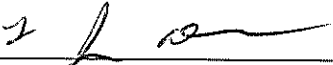
- b. *Water, Air, & Soil Pollution*, Volume 80, Issue 1-4, dated February 1995 and containing the article “Mercury stack emissions from U.S. electric utility power plants” by Chu, P. and Porcella, D. B. was received by the University of Pittsburgh Libraries on August 10, 1995 and was made available to the public within a few days of receipt, and certainly within one week. The University of Pittsburgh Libraries had a subscription to the print version of the *Water, Air, & Soil Pollution* periodical from 1971 to 2003. A copy of the first few pages of the periodical issue, including the page having the “date received” stamp, as it is maintained in the Library's collection, plus the article in question, is attached as Exhibit B.
- c. *Fuel Processing Technology*, Volume 63, Issue 2, dated April 2000 and containing the article “Gas-phase transformations of mercury in coal-fired power plants,” by Senior, C.L., Sarofim, A.F., Zeng, T., Helble, J.J., and Mamani-Paco, R. was received by the University of Pittsburgh Libraries on March 21, 2000 and was made available to the public within a few days of receipt, and certainly within one week. The University of Pittsburgh Libraries had a subscription to the print version of the *Fuel Processing Technology* periodical from 1980 to 2003. A copy of the first few pages of the periodical issue, including the page having the “date received” stamp, as it is maintained in the Library's collection, plus the article in question, is attached as Exhibit C.
- d. *Fuel Processing Technology*, Volumes 65-66, dated June 2000 and containing the articles (1) “Mercury transformations in coal combustion flue gas” by Galbreath, K.C. and Zygarlicke, C.J.; and (2) “Towards the development of a chemical kinetic model for the homogeneous oxidation of mercury by chlorine species”, was received by the University of Pittsburgh Libraries on June 23, 2000 and was made available to the public within a few days of receipt, and certainly within one week. A copy of the first few pages of the periodical issue, including the page having the “date received” stamp, as it is maintained in the Library's collection, plus the articles in question, is attached as Exhibit D.
- e. *Environmental Science & Technology*, Volume 34, Issue 1, dated January 2000 and containing the article “Impact of flue gas conditions on mercury uptake by sulfur-impregnated activated carbon” by Liu, W., Vidic, R.D., Brown, T.D. was received by the University of Pittsburgh Libraries on January 07, 2000 and was made available to the public within a few days of receipt, and certainly within one week. The University of Pittsburgh Libraries had a subscription to the print version of the *Environmental Science & Technology* periodical from 1967 to 2008. A copy of the first few pages of the periodical issue, including the page having the “date received” stamp, as it is maintained in the Library's collection, plus the article in question, is attached as Exhibit E.
- f. *Environmental Science & Technology*, Volume 34, Issue 3, dated February 2000 and containing the article “Optimization of high temperature sulfur impregnation in activated carbon for permanent sequestration of mercury” by Liu, W., Vidic, R.D., Brown, T.D., was received by the University of Pittsburgh Libraries on February 21, 2000 and was made available to the public within a few days of

receipt, and certainly within one week. A copy of the first few pages of the periodical issue, including the page having the "date received" stamp, as it is maintained in the Library's collection, plus the article in question, is attached as Exhibit F.

- g. *Industrial & Engineering Chemistry Research*, Volume 39, Issue 4, dated April 2000 and containing the article "Novel sorbents for mercury removal from flue gas" by Granite, E.J., Pennline, H.W. and Hargis, R.A., was received by the University of Pittsburgh Libraries on April 13, 2000 and was made available to the public within a few days of receipt, and certainly within one week. The University of Pittsburgh Libraries had a subscription to the print version of the *Industrial & Engineering Chemistry Research* periodical from 1987 to 2008. A copy of the first few pages of the periodical issue, including the page having the "date received" stamp, as it is maintained in the Library's collection, plus the article in question, is attached as Exhibit G.

5. I declare under penalty of perjury under the laws of the United States of America that this declaration is true, complete, and accurate to the best of my knowledge. I further acknowledge that willful false statements and the like are punishable by fine or imprisonment, or both (18 U.S.C. § 1001).

Executed at Pittsburgh, Pennsylvania, on June 2, 2025.



Tracey J. Olanyk
Associate University Librarian
University of Pittsburgh
Resource Acquisition and Discovery Department

EXHIBIT A

POWER Engineering®

the magazine of power generation

Hydro Power: The Versatile Renewable



Hydrogen safety
Supporting variable
renewable resources
Coping with a busy
nuclear autumn

#BXNMSLB *****CAR-RT LOT**C-099
024 POE
#0048353/CB/D#
UNIV OF PITTSBURGH
ENG PERIODICALS 09
7500 THOMAS BLD RD RM 339
313
96
288132
1

POWER Engineering®

Vol. 113, No. 6, June 2009

UNIVERSITY OF PITTSBURGH

1421 South Sheridan Road
Tulsa, OK 74112
P.O. Box 1260, Tulsa, OK 74101
Telephone: (918) 835-3161
Fax: (918) 831-9834
E-mail: pe@pennwell.com
World Wide Web: <http://www.powereng.com>

JUN 22 2009

POWER ENGINEERING LIBRARY

CHIEF EDITOR—David Wagman
(918) 831-9866 davidw@pennwell.com

SENIOR EDITOR—Nancy Spring
(918) 831-9492 nancys@pennwell.com

ASSOCIATE EDITOR—Steve Blankinship
(214) 739-4756 steveb@pennwell.com

ON-LINE EDITOR—Jeff Postelwait
(918) 832-9339 jeffp@pennwell.com

CONTRIBUTING EDITOR—Robynn Andracssek
CONTRIBUTING EDITOR—Brad Buecker
CONTRIBUTING EDITOR—Anthony Carrino
CONTRIBUTING EDITOR—Brian Schimmoller
CONTRIBUTING EDITOR—Rob Swanekamp, P.E.

PRODUCTION SUPERVISOR—Deanna Priddy Taylor
(918) 832-9378 deannat@pennwell.com

SUBSCRIBER SERVICE

P.O. Box 3271, Northbrook, IL 60065
Phone: (847) 559-7501
Fax: (847) 291-4816
E-mail: poe@omeda.com

MARKETING MANAGER—Wendy Lissau
(918) 832-9391 wendyl@pennwell.com

**VICE PRESIDENT, NORTH AMERICAN POWER
GENERATION GROUP**—Richard Baker
(918) 831-9187 richardb@pennwell.com

NATIONAL BRAND MANAGER—Rick Huntzicker
(770) 578-2688 rickh@pennwell.com

CORPORATE HEADQUARTERS—PennWell Corp.
1421 S. Sheridan Road, Tulsa, OK 74112
Telephone: (918) 835-3161

CHAIRMAN—Frank T. Lauinger
PRESIDENT/CEO—Robert F. Biolchini
CHIEF FINANCIAL OFFICE/SENIOR VICE PRESIDENT—Mark C. Wilmoth

CIRCULATION MANAGER—Linda Thomas
CIRCULATION DIRECTOR—Gloria Adams
PRODUCTION MANAGER—Katie Noftsgar

POWER ENGINEERING, ISSN 0032-5961, USPS 440-980, is published 12 times a year by PennWell Corp., 1421 S. Sheridan Rd., Tulsa, OK 74112; phone (918) 835-3161. ©Copyright 2009 by PennWell Corp. (Registered in U.S. Patent Trademark Office). Authorization to photocopy items for internal or personal use, or the internal or personal use of specific clients, is granted by *POWER ENGINEERING*, ISSN 0032-5961, provided that the appropriate fee is paid directly to Copyright Clearance Center, 222 Rosewood Drive, Danvers, MA 01923 USA 508-750-8400. Prior to photocopying items for educational classroom use, please contact Copyright Clearance Center, Inc., 222 Rosewood Drive, Danvers, MA 01923 USA 508-750-8400. Periodicals postage paid at Tulsa, OK and additional mailing offices. Subscription: U.S.A. and possessions, \$98 per year; Canada and Mexico, \$98 per year; international air mail, \$242 per year. Single copies: U.S., \$14, Outside U.S. \$23. Back issues of *POWER ENGINEERING* may be purchased at a cost of \$14 each in the United States and \$16 elsewhere. Copies of back issues are also available on microfilm and microfiche from University Microfilm, a Xerox Co., 300 N. Zeeb Rd., Ann Arbor, MI 48103. Available on LexisNexis, Box 933, Dayton, OH 45402; (800) 227-4908. POSTMASTER: Send change of address, other circulation information to *POWER ENGINEERING*, PO Box 3271, Northbrook, IL 60065-3271. "POWER ENGINEERING" is a registered trademark of PennWell Corp. Return undeliverable Canadian addresses to P.O. Box 122, Niagara Falls, ON L2E 6S4.



Member
American Business Press
BPA International



PRINTED IN THE U.S.A. GST NO. 126813153
Publications Mail Agreement No. 40052420

Plant
Design
Suite

Easy
Open
Scalable

CADWorx®

Why is CADWorx one of the fastest growing and most productive plant design suites on the market?

Because it has all the tools to produce intelligent plant designs, including:

- Piping
- Steel
- Cable trays/ducting
- Collision detection
- Equipment
- Bills of material
- Isometrics
- Flow schematics
- Instrument loop diagrams
- Bi-directional links to analysis programs
- Walkthrough and visualization

AutoCAD
2010
Compatible

Autodesk

CADWorx delivers!

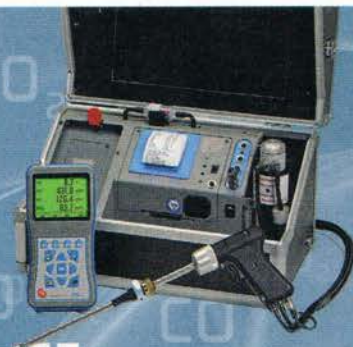
Contact us to find out how you can improve your design efficiency.

+1 281-890-4566
sales@coade.com

DOWNLOAD FREE DEMO
www.coade.com

COADE®
Plant Focused. Industry Driven.

For info. <http://powereng.hotims.com> RS# 2



Use
the
analyzer
that
smokes
the
rest.

ecom®

Rugged Reliable Accurate

EMISSION ANALYZERS

ecomusa.com

877-326-6411

AMEREN ILE EXHIBIT 1082
For info. <http://powereng.hotims.com> RS# 3
Page 6

A Variety of Hg Capture Solutions Are Available

By Steve Blankinship, Associate Editor

While vacating the Clean Air Mercury Rule (CAMR) has postponed implementation of mercury capture to some extent, improvements in ways to capture – and monitor – Hg have continued to wend their way through the pilot testing phases and into the commercial market.

Overall, all the coal plants in the United States emit about 50 tons of mercury per year. To place this into perspective, coal plants emit about a million tons of sulfur dioxide (SO₂) per year. CAMR was to ultimately reduce the 50 tons to 15 tons a year and Phase 1 was supposed to take effect January 1. But court challenges led to the vacating of the rule, thereby delaying indefinitely enforcement of the early phases of emission and monitoring compliance with federal rules. That didn't change the forward path of local rules adopted by close to two dozen states that elected to enact their own restrictions on mercury emissions from power plants and other industrial facilities.

"I'm not aware of any plants that complied with the former Clean Air Mercury Rule (CAMR) before it was vacated, but a number of plants have had to comply with state mandates," says George Offen, manager of air emission reduction programs and the beneficial use of coal combustion products for EPRI. There are about 20 states that have their own mercury rules."

The original CAMR concept espoused by EPA was for the initial reduction in Hg from coal-fired facilities to come largely as a co-benefit resulting from SO₂ and NO_x reduction measures required under CAIR Phase I, says Offen. "So almost everyone who was not under a state mandate to reduce mercury emissions was probably waiting for Phase II of CAMR. A few installed activated carbon Hg reduction systems, but we've been told that they aren't operating now unless under state rules."

Monitoring mercury, essential in order to verify compliance with reduction rules, is a real challenge. Two things make monitoring difficult. Concentrations of mercury in most coals are extremely low. SO₂ is measured in parts per thousand. Uncontrolled SO₂ in the flue gas of a coal-fired boiler can be 1,000 to 4,000 parts per million, which today's emission control system reduce to 20 to 50 parts per million. Hg in coal flue gas is measured in parts per billion, and it's hard to measure such low quantities. In addition, the concentration of mercury varies greatly, further adding to the difficulty of obtaining a reliable percent reduction measurement.

"The monitors today are reasonably close to being commercial," said George Offen, manager of air emission reduction programs and the beneficial use of coal combustion products for EPRI. "A lot has happened in the past two years with monitoring." Reliability and consistency have improved and monitors also have a much lower failure rate. "The challenge we're facing is we don't yet have National Institute of Science and Testing (NIST) traceable calibration standards." Major manufacturers in the mercury

monitoring sector include Tekran and Thermo Scientific.

The other difficulty with monitoring is that Hg readily reacts with ash and other materials such as chlorine. "But when measuring it for compliance you're only measuring vapor phase mercury and you have hardly any particulates so that helps some," said Offen. "On the other hand, you also have water, especially behind a scrubber."

Strategy

Mercury concentrations vary enormously in any given type of coal, so with the possible exception of Texas lignite (which has substantially higher mercury than other coals) the bands of mercury content overlap across coals. That means using existing selective catalytic reduction (SCR) and flue gas desulfurization (FGD) to make them capture Hg as well as other emissions. One way of enhancing Hg capture from FGD and SCR at power plants that cannot meet their mercury emission limits through co-benefits alone is to treat the coal (which typically for these situations lacks enough chlorine to force the mercury into a soluble compound) by adding something to it. Alstom's KNX process, for example, uses calcium bromide. Bromide can be added to the boiler or to the coal to oxidize the mercury and facilitate its capture in wet scrubbers. Newly under consideration is the practice of injecting activated carbon upstream of the FGD to improve its mercury capture performance even more. Of course, a plant could increase its mercury capture rate, if needed, by using conventional activated carbon injection.

Power plants without an FGD would likely use sorbent injection, mostly an activated carbon, upstream of a particulate control device. The particulate control can be either the plant's existing device or a compact baghouse installed following the primary particulate control, with sorbent injection between the primary control and the new baghouse. Activated carbon and brominated activated carbon injection technology are being deployed at a number of power plants. Activated carbon is being offered by ADA-ES, Calgon, Norit, Sorbent Technologies and others. Although variations exist, "all of them revolve around some kind of activated carbon," said EPRI's Ramsay Chang, technical executive for emission controls.

ADA-ES, a leading sorbent supplier, has begun to build an activated carbon manufacturing plant in Red River Parish, Louisiana and plans to begin partial operation this summer and full operation this fall. The company has signed multi-year, off-take contracts to supply activated carbon to major utilities, with an aggregate value in excess of \$160 million.

There are also variations of sorbent injection that provide ways to introduce activated carbon into flu gas. It can be injected in front of the air heater instead of behind it to provide more flue gas reaction time. There are also ways to agglomerate the carbon or grind it finer on site to achieve better mass transfer. These processes are also being offered commercially. The post

combustion Mer-Cure process Alstom offers is a combination of some of those methods.

Another type of sorbent injection, referred to by EPRI as alternative sorbents, are designed to be tolerant to higher temperatures making them more ash compatible. That means when the carbonate mixes with the ash it has less affect on the ash than normal activated carbon. Another group of non-carbon sorbents are known as amended silicane. "A lot of these are mineral-based non-carbons that show some promise but from our point of view are not yet consistent," said Chang.

For several years, Hitachi has offered its TRAC mercury capture enhancement solution. (See accompanying story beginning on page 50.)

Pre-Combustion and Post-Combustion

Alstom is attacking Hg from two different approaches that, in some cases, might be used simultaneously. Alstom's KNX pre-combustion offering applies calcium bromide to the coal prior to combustion to promote mercury oxidation. "If you can oxidize the mercury, you can collect it in downstream equipment," said Sean Black, director of Air Quality Control Systems and CO₂ marketing for Alstom. "It can be stand-alone to enhance the capabilities of the existing air quality control system or can be applied in combination with another mercury control technology such as our Mer-Cure post-combustion technology or activated carbon injection."

Halogenes are known to improve mercury oxidation in the combustion area at higher temperatures as coal is being burned, and although chlorine or other halogenes can be applied, Alstom found that bromine is the most effective halogen to use. In addition to being economical, it can be applied in concentrations where it enhances mercury oxidation without causing other concerns such as corrosion in the boiler. Calcium bromide is a commercially available solution in the marketplace.

Alstom's KNX business model is to offer the technology and let the customer supply the additive. "There is some equipment used to inject the solution," said Black, "but it's a fairly simple approach. It can be a capital solution or just a technology approach."

"Mer-Cure is essentially an enhanced carbon injection system," said John Iovino, product manager for Alstom Power. "It has a silo, feed system and injection lances that inject the activated carbon into the duct work, similar to other systems on the market."

There are, however, two basic differences between Mer-Cure and other post-combustion activated carbon systems. Mer-Cure has an on line processor that keeps the resulting material from sticking together and de-agglomerates it to create smaller particle sizes and greater surface area. The second feature is the injection location of the sorbent upstream of the air heater. The benefits of upstream injection is that it's a higher temperature region with more internal duct area and provides more residence time for the sorbent to absorb the mercury.

Although Mer-Cure is targeted primarily to ESP configurations, Alstom has also installed it on wet scrubber applications where the combination of Mer-Cure and KNX worked well. "There are some instances where the KNX by itself provides the benefits and there are some cases where Mer-Cure alone can provide the desired benefits. There are many cases where the combination of the two work very effectively together," said Iovino. The KNX applied to the coal provides

better oxidation of the mercury at a lower cost than brominated sorbents, allowing the Mer-Cure system further downstream to capture the mercury more efficiently."

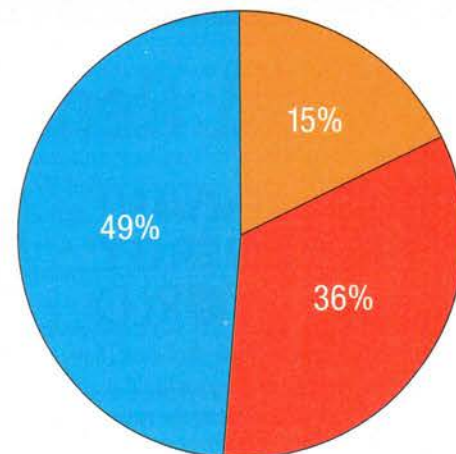
When a customer burns coal with high concentrations of elemental mercury emissions coming from the boiler, they don't get a lot of capture in the existing wet scrubber," said Black. "So we might see 20 to 30 percent mercury removal with the existing AQCS system. When they apply the KNX to the coal it goes from 20 to 30 percent removal to 80 to 90 percent. You may find other cases where they are burning a coal that is not sub-bituminous and you may already have a relatively high mercury removal of say 60 to 80 percent and we can enhance that even 90 percent removal."

Alstom says KNX is most attractive for a client burning sub-bituminous coal because those coals tend to have relatively low halogen content. Alstom has the exclusive license to market the technology in North America. Bromine can be injected in low concentrations to achieve the mercury removal needed without introducing significant halogenes to the boiler. Using chlorine would achieve the same mercury removal but would increase corrosion including tube leaks. Lignite can be a good candidate for the process as well Bituminous offers a lesser value because of the relative degree of improvement is not as great. Bituminous is amenable to mercury capture to start with.

Iovino said the business model for Mer-Cure is a bit different from KNX. The customer purchases the rights to use KNX via a license agreement, whereas Mer-Cure is supplied as a complete system. Mer-Cure reduces sorbent usage about 50 percent compared to traditional activated carbon systems. As a result, significant O&M savings can be realized by dramatically reducing sorbent costs. By the end of this year Alstom expects to have 18 Mer-Cure systems installed and operational. **pe**

PE Online Question of the Week

Are the prospects for new nuclear power plants being built in the U.S. better or worse than they were a year ago?



● Better ● The Same ● Worse

(For more Questions, visit www.power-eng.com.)

EXHIBIT B

WATER, AIR, & SOIL POLLUTION



an international journal
of environmental pollution

80/1-4

This issue is Volume 80

**SPECIAL ISSUE ON
MERCURY AS A GLOBAL POLLUTANT**

Guest Editors: Don Porcella, John Huckabee
and Brian Wheatley

ISSN 0049-6979

CODEN WAPLAC

AMEREN UE EXHIBIT 1082
Page 10

MERCURY STACK EMISSIONS FROM U.S. ELECTRIC UTILITY POWER PLANTS

P. CHU and D.B. PORCELLA

Electric Power Research Institute, 3412 Hillview Avenue, Palo Alto, CA USA

Abstract. Literature estimates for worldwide anthropogenic mercury (Hg) emissions range from 900 to 6200 t/yr. EPA recently estimated that U.S. electric utilities emit about 93 t/yr. EPRI, DOE, and others have recently conducted field measurements to better quantify electric utility emissions of Hg and other trace substances. Hg emissions inventories based on these recent measurements indicate that total electric utility Hg emissions are about 40 t/yr - about half of these previous estimates. Furthermore, the results have indicated that Hg emissions are quite variable and are not consistently captured by conventional air pollution control technologies - electrostatic precipitators, fabric filters, and flue gas desulfurization systems.

1. Introduction

Title III of the 1990 Clean Air Act Amendments (CAAA) mandated that the U.S. Environmental Protection Agency (EPA) evaluate emissions and health risks associated with 189 hazardous air pollutants from electric utility steam generating stations. Hg was singled out for two separate studies that will examine emissions from utilities and other sources and define the thresholds at which Hg affects health and ecology. In anticipation of the CAAA, the Electric Power Research Institute (EPRI) initiated the Power Plant Integrated Systems: Chemical Emission Studies (PISCES) research program in 1988 (Chow 1991).

As part of the PISCES program, the Field Chemical Emission Monitoring (FCEM) program was undertaken to fill critical data gaps in the literature. To date, the EPRI FCEM program has sampled at 35 utility sites - encompassing a range of fuels, boiler configurations, particulate control technologies, flue gas desulfurization systems, and NO_x control technologies. Parallel to EPRI's efforts, the Department of Energy (DOE) has conducted field measurements as part of two DOE studies - the Clean Coal Technology program and the Comprehensive Assessment of Air Toxic Emissions from Coal-Fired Power Plants (Schmidt and Brown 1994). The combined studies provide the most extensive quality-controlled data set extant for estimating Hg (as well as other trace substances) emissions from electric utilities.

Parallel to the FCEM program, EPRI's work in Hg cycling highlighted the need to characterize the various species of Hg in stack emissions. EPRI sponsored development of a technique to speciate Hg, and at select sites, Hg speciation measurements were conducted. This paper summarizes recent Hg field results and quantifies total Hg emissions from electric utility power plants.

2. Literature

Various authors have estimated global anthropogenic Hg emissions. Using the geometric mean of the range of Hg emissions compiled by Nriagu and Pacyna (1988), present day worldwide fossil-fuel combustion was estimated to produce about 1500 t(1000kg)/yr (290 from electricity generation and 1210 from other industrial use). The U.S. EPA has compiled information about present day estimates of Hg emissions from many sources to the atmosphere in the U.S. that amount to about 300 t/yr in 1990 (MRI 1993). This study estimated that coal-fired power plants emit 89 t/yr, with total power plant Hg emissions of 93 t/yr. This estimate was based largely on Hg in coal data from the U.S. Geological Survey (USGS). The USGS analyzed thousands of channel and core samples of coal for various coal quality

Water, Air, and Soil Pollution 80: 135-144, 1995.
© 1995 Kluwer Academic Publishers. Printed in the Netherlands.

parameters, including Hg content. These data represent "in-the-ground" coals which are often different in Hg content from "as-fired" coals. After the coal is mined, the coal may be washed before it is pulverized and burned.

3. Recent Field Studies

The PISCES program was initiated in 1988, and the initial phase involved a compilation of an interim chemical emissions database based on literature information. EPRI and the Utility Air Regulatory Group (UARG) concluded that the literature data (1) contained significant gaps -- especially with regard to internal plant streams, (2) were highly variable for a given plant characteristic, and (3) were conducted using inconsistent sampling and analytical procedures (Radian 1992). The limitations in the database became the impetus for EPRI and DOE's intensive field data acquisition efforts. To date, 48 fossil fuel-fired power plants have been sampled by EPRI and DOE. Because some sites were tested under different configurations (i.e. pilot facilities, pre- and post-low NO_x burners, upstream and downstream of an flue gas desulfurization (FGD) system), more than one data set was obtained at some sites. The combined field studies include every significant coal type, boiler configuration, and particulate, SO₂, and NO_x control technology. The two sampling programs followed generally consistent sampling and analytical protocols. Triplicate samples were collected at each field site over a period of about 3 to 5 days. The results of these field studies provide a reasonable estimate of expected Hg emissions from utility power plants. However, because of the low concentrations of Hg and the nature of Hg, sampling and analysis have generally been difficult and significant uncertainty exists in the data.

3.1 HG IN FOSSIL-FUELS

The U.S. electric utility industry burns three major classifications of fossil fuels - coal, fuel oil, and natural gas. Figure 1 compares the measured Hg concentrations from the recent field sites with those in the literature for the three fossil fuels - coal, oil, and gas. The recent measurements have indicated Hg levels in U.S. coal range from 0.02 to 0.25 $\mu\text{g/g}$ (emissions in the range: 0.5 to 10 $\mu\text{g/MJ}$; multiply $\mu\text{g/MJ}$ by 2.3 to obtain $\text{lb}/10^{12}$ Btu). Hg levels in coal tend to be 1 to 4 orders of magnitude greater than in fuel oil and natural gas; thus it makes sense to discuss Hg emissions by these different fuel types.

3.1.1 Coal

The more recent measurements tend to be within the data range of the literature values, but do not include some of the high literature results. Because of the limited sample size from EPRI's field studies and in order to better quantify Hg concentrations in coal, EPRI and UARG sponsored a study to analyze 123 different "as fired" coals (Baker, Bloom). At select power plants, multiple samples were taken at different time intervals in order to evaluate variability. A total of 154 samples (106 bituminous, 37 sub-bituminous, and 11 lignite) were analyzed. These coal samples represent a significant portion of the current and anticipated future coal supplies for the U.S. utility industry. These include samples of coal from a total of 76 counties in all 18 major coal-producing states in the U.S. In aggregate, this study provides a broad-based representation of the Hg content in U.S. coals. The results are summarized in Table I. The overall mean Hg concentration in the 154 samples was 0.085 $\mu\text{g/g}$ (standard deviation of 0.074 $\mu\text{g/g}$). The multiple samples from the select plants varied within 10 percent but did not significantly affect the mean. The mean of the 123 different coals was 0.088 $\mu\text{g/g}$.

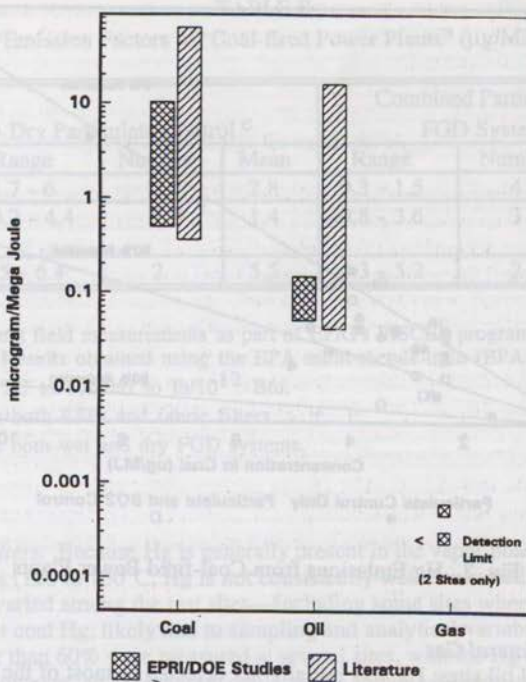


Fig. 1. Hg Levels in Fossil Fuels

TABLE I
Summary of Hg Concentrations by Coal Rank (Baker 1994)

Coal Type	Number of Samples	Arithmetic Mean ($\mu\text{g/g}$)	Standard Deviation ($\mu\text{g/g}$)
Bituminous	87	0.087	0.070
Sub-bituminous	37	0.053	0.027
Lignite	11	0.177	0.118
All Ranks	154	0.085	0.074

The results showed lower levels of Hg in the coal than the revised USGS coal database. The mean Hg concentration for bituminous coals from the EPRI/UARG study was 0.087 $\mu\text{g/g}$. This compares with an average of 0.21 for bituminous coals based on the USGS database. As noted earlier, the USGS database represents as-mined core samples, while the EPRI study represents as-fired coal samples. Thus process steps such as coal washing remove some Hg and are not accounted for in the USGS analyses.

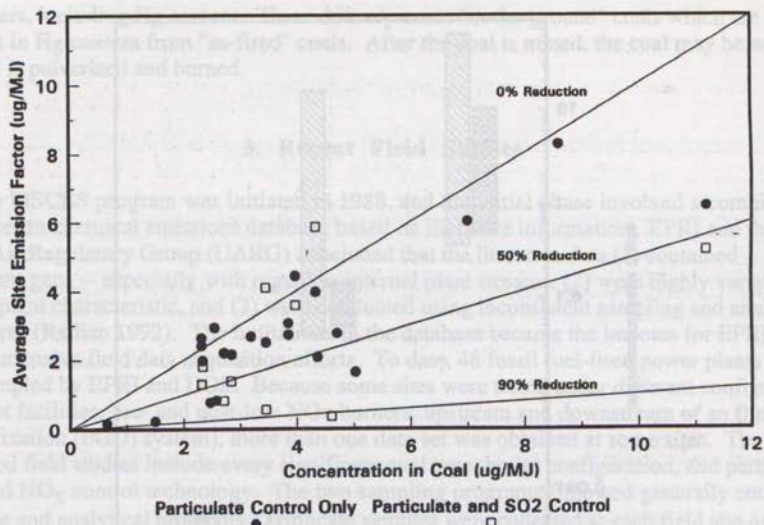


Fig. 2. Hg Emissions from Coal-fired Power Plants

3.1.2 Fuel Oil and Natural Gas

In the EPRI fuel oil sites, Hg was initially not detected in most of the fuel oil samples. To obtain lower detection limits, INAA (instrument neutron activation analysis) was used instead of CVAAS (cold vapor atomic absorption spectrophotometry). Using INAA with standards and blanks to ensure no loss of Hg, Hg was measured in the 0.002 to 0.008 $\mu\text{g/g}$ range (0.04 to 0.13 $\mu\text{g/MJ}$). This is 1 to 2 orders of magnitude less than in coal. Natural gas samples were analyzed for Hg at only two sites. Hg was detected at 0.02 $\mu\text{g/m}^3$ (0.00056 $\mu\text{g/MJ}$) at one site and below the detection limit of 0.01 $\mu\text{g/m}^3$ (0.00028 $\mu\text{g/MJ}$) at the other site.

3.2 FLUE GAS STACK EMISSIONS

All coal-fired plants employ some type of particulate control technology and some plants also include an FGD system. This is significant because particulate and SO_2 control systems may remove Hg. Only a fraction of the oil-fired plants have a particulate control device, and no commercial oil-fired plants use an FGD system. Gas-fired power plants are generally uncontrolled.

3.2.1 Coal-fired Power Plants

Figure 2 compares the Hg specific emission factors with the inlet coal feed for coal-fired units. Both the individual Hg emission rates and the inlet coal concentration are normalized to mass of Hg per unit of heat input ($\mu\text{g/MJ}$) to calculate Hg removals for each site. Hg removal is defined as the reduction in total Hg stack emissions relative to potential Hg emissions based on the Hg in coal concentrations. The results are presented for the two general air pollution control technologies - dry particulate control (ESP and fabric filters) and FGD systems (spray dryer absorbers and wet FGD systems).

TABLE II
Hg Emission Factors for Coal-fired Power Plants^a ($\mu\text{g}/\text{MJ}$)^b

Coal Type	Dry Particulate Control ^c			Combined Particulate and FGD Systems ^d		
	Range	Number	Mean	Range	Number	Mean
Bituminous	1.7 - 6	15	2.8	0.3 - 1.5	4	0.6
Sub-bituminous	< 0.2 - 4.4	7	1.4	0.8 - 3.6	3	2.1
Lignite	4.5 - 6.4	2	5.5	4.3 - 5.2	2	4.7

^a Based on recent field measurements as part of EPRI's PISCES program and DOE's field test efforts. Results obtained using the EPA multi-metals train (EPA Method 29).

^b Multiply by 2.3 to convert to $\text{lb}/10^{12}$ Btu.

^c This includes both ESPs and fabric filters.

^d This includes both wet and dry FGD systems.

ESPs and Fabric Filters. Because Hg is generally present in the vapor phase at particulate control temperatures (120 to 150°C, Hg is not consistently well controlled by an ESP or fabric filter. Hg removal varied among the test sites—including some sites where the outlet Hg was greater than the inlet coal Hg, likely due to sampling and analytical variability. By contrast, Hg removals greater than 60% were measured at several sites, with the Hg accounted for in the collected fly ash. However, an explanation could not be found why certain plants or coals yield more particulate phase Hg. The mean removal efficiency for all coal-fired plants with dry particulate controls was about 30%.

Wet FGD Systems. Hg removal efficiencies for a combined ESP (or fabric filter) and wet FGD systems were highly variable and gave poor correlation with the FGD design, coal composition, or measured Hg valence (oxidation) state. The Hg removal efficiencies for ESP/FGD systems ranged from as low as 0% to as high as 90%. Research has shown that oxidized Hg appears to be removed to a greater degree than elemental Hg (Peterson et al. 1994). However, only poor correlation was obtained with oxidized Hg or with Hg removal efficiency by FGD systems. The mean Hg removal efficiency for the combined ESP/FGD system was about 45%. EPRI, DOE, and other organizations are continuing work in this area to better understand Hg chemistry.

Emission Factors - The Hg emission results for coal-fired plants are presented for the three major coal classifications as well as the two general air pollution control technologies - dry particulate control (ESP and fabric filters) and FGD systems (spray dryer absorbers and wet FGD systems). The database is quite small for most of the categories, and this should be considered when applying the results in Table II. For example, the average Hg emission factor for units burning sub-bituminous coals with only particulate controls was actually less than the average Hg emission factor for the combination of the particulate and FGD system. This artifact was due to the small number of units studied. Two of the FGD systems had less than 25% Hg removal, while four of the dry particulate control sites achieved greater than 65% removal. Only two sites were tested that burn lignite coal; thus the confidence interval around the average emissions for these units is broad. The sites tested include both North Dakota and Texas lignite coals.

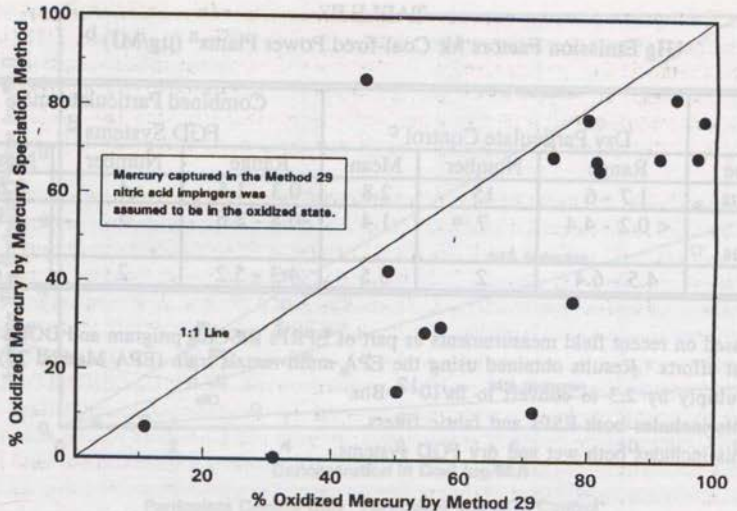


Fig. 3. Comparison of Hg Speciation Methods

Hg Speciation. Hg emissions may be present in several valence states - elemental (Hg^0) and oxidized (Hg^{+2}). This has significance for several reasons. The chemical form of the Hg may affect the degree of removal, as well as atmospheric fate, health effects, and risk assessment. EPRI has applied two sampling methods to quantify Hg emissions - the EPA multi-metals train (EPA draft Method 29) and the mercury speciation adsorption (MESA) method (Prestbo and Bloom 1995). EPRI has used both methods to provide some estimate of oxidized and elemental Hg. Neither method has been validated for Hg speciation. At some sites, the flue gas was sampled downstream of the ESP and some oxidation/reduction of Hg may occur before exiting the stack. In addition, oxidation/reduction of Hg may occur in the sampling system as well. Both methods are still experimental for Hg speciation, and further validation studies are planned. The multi-metals train uses two sets of impingers to capture the vaporous Hg. The first set of impingers consists of HNO_3/H_2O_2 and the second set consists of $KMnO_4$. Method 29 was not designed to speciate Hg, but it has been suggested that only oxidized Hg is captured in the HNO_3/H_2O_2 impingers, thus all remaining Hg (which should be elemental Hg) is captured in the $KMnO_4$ impingers. The MESA method, designed to speciate flue gas Hg, follows a similar approach except it uses a different medium to capture the Hg. This method employs solid sorbent traps - consisting of soda lime and iodated carbon - to capture the oxidized and elemental Hg, respectively.

The oxidized Hg concentrations from Method 29 (this assumes that the Hg captured in the HNO_3/H_2O_2 impingers is oxidized Hg) generally appear to be higher than the oxidized Hg concentrations from the MESA method. Figure 3 compares the measured levels of oxidized Hg based upon these two methods. Because the two methods generally agree for total Hg (some sites having large discrepancies), it would appear that one or both methods does not accurately quantify oxidized Hg. The purpose of the HNO_3/H_2O_2 impingers in Method 29 was to capture the volatile trace metals (such as arsenic, chromium, and nickel) and was not intended to selectively capture oxidized Hg. Thus, some elemental Hg may be captured in the HNO_3/H_2O_2 impingers. The other possibility is that the MESA method does not efficiently capture all the oxidized Hg. Recent research has shown that the oxidized Hg capture efficiency in the soda lime traps is a function of the sampling temperature. Some of the early runs were

not conducted at optimum temperatures and it is possible some of the oxidized Hg was not captured in the soda lime traps—thus underestimating oxidized Hg. In addition, the MESA was not designed to sample flue gas isokinetically, thus the train may not obtain a representative sample of particulates. However, when detected, the particulate phase Hg has generally been a small fraction (<1%) of the total Hg. In addition to being present at very low levels in the particulate phase, the ESP or fabric filter would be expected to capture most of the particulate phase Hg.

For dry particulate controls (ESPs and fabric filters), the mean percentage of oxidized Hg levels based on the sorbent speciation and Method 29 trains were 55 and 70%, respectively. The mean percentage of oxidized Hg for FGD systems were 25 and 45%, respectively.

The ratio of oxidized and elemental Hg is potentially a function of the coal type and composition as well as flue gas conditions. Data were insufficient to determine any definitive correlations to predict levels of oxidized and elemental Hg—other than by direct measurement. Figures 4 and 5 compare the concentration of oxidized Hg (in $\mu\text{g}/\text{Nm}^3$ - normal [25°C, 1 atm]) as a function of Cl in the coal for the multi-metals and sorbent speciation methods. The results from the MESA method show a trend toward higher oxidized Hg concentrations with increasing Cl content in the coal. This trend was not apparent with the Hg speciation results from Method 29. It is important to note that some results appear to be "outliers" and there is significant scatter among the data. This may be due to other factors that affect Hg speciation and that have not been completely considered. In addition, some of this scatter may be due to process variability as well as sampling and analytical methods.

3.2.2 Fuel Oil-fired Power Plants

As part of the State of California AB2588 study, utilities attempted to measure Hg (as well as other trace substances) emissions from oil-fired power plants. The method detection limits were not sufficient to quantify the concentrations of Hg in either the fuel oil or the stack. In EPRI field sites, more sensitive analytical methods were used to achieve lower detection limits in both the fuel oil and stack measurements. INAA was used to analyze the fuel oil - instead of CVAAS. Using INAA, Hg in fuel oil was measured in the 0.002 to 0.008 $\mu\text{g}/\text{g}$ (0.04 to 0.13 $\mu\text{g}/\text{MJ}$) range. Assuming that all the Hg in the fuel oil is emitted in the stack, the Hg concentration in the flue gas would be approximately 0.1 to 0.4 $\mu\text{g}/\text{Nm}^3$. Because the Hg method detection limit (flue gas measurements) have ranged from 0.1 to 0.5 $\mu\text{g}/\text{Nm}^3$, these low levels of Hg have led to difficulties in quantifying the Hg concentration in flue gas for oil-fired power plants. Measured Hg stack emissions have ranged from 0.2 to 1.7 $\mu\text{g}/\text{Nm}^3$ (0.07 to 0.6 $\mu\text{g}/\text{MJ}$). The measured emission levels have been highly variable and have sometimes been much greater than the inlet fuel levels. Trace metals emissions data from fuel oil plant appear to be log normal, thus a geometric mean for Hg appears to be more appropriate than an arithmetic mean. A geometric mean reduces the emphasis on the very high measurements which are likely due to sampling and analytical difficulties. The geometric mean is 0.2 $\mu\text{g}/\text{MJ}$ (Table III); this emission factor is conservative since this is higher than the Hg levels in the fuel oil.

3.2.3 Gas-fired Power Plants

Field tests were conducted at two electric utility gas boiler sites. Hg was not detected at the stack at either site. The detection limit was about 0.5 $\mu\text{g}/\text{Nm}^3$ (0.17 $\mu\text{g}/\text{MJ}$) which was three orders of magnitude higher than the expected levels based on the natural gas analyses. The Hg concentration in the natural gas was measured at 0.00056 $\mu\text{g}/\text{MJ}$ (near the detection limit) at one boiler and less than the detection limit of 0.00027 $\mu\text{g}/\text{MJ}$ at the other. This yields an average of 0.00034 $\mu\text{g}/\text{MJ}$ (assumes half of the detection limit for the not detected value). The best estimate for Hg emissions would be to use the natural gas analyses and assume all the Hg is emitted in the stack (Table III).

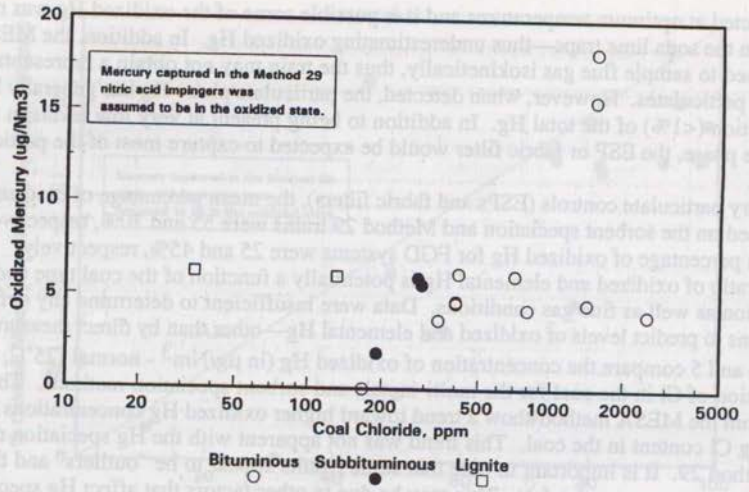


Fig. 4. ESP Outlet Oxidized Hg Concentration (Method 29) as a Function of Chloride Level

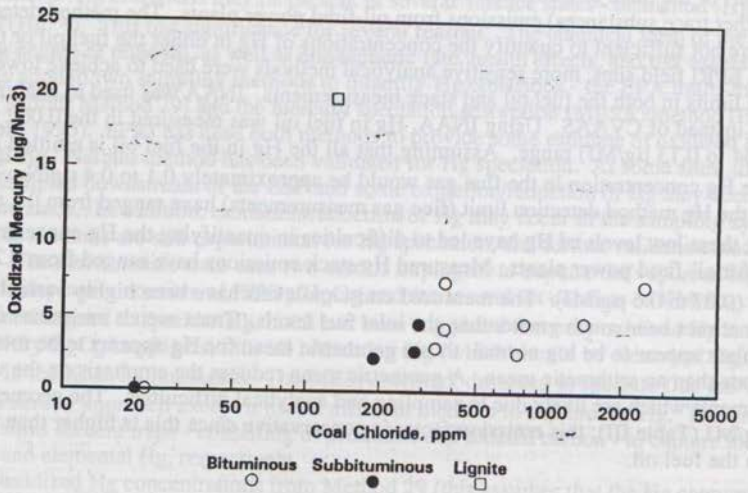


Fig. 5. ESP Outlet Oxidized Hg Concentration (MESA) as a Function of Chloride Level

TABLE III
Hg Emission Factors for Oil and Gas-fired Power Plants ($\mu\text{g}/\text{MJ}$)^a

Fuel Type	Range	Number	Mean
Fuel Oil	0.07 - 0.6	5	0.20 ^b
Natural Gas	<0.00026 - 0.00056	2	0.00034 ^c

- ^a Multiply by 2.3 to convert to $\text{lb}/10^{12}$ Btu.
^b Hg stack emission results for oil plants were assumed log normally distributed. This emission factor is a conservative estimate for oil-fired plants with ESPs.
^c Natural gas emission factors are based upon Hg in the inlet natural gas analyses, assuming that all Hg was emitted in the flue gas.

4. Total Electric Utility Emissions

Based on these recent and relatively extensive fuel and stack measurements, two approaches additional to MRI (1993) were employed to estimate total electric utility emissions from fossil-fueled power plants.

1. The more detailed approach incorporated the coal purchases for each individual power plant (EIA/DOE 1993) and average Hg concentrations based on the Hg coal analyses study (Baker, Bloom 1994) to estimate input Hg. Average removal efficiencies as calculated from the recent EPRI/DOE studies were then applied to estimate Hg emissions at each power plant. The individual Hg emissions were then summed to yield about 39 t/yr for the U.S. electric utility coal fired plants. Hg emissions from oil- and gas-fired utility plants estimated based on heat input data (MRI 1993) and average emission factors (Table III) were less than 0.3 t/yr.
2. An alternative approach applied the average emission factors for each category of fuel type and control technology from Tables II and III and the total heat input data for the U.S. utility industry. The UDI Power Statistics Database (1989) was used to calculate a weighted emission factor based on each of the categories of fuel type and control technology. This simplistic approach is similar to the methods used by other surveys such as MRI (1993), and yields a similar Hg emissions estimate as the detailed approach (described above) of 41 t/yr for the coal-fired power plants.

The estimated Hg emissions from these two approaches are compared with MRI's estimates in Table IV. Both approaches provide estimates of utility Hg inventory on the order of 40 t/yr for the 1990 period - less than half of MRI's estimate. Thus the revised U.S. total for Hg from all sources would likely be on the order of 250 t/yr (MRI 1993) - assuming the Hg emissions data for all other sources were correct. Power plants would amount to about 15 to 20% of the U.S. total, a number likely to decrease as newer generation technologies coming on-line.

TABLE IV
Total Hg Emission from Fossil Fuel-fired Power Plants (t/yr - in 1990)

Fuel Type	MRI ^a	EPRI Estimates	
		Fuel/Removal Efficiencies Methodology ^b	Emission Factors Methodology ^c
Coal	89	39	41
Oil	3.8	0.3 ^d	0.3
Natural gas	not estimated	0.001 ^d	0.001
Total	93	39.3	41.3

^a Midwest Research Institute (1993).

^b This methodology employs recent data on Hg in fuels and average removal efficiencies for ESP/fabric filters and ESP/FGD systems for coal fired power plants.

^c This methodology employs average emission factors and heat inputs. The emission factors were based on actual measured Hg concentrations in flue gases. This calculation is the same approach as MRI (1993), but uses the recent emission factors in Table II.

^d Based on recent emission factors in Table III.

5. Conclusions

Recent field measurements by EPRI and DOE better quantify Hg levels in fossil fuels and in flue gas emissions from electric utility power plants. These measurements show total Hg emissions from electric utility fossil-fuel fired power plants are about half of previous estimates. Hg is relatively volatile at nominal power plant stack temperatures, and is not consistently captured in conventional particulate and SO₂ control devices. The factors that affect Hg removal efficiencies could not be determined from the limited results available. Further, experiments on Hg speciation show the need for additional development work to develop reliable methods.

References

- Baker, S.S., EPRI Mercury in Coal Study: A Summary Report for Utilities That Submitted Samples, May 1994.
- Bloom, N.S. and E. M. Prestbo. In press. A New Survey of Mercury in U.S. Fossil Fuels. Pittsburgh Coal Conference. Pittsburgh PA 1993.
- Prestbo, E. M. and N. S. Bloom. Mercury Speciation Adsorption (MESA) method for Combustion Flue Gas : Methodology, Intercomparison and Atmospheric Implications. Accepted. WASP. This Volume/
- Chow, W., et al., Managing Air Toxics: Status of EPRI's PISCES Project, Proceedings of the Conference on Managing Air Toxics: State of the Art, November 4-6, 1991, Washington, D.C.
- Energy Information Administration, U.S. Department of Energy, Cost and Quality of Fuels for Electric Utility plants 1992, August 1993.
- Midwest Research Institute (MRI). Locating and Estimating From Sources of Mercury and Mercury Compounds. EPA-454/R-93-023, September 1993.
- Nriagu, J.O. and J.M. Pacyna, Quantitative Assessment of Worldwide Contamination of Air, Water, and Soils by Trace Metals, Nature 356:389, 1988.
- Peterson et al. "Mercury Removal By Wet Limestone Fgd Systems. EPRI HSTC Results." Proceedings of the 87th Annual Meeting and Exhibition of the Air & Waste Management Association, Paper 94-RP114B.01, June 19-24, 1994.
- Public Law 101-549, November 15, 1990.
- Radian Corporation, Evaluation of Emissions Information in the PISCES Database, Report DCN 92-213-161-02, March 1992.
- Schmidt, C.R. and T.D. Brown, Comprehensive Assessment of Air Toxic Emissions from Coal-Fired Power Plants, Proceedings of the 87th Annual Meeting and Exhibition of the Air & Waste Management Association, Paper 94-WA-68A.03, June 19-24, 1994.
- Utility Data Institute Power Statistics Directory Database, 1989.

EXHIBIT C



Fuel Processing Technology



MAR 16 2000

BEVIER ENGINEERING LIBRARY

FUEL PROCESSING TECHNOLOGY

An international journal devoted to all aspects of processing
and beneficiation of coal, petroleum, oil shale, tar sands and peat

Editor

Gerald P. Huffman,
Lexington, KY, USA

Regional Editor for Europe

A.M. Mastral
Zaragoza, Spain

Regional Editor for the Far East

Peng Chen,
Beijing, P.R. China

Honorary Editor

Larry L. Anderson,
St. George, UT, USA

Editorial Board

S.A. Benson, Grand Forks, ND, USA
J.C. Crelling, Carbondale, IL, USA
E. Ekinci, Istanbul, Turkey
R.A. Graff, New York, NY, USA
W.R. Jackson, Clayton, Vic., Australia
J. Jin, Beijing, P.R. China
I.A. Korobetski, Kemerovo, Russia
B. Li, Taiyuan, P.R. China
R. Markuszewski, Des Plaines, IL, USA
A. Marzec, Gliwice, Poland
T.C. Miin, Ann Arbor, MI, USA

Y. Nishiyama, Sendai, Japan
M. Nomura, Osaka, Japan
Y. Sato, Tsukuba, Japan
H.H. Schobert, University Park, PA, USA
H. Schulz, Karlsruhe, Germany
A. Tomita, Sendai, Japan
I. Wender, Pittsburgh, PA, USA
W.H. Wisler, Salt Lake City, UT, USA
K.-C. Xie, Taiyuan, P.R. China
Y. Yürüm, Ankara, Turkey

Volume 63 (2000)



ELSEVIER

Amsterdam - Lausanne - New York - Oxford - Shannon - Tokyo

0378-3820/00/0 - see front matter © 2000 Elsevier Science B.V. All rights reserved.
ISSN: 0378-3820(99)00068-5



ELSEVIER

Fuel Processing Technology 63 (2000) 197–213

FUEL
PROCESSING
TECHNOLOGY

www.elsevier.com/locate/fuproc

Gas-phase transformations of mercury in coal-fired power plants

Constance L. Senior ^{a,*}, Adel F. Sarofim ^{b,1}, Taofang Zeng ^{b,2},
Joseph J. Helble ^c, Ruben Mamani-Paco ^c

^a Physical Sciences Inc., 20 New England Business Center, Andover, MA 01810, USA

^b Department of Chemical Engineering, Massachusetts Institute of Technology, Cambridge, MA, USA

^c Department of Chemical Engineering, University of Connecticut, CT, USA

Received 1 January 1999; received in revised form 20 September 1999; accepted 20 September 1999

Abstract

Because mercury enters the food chain primarily through atmospheric deposition, exposure models require accurate information about mercury emission rates and mercury speciation from point sources. Since coal-fired power plants represent a significant fraction of the anthropogenic emissions of mercury into the atmosphere, the speciation of mercury in coal-fired power plant flue gas is currently an active topic of research. We have demonstrated that the assumption of gas-phase equilibrium for mercury-containing species in coal-fired power plant exhaust is not valid at temperatures below approximately 800 K (500°C). Chlorine-containing species have been shown to be the most important for oxidation of elemental mercury in the post-combustion gases. The conversion of HCl to Cl₂ in the flue gas of a coal-fired power plant is kinetically limited. Kinetic calculations of the homogeneous oxidation of elemental mercury by chlorine-containing species were carried out using global reactions from the literature. The levels of mercury oxidation, while of comparable magnitude to field observations, are still below the 40% to 80% oxidation typically observed in field measurements. © 2000 Elsevier Science B.V. All rights reserved.

Keywords: Mercury; Coal-fired power plant; Flue gas

* Corresponding author. Fax: +1-978-689-3232; e-mail: senior@psicorp.com

¹ Present address: Department of Chemical Engineering, University of Utah, USA.

² Present address: Department of Mechanical and Aerospace Engineering, UCLA, USA.

1. Introduction

A recent report by the Environmental Protection Agency (EPA) on emission of hazardous air pollutants by electric utilities predicted that emissions of air toxics from coal-fired utilities would increase by 10% to 30% by the year 2010 [1]. Mercury from coal-fired utilities was identified as the hazardous air pollutant of greatest potential public health concern.

Anthropogenic emissions of mercury account for 10% to 30% of the world-wide emissions of mercury [2]. EPA has estimated that during the period 1994–1995 annual emissions of mercury from human activities in the United States were 159 tons [1]. Approximately 87% of these emissions were from combustion sources. Coal-fired utilities in the U.S. were estimated to emit 51 tons of mercury per year into the air during this period.

The form of mercury emitted from point sources is a critical variable in modeling the patterns and amount of mercury deposition from the atmosphere [1,3]. Both elemental and oxidized mercury are emitted to the air from combustion point sources. Elemental mercury has a lifetime in the atmosphere of up to a year, while oxidized forms of mercury have lifetimes of a few days or less [1] as a result of the higher solubility of Hg^{+2} in atmospheric moisture. Elemental mercury can thus be transported over long distances, whereas oxidized and particulate mercury deposit near the point of emission. Once mercury has deposited on land or water, it can transform into methylmercury, an organic form, and thereby enter the food chain. Humans are most likely to be exposed to methylmercury through consumption of fish.

Mercury is present in coal in low concentrations, on the order of 0.1 ppmw. In the combustion zone of a coal-fired power plant, all the mercury in coal is vaporized as elemental mercury, yielding vapor concentrations of mercury in the range of 1 to 20 $\mu\text{g}/\text{m}^3$ (1 to 20 ppbw). At furnace exit temperatures (1700 K), all of the mercury is expected to remain as the thermodynamically favored elemental form in the gas. As the gas cools after combustion, oxidation reactions can occur, significantly reducing the concentration of elemental mercury by the time the post-combustion gases reach the stack. Measurements of the concentration of mercury species taken in the stacks of pilot and full scale coal combustion systems show more than half of the vapor phase mercury as the oxidized form which is likely to be HgCl_2 [4–6]. Current measurement methods cannot identify specific oxidized species of mercury. The range of observed values is broad: one study consisting of mercury speciation measurements from fourteen different coal combustion systems reported anywhere from 30% Hg^{+2} to 95% Hg^{+2} upstream of the air pollution control device (APCD) [4].

Although we can identify the major reaction pathways for mercury in coal combustion flue gas with some degree of confidence, we cannot yet make quantitative predictions of the emissions of specific mercury species from coal-fired power plants. In our work, the goal is to advance the state of knowledge such that a predictive model for emissions of total mercury and specific mercury species can be formulated. Specifically, we want to predict the rate of oxidation of elemental mercury from the furnace exit to the convective air heater, leading to prediction of gas-phase mercury speciation at the

inlet to the APCD. In this paper, we examine methods for calculation of the speciation of mercury in coal combustion flue gas.

2. Equilibrium calculations

As a starting point, the distribution of mercury species in coal combustion flue gas were calculated using equilibrium calculations. Such equilibrium calculations have been carried out before [7]. However, no one has yet explored whether the assumption of equilibrium is valid for mercury species in coal-fired utility flue gas given the time–temperature history in the post-combustion region. If equilibrium is a valid assumption for a particular element, then predicting the fate of the element is relatively straightforward. On the other hand, if equilibrium will not be attained in the flue gas, constrained equilibrium or kinetic models will need to be developed.

Equilibrium calculations were conducted using SOLGASMIX [8]. The thermochemical database in the HSC package provided thermochemical data on the species of interest [9]. Calculations were carried out for four coals using the material balances in Table 1. A stoichiometric ratio of 1.2 was assumed for the combustion process. The species considered in the equilibrium calculation were as follows:

Gas: CO, CO₂, Cl₂, H₂, HCl, H₂O, Hg, HgCl₂, HgO, N₂, NO, NO₂, O₂, SO₃

Condensed: C, Hg, HgO, HgSO₄.

Table 1
Compositions for equilibrium calculations at SR = 1.2

	Elkhorn/Hazard (bituminous)	Pittsburgh (bituminous)	Illinois 6 (bituminous)	Wyodak (sub-bituminous)
<i>Ultimate analysis (wt.%)</i>				
H	4.85	4.98	5.1	7.04
C	74.87	76.62	67.7	52.84
N	1.43	1.48	1.18	0.7
S	0.82	1.64	3.6	0.39
O	10.45	8.19	12.14	34.54
Ash	7.41	7.01	10.26	4.49
<i>Minor species (ppmw)</i>				
Cl	1700	980	340	550
Hg	0.13	0.11	0.11	0.11
<i>Gas composition at SR = 1.2 (in vol.%)</i>				
CO ₂	14.5	14.44	14.26	13.86
H ₂ O	5.7	5.69	6.51	11.13
O ₂	4.13	3.86	4.21	6.27
N ₂	76.49	76.59	75.8	72.17
<i>(in ppmv)</i>				
SO ₂	594	1166	2837	383
HCl	111	62	24	49
Hg	0.0015	0.00124	0.0014	0.00172
SO ₃ ^a	8.2	15.5	39.6	6.5

^aCalculated assuming frozen equilibrium at 1400 K.

Unlike previous calculations [7], the equilibrium between SO_2 and SO_3 was frozen in these calculations. Without this assumption, all of the sulfur is predicted by the equilibrium calculations to exist as SO_3 at low temperatures. This result is contrary to observations from coal-fired power plants in which on the order of 3% of the sulfur is present as SO_3 in stack gases. The formation and destruction of SO_3 is dominated by radical reactions which become slow as the combustion products are cooled below about 1500 K [10]. The concentration of SO_3 in the flue gas was set equal to that predicted by equilibrium at 1400 K for each coal based on these kinetic arguments.

Typical results from 500 to 1100 K are shown in Fig. 1 for the Pittsburgh coal. Below about 425 K (150°C) condensation of HgSO_4 is predicted, but results of the equilibrium calculations are not shown for this temperature in the figure for two reasons. First, below the acid dewpoint temperature (typically 400 K), the simple equilibrium approach employed for this analysis cannot adequately model the formation of multi-component aqueous solutions containing sulfates. Second, heterogeneous reactions appear to be important for oxidation of mercury at temperatures as high as 600 K [11].

Results for the other three coals are qualitatively similar to those shown in Fig. 1. Below 725 K (450°C) all of the Hg is predicted to exist as HgCl_2 . Above about 975 K (700°C) 99% of the Hg is predicted to exist as gaseous Hg. The rest (1%) is predicted to be gaseous HgO . Between 725 and 975 K, the split between HgCl_2 and Hg is determined by the chlorine content of the coal (Fig. 2). The mercury content of the coal has no effect on the equilibrium distribution of mercury species. Equilibrium HCl concentrations in the gas are predicted to be in the range of 24 to 111 ppm for the coals studied here. Even at these low concentrations, the reaction between Hg and HCl dominates the equilibrium chemistry. At temperatures representative of the inlet to the APCD, therefore, all the mercury should exist in the gas phase as HgCl_2 , if equilibrium were attained in the flue gas.

It is unlikely, however, that equilibrium is attained for mercury species in the post-combustion gas of practical combustion systems. Consider Fig. 3, an idealized

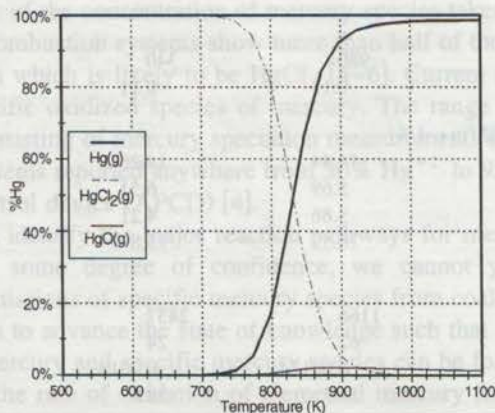


Fig. 1. Equilibrium mercury speciation in flue gas as a function of temperature (Pittsburgh coal).

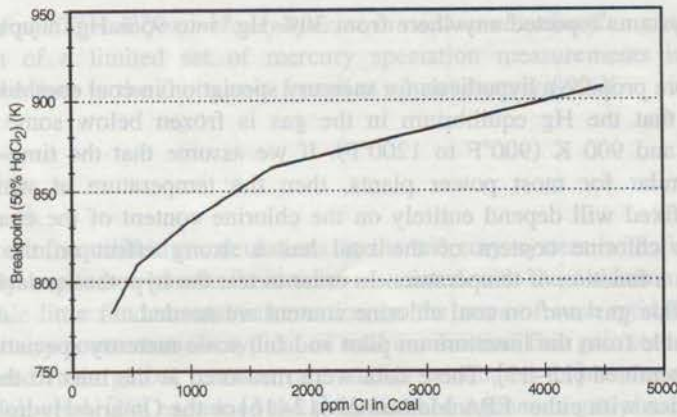


Fig. 2. Equilibrium mercury speciation in flue gas: temperature of 50% HgCl₂ in gas as a function of coal chlorine content.

temperature history for a coal-fired power plant. The flue gas cools rapidly as heat is transferred to water and steam. Observations of kinetic limitations for other species in practical combustion systems and measurements of mercury speciation in coal-fired power plants suggest that equilibrium will not be attained for mercury in coal-fired power plant flue gas. Minor species in the flue gas such as CO and SO₂ do not have time to equilibrate as the gas cools [10]. Similarly for trace species, equilibrium may not be attained as the flue gas cools.

The evidence from pilot-scale and full-scale combustion systems is not consistent with the assumption of equilibrium for mercury species in flue gas at the temperatures corresponding to the location of the APCD. The amount of mercury in the oxidized form when measured at the APCD inlet is almost always less than 100%. For example, one study consisting of mercury speciation measurements from fourteen different coal

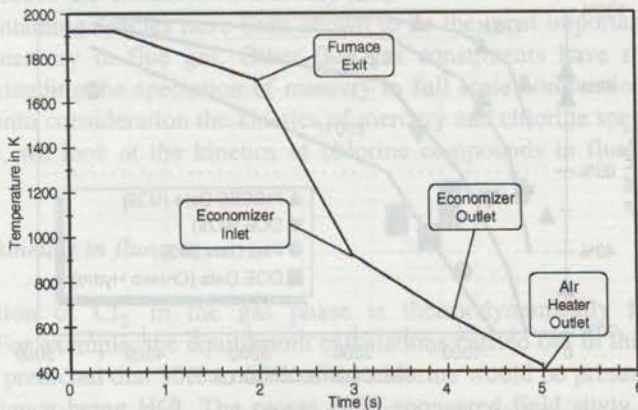


Fig. 3. Time-temperature history for pulverized coal-fired boiler.

combustion systems reported anywhere from 30% Hg^{+2} to 95% Hg^{+2} upstream of the APCD [4].

We therefore propose a hypothesis for mercury speciation in coal combustion flue gas which states that the Hg equilibrium in the gas is frozen below some temperature between 750 and 900 K (900°F to 1200°F). If we assume that the time–temperature history is similar for most power plants, then the temperature at which mercury speciation is fixed will depend entirely on the chlorine content of the coal. As Fig. 2 indicated, the chlorine content of the coal has a strong effect on the equilibrium distribution as a function of temperature. In order to test the hypothesis, data on mercury speciation in flue gas and on coal chlorine content are needed.

Data available from the literature on pilot and full scale mercury speciation measurement were assembled [12–17]. These data were measured at the inlet to the particulate collection device with either EPA Method 29 [12–16] or the Ontario Hydro method [17] used to measure mercury speciation. The mercury speciation results are compared with equilibrium predictions in Fig. 4. The percentage of mercury as gaseous Hg^{+2} is plotted as a function of coal chlorine content. The lines indicate hypothetical temperatures at which the equilibrium is frozen. Considerable scatter is seen in the data over a range of frozen equilibrium temperatures. However, the mercury speciation data were obtained using both EPA Method 29 and the newer Ontario Hydro method. The former method may overestimate the amount of Hg^{+2} by as much as 10% to 30% [18]. Such a correction to the Method 29 data would bring them closer to the Ontario Hydro data. The data are consistent with a cut-off temperature for mercury oxidation in the range of 800 to 850 K (980°F to 1070°F). Further work will be required to gather field data that provides a validation of this hypothesis.

In summary, equilibrium predicts complete oxidation of elemental mercury to HgCl_2 in coal-fired combustion flue gas at temperatures below about 725 K. The chlorine content of the coal determines the temperature below which HgCl_2 is thermodynamically stable.

Measurements in full scale combustion systems (circa 400 K) do not show complete oxidation of elemental mercury as predicted by equilibrium. We conclude that the

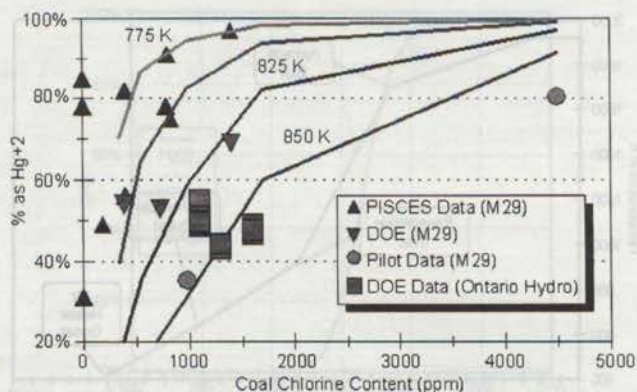


Fig. 4. Fraction of mercury as oxidized in flue gas at APCD inlet conditions as a function of coal chlorine content, comparison of field and pilot data with frozen equilibrium hypothesis.

assumption of equilibrium for mercury species in coal combustion flue gas is not valid. Consideration of a limited set of mercury speciation measurements indicates that mercury equilibrium in the flue gas is frozen at approximately 800 K.

3. Kinetics

Comparison of equilibrium calculations in the mercury system with field measurements strongly implicates kinetic limitations associated with the oxidation of elemental mercury. While little fundamental information on the rates of such oxidation reactions exists for mercury concentrations typical of coal combustion flue gas, some information can be obtained from global reaction rate studies conducted under waste incineration conditions. Hall et al. [19] examined the potential homogeneous gas phase reactions of mercury with Cl_2 , HCl , O_2 , NH_3 , NO , NO_2 , SO_2 , and H_2S at atmospheric pressure and temperatures ranging from ambient to 900°C . Reactions of elemental mercury (Hg^0) were evaluated through measurement of total gaseous Hg and Hg^0 in experiments conducted under both isothermal and decreasing temperature conditions. Reactions with HCl occurred rapidly at temperatures ranging from 500°C to 900°C , with approximately 90% reaction noted in 0.7 s in isothermal measurements at the highest temperature. Reactions with Cl_2 were also rapid, with 70% conversion occurring in 1.1 s at 500°C . Similarly, Gaspar et al. [20] examined the reaction of Hg^0 in simulated incinerator flue gas at temperatures of 400°C to 900°C and concluded that the process was kinetically limited.

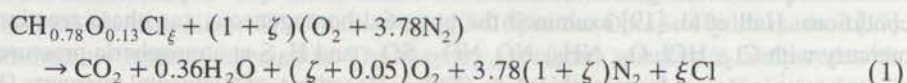
Other components of combustion flue gas also influence mercury oxidation in a minor way. Nitrogen dioxide has been shown to oxidize elemental mercury in the temperature range of 773 to 973 K (500°C to 700°C) [19,21], but the rates are much lower than those for HCl or Cl_2 . High concentrations (~ 1000 ppm) of NO_2 oxidized only 10% of elemental mercury in simulated flue gas at 613 K [19]. Elemental mercury does not react directly with SO_2 [19], but the presence of SO_2 in the gas reduces the amount of elemental mercury oxidized by HCl [21,22]. The presence of water vapor also was noted to reduce the oxidation of mercury [22].

Chlorine-containing species have been shown to be the most important for oxidation of elemental mercury in flue gas. Other flue gas constituents have relatively minor effects. Understanding the speciation of mercury in full scale combustion systems must therefore take into consideration the kinetics of mercury and chlorine species in flue gas. As a first step, we look at the kinetics of chlorine compounds in flue gas at realistic cooling rates.

3.1. Chlorine kinetics in flue gas

The formation of Cl_2 in the gas phase is thermodynamically favored at low temperatures. For example, the equilibrium calculations carried out in this study on four different coals predicted that 30% to 60% of the chlorine would be present as Cl_2 at 423 K with the balance being HCl . The recent DOE-sponsored field study of emission of HAPs from utility boilers reported molecular chlorine levels of 4%, 5%, and 45% of

total chlorine for the three plants reporting such data [23]. The formation of Cl_2 may be kinetically limited in the rapidly cooling flue gas which might reduce the gas-phase oxidation of elemental mercury relative to the equilibrium value. Kinetic calculations for the C–H–O–N–Cl system were carried out using the SENKIN code developed at the Sandia National Laboratories. This code models the time evolution of a homogeneous reacting gas mixture in an open system with a constant flow rate using the system mass balance, energy balance, and reaction rate expressions as the governing equations. Calculations were then carried out for chlorine transformations under conditions similar to those in a coal-fired boiler by using the CH_3Cl mechanism in the standard CHEMKIN-II code. The CH_3Cl mechanism includes 264 elementary reactions (documented in Ref. [24]). The initial composition was calculated according to the overall combustion reaction:



where ζ is the amount of excess air relative to stoichiometric and ξ is the chlorine content of the coal. The code used in this study assumes constant pressure, but allows the temperature to vary as a function of time. Prior to initiating the temperature-variant kinetic calculations, the system is allowed to react at 1925 K for 0.5 s to generate an equilibrium mixture of species and thus convert most of the chlorine to HCl. We then use either an idealized temperature history from furnace exit to APCD inlet for a coal fired power plant (Fig. 3) corresponding to an average cooling rate of approximately 300 K s^{-1} or a constant cooling rate of 200 or 500 K s^{-1} to examine homogeneous chlorine chemistry. The amount of excess air and the coal chlorine content were varied in the calculations in order to investigate their effects on chlorine speciation in the flue gas.

Fig. 5 shows the percentage of total chlorine calculated to be Cl_2 as a function of time. The initial chlorine content of the coal was assumed to be 2000 ppmw and 25% excess air was assumed for the combustion stoichiometry. It can be seen that Cl_2 is produced only when the temperature falls below 1200 K. At the end condition, 0.7% of the total initial chlorine has been transformed into Cl_2 .

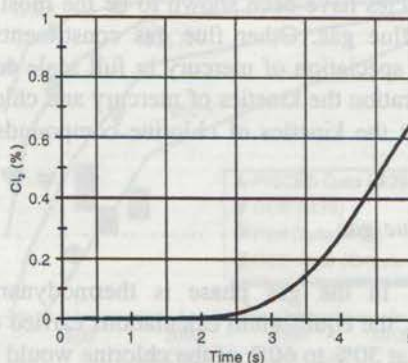


Fig. 5. Percentage of total chlorine in flue gas found as Cl_2 as a function of time assuming 2000 ppm Cl in coal and 25% excess air.

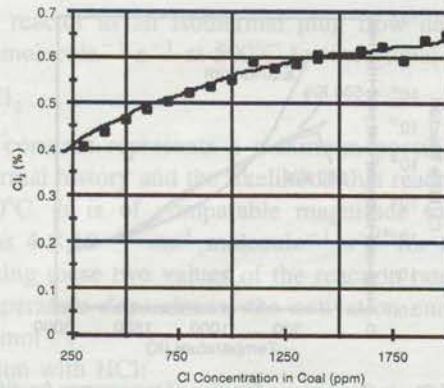


Fig. 6. Final percentage of total chlorine in flue gas found as Cl_2 as a function of chlorine content of coal, assuming 25% excess air.

Fig. 6 shows that as the concentration of chlorine in the coal increases, more is transformed into Cl_2 at the end condition. However, a 10-fold increase in coal chlorine content only increases the amount converted to Cl_2 by a factor of two. This shows that the conversion has a weak dependence on concentration. The effect of changes in excess air is shown in Fig. 7. As the excess air increases, more chlorine will be transformed into Cl_2 , but the increase is very small. At stoichiometric conditions, calculations showed almost no production of Cl_2 . A possible explanation is that the concentration of OH radical is lower for the stoichiometric case. OH is needed to produce significant amounts of atomic Cl, which then forms Cl_2 .

The production of molecular chlorine falls far below equilibrium levels given the high cooling rates in power plant flue gas. This is illustrated in Fig. 8 which compares the concentration of Cl_2 in the flue gas as a function of temperature calculated from reaction kinetics using cooling rates of 200 K s^{-1} and 500 K s^{-1} and from equilibrium.

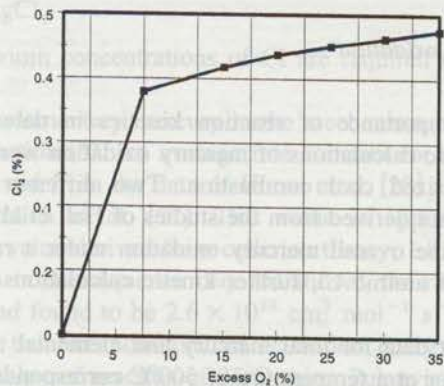


Fig. 7. Final percentage of total chlorine in flue gas found as Cl_2 as a function of excess air, assuming 500 ppm Cl in coal.

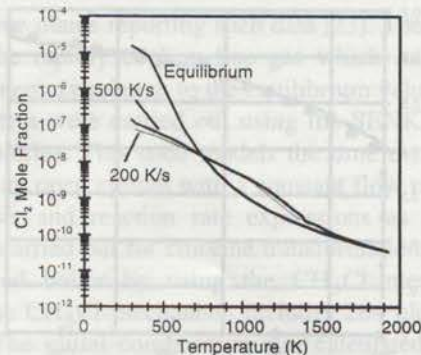


Fig. 8. Concentration of Cl_2 in flue gas as a function of temperature for different cooling rates.

Between 1400 and 750 K, the kinetically calculated concentration of Cl_2 with flue gas cooling is slightly higher than the equilibrium concentration. As the temperature drops below 750 K, the concentration of Cl_2 with flue gas cooling is much lower than the equilibrium value. A more detailed examination of the kinetic mechanism shows the three body reaction:



to be the pathway for production of Cl_2 . For the high cooling rates of practical combustion systems, this reaction is not fast enough at temperatures below 750 K to produce much molecular chlorine. The kinetic model thus predicts super-equilibrium concentrations of the chlorine radical at temperatures below 1500 K.

These calculations show that the conversion of HCl to Cl_2 in the flue gas of a coal-fired power plant is kinetically limited. At flame temperatures, chlorine is predicted to be HCl. At APCD inlet temperatures, equilibrium predicts as much as half of the chlorine to be in the form of Cl_2 , but kinetic calculations show that less than 1% of the chlorine is converted to Cl_2 .

3.2. Kinetics of mercury oxidation

To investigate the importance of reaction kinetics in determining the extent of mercury oxidation, kinetic calculations of mercury oxidation were conducted for conditions relevant to pulverized coal combustion. Two different kinetic models were considered. Global kinetics derived from the studies of Hall et al. [19] and Gaspar et al. [20] were used to examine overall mercury oxidation under a range of conditions. To assess the importance of atomic Cl, further kinetic calculations were conducted using elementary reactions.

Hall et al. [19] report data for total mercury and elemental mercury concentrations obtained in a flow reactor at a temperature of 500°C corresponding to a residence time of approximately 1.5 s. Upstream of the sampling point, temperatures are greater than 600°C [25], but peak temperatures and temperature profiles are not provided by the

authors. Modeling the reactor as an isothermal plug flow device, a rate constant of $k = 1.07 \times 10^{-15} \text{ cm}^3 \text{ molecule}^{-1} \text{ s}^{-1}$ at 500°C for the global reaction:



is obtained. This rate constant represents a maximum possible value because of the uncertainties in gas thermal history and the likelihood that reaction occurred at temperatures greater than 500°C. It is of comparable magnitude to the value reported by Schroeder et al. [26] as $4 \times 10^{-16} \text{ cm}^3 \text{ molecule}^{-1} \text{ s}^{-1}$ for the same reaction under ambient conditions. Using these two values of the reaction rate constant and assuming an Arrhenius-type temperature dependence, the activation energy for this reaction is estimated to be 3.7 kJ mol^{-1} .

For the global reaction with HCl:



Gaspar et al. [20] report a rate constant of $k = 2.20 \times 10^7 \exp(-3460/T) \text{ l mol}^{-1} \text{ s}^{-1}$ over the temperature range 400°C to 900°C. This latter rate constant was derived from experiments conducted at HCl concentrations of 300 and 3000 ppmv, mercury concentrations of 0.37 ppmv (approximately 10 to 20 times greater than typical values associated with pulverized coal combustion), and approximate residence times of 1 s.

In considering the global reactions of Hg with Cl_2 and HCl (Eqs. (3) and (4)), we ran both “reactions” simultaneously. The reason for doing this was that the rates were derived from studies in which only Cl_2 or HCl was injected, and thus represent reactions derived from those species alone. Since we believe Cl atom is responsible at the elementary level, this choice (considering both “reactions” simultaneously) ignores interplay between Cl derived from Cl_2 and HCl, and could thus be considered a maximum rate of conversion.

Studies of the mechanism of mercury oxidation at temperatures of 600°C and above by Kramlich et al. [27] suggest that the key oxidizing species is atomic Cl. Kramlich et al. propose a homogeneous pathway, governed by two principal steps:



Note that super-equilibrium concentrations of Cl are required to account for observed HgCl_2 concentrations.

The consumption of elementary mercury in the mechanism proposed by Kramlich et al. [27] proceeds by reaction (5). An average rate constant for this reaction, $1.5 \times 10^{13} \text{ cm}^3 \text{ mol}^{-1} \text{ s}^{-1}$, is derived from the data of Horne et al. [28] and is equal to the value recommended by Kramlich et al. [27]. This value is approximately one order of magnitude less than the value derived from collision theory, $1.8 \times 10^{14} \text{ cm}^3 \text{ mol}^{-1} \text{ s}^{-1}$. For the second reaction in the sequence (Eq. (6) above), the rate constant was derived from collision theory and found to be $2.6 \times 10^{14} \text{ cm}^3 \text{ mol}^{-1} \text{ s}^{-1}$ at 2000 K. Assuming an Arrhenius form for the rate constant, an activation energy of 15 kJ mol^{-1} was estimated from the enthalpy of reaction at 25°C using Polanyi–Semenov methods. The pre-exponential factor was set equal to the value of the collision limited rate constant at 2000 K since at this temperature the exponential term approaches unity.

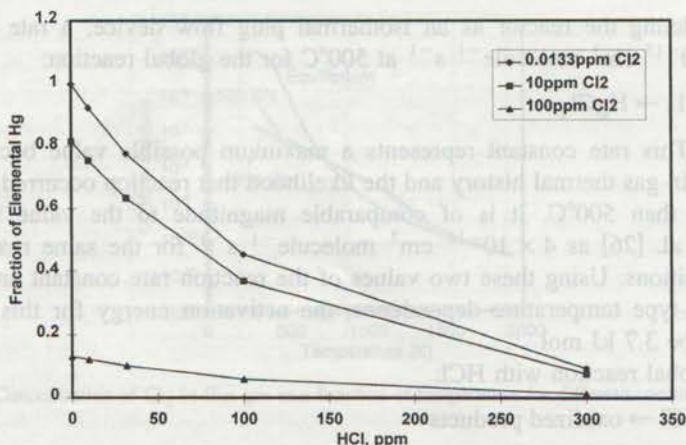


Fig. 9. Hg conversion as a function of HCl concentration at 773 K using global kinetics.

We considered the reverse of reaction (5) in the two-step elementary reaction sequence as well. The reverse rate constant was derived from the equilibrium constant using data from HSC and checked by evaluating free energy of formation values in the JANAF tables. No effect on the results was seen by including the reverse reaction. We did not consider the reverse of reaction (6). We assumed that HgCl levels would not build up in the vapor phase, so that the proposed two-step reaction mechanism converts the HgCl at collision-limited rates to HgCl₂.

3.3. Results of mercury kinetic calculations

Mercury consumption rates were derived from kinetic calculations conducted using the global reaction sequence (both Eqs. (3) and (4)) and the two primary steps of the mechanistic pathway (Eqs. (5) and (6)). Mercury concentrations of 0.15 ppmw in the

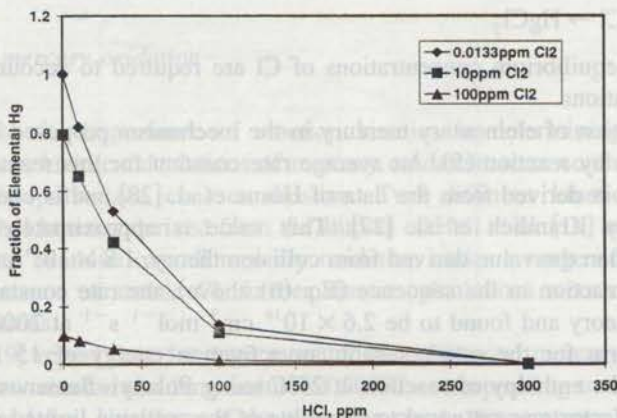


Fig. 10. Hg conversion as a function of HCl concentration at 973 K using global kinetics.

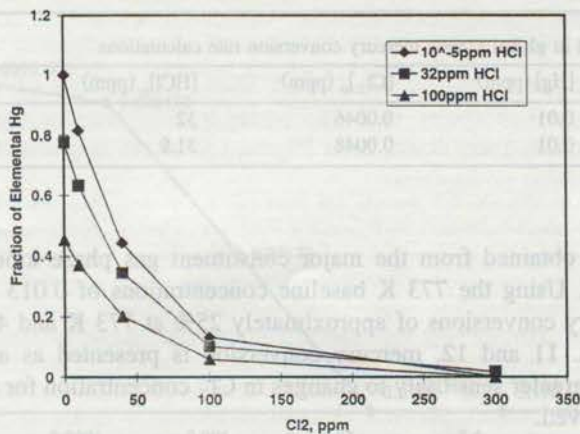


Fig. 11. Hg conversion as a function of Cl₂ concentration at 773 K using global kinetics.

coal, corresponding to 0.01 ppmv in the flue gas, were used. Concentrations of the oxidants HCl, Cl₂, and Cl were taken from the combustion gas kinetic calculations described above. Reactions were examined at the isothermal conditions of 773 and 973 K as well as under cooling rates of 200 and 500 K s⁻¹, in each case starting from a peak temperature of approximately 973 K. Note that the starting temperature of 973 K is outside of the 300–773 K range used to derive the rate constant for the global reaction involving molecular chlorine (Eq. (3)). We are therefore assuming that the moderate temperature dependence of this reaction rate remains unchanged between 773 and 973 K, an assumption necessitated by a lack of high temperature rate data.

In Figs. 9 and 10, mercury conversion under isothermal conditions is presented as a function of HCl concentrations at temperatures of 773 and 973 K, respectively. A residence time of 2 s was used in these calculations. Baseline Cl₂ and HCl concentra-

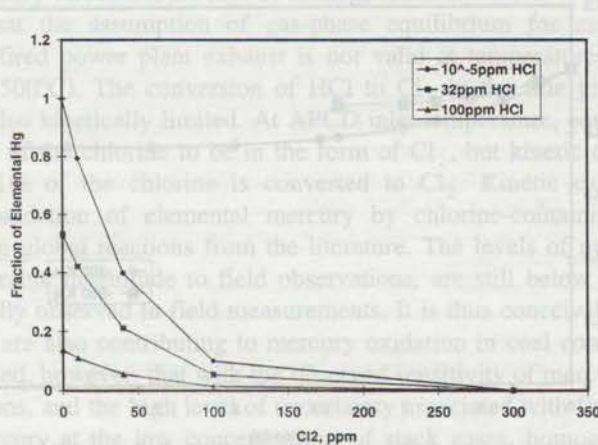


Fig. 12. Hg conversion as a function of Cl₂ concentration at 973 K using global kinetics.

Table 2
Initial conditions used in global kinetic mercury conversion rate calculations

dT/dt	[Hg] (ppm)	$[Cl_2]_0$ (ppm)	$[HCl]_0$ (ppm)	T range (K)
-200 K s^{-1}	0.01	0.0046	32	962.6–300
-500 K s^{-1}	0.01	0.0048	31.9	971.4–300

tions were those obtained from the major constituent gas phase kinetic simulation at each temperature. Using the 773 K baseline concentrations of 0.013 ppm Cl_2 and 32 ppm HCl, mercury conversions of approximately 25% at 773 K and 45% at 973 K are obtained. In Figs. 11 and 12, mercury conversion is presented as a function of Cl_2 concentration. A greater sensitivity to changes in Cl_2 concentration for the global kinetic sequence is observed.

To investigate mercury oxidation under thermal profiles associated with coal combustion, calculations using the combined global reactions were also conducted at cooling rates of 200 and 500 $K s^{-1}$. Initial conditions for these calculations are presented in Table 2. As shown in Fig. 13, mercury conversion is higher at the slower cooling rate, a result of increased residence time at higher temperatures. For the cooling rate of -200 K s^{-1} , an overall conversion of 24% is achieved in 2 s. At the higher cooling rate, an asymptotic value of 10.5% conversion is reached in 1 s.

Mercury concentration profiles derived from the elementary reaction sequence (5)–(6) at a temperature of 773 K are presented in Fig. 14. Use of this reaction sequence is seen to result in complete conversion of elemental mercury within 1 s. Order of magnitude reductions in the atomic Cl concentration significantly reduced the conversion, however. Mercury conversions of comparable magnitude to the field data were obtained at atomic Cl concentrations of 0.00173 ppm, 100-fold less than those suggested by the major constituent gas phase reaction chemistry. This suggests that accurate prediction of

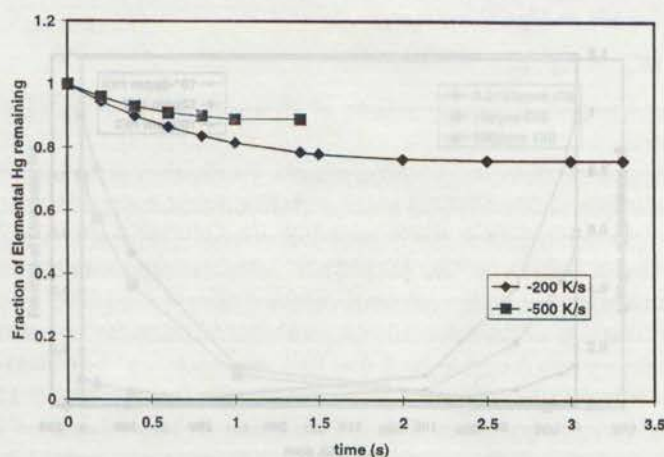


Fig. 13. Hg conversion for two different cooling rates.

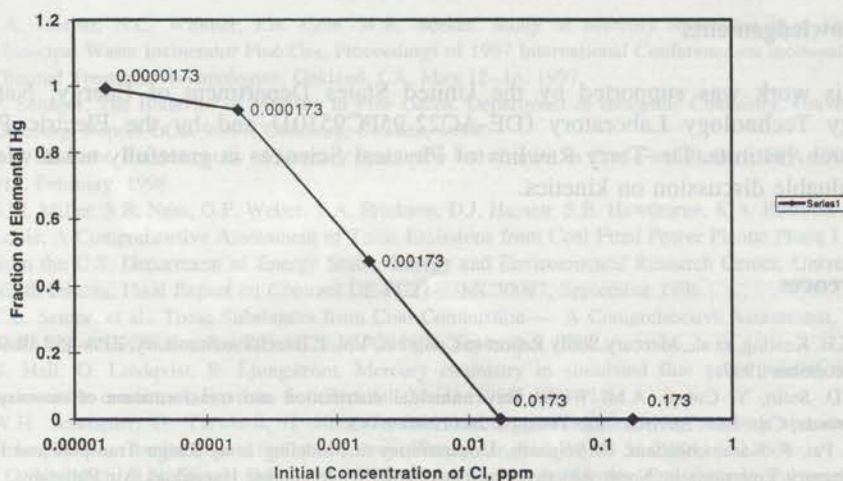


Fig. 14. Hg conversion as a function of Cl atom concentration at 773 K and 1 s residence time.

mercury speciation in coal combustion systems using a mechanistic model will require detailed knowledge of the super-equilibrium chlorine atom concentrations as a function of temperature and cooling rate.

4. Conclusions

Chlorine-containing species have been shown to be the most important for oxidation of elemental mercury in flue gas. Other flue gas constituents (e.g., H_2O , SO_2 , NO_2) may have secondary effects on the rate of homogeneous oxidation of mercury. We have demonstrated that the assumption of gas-phase equilibrium for mercury-containing species in coal-fired power plant exhaust is not valid at temperatures below approximately 800 K (500°C). The conversion of HCl to Cl_2 in the flue gas of a coal-fired power plant is also kinetically limited. At APCD inlet temperature, equilibrium predicts as much as half of the chlorine to be in the form of Cl_2 , but kinetic calculations show that less than 1% of the chlorine is converted to Cl_2 . Kinetic calculations of the homogeneous oxidation of elemental mercury by chlorine-containing species were carried out using global reactions from the literature. The levels of mercury oxidation, while of comparable magnitude to field observations, are still below the 40% to 80% oxidation typically observed in field measurements. It is thus conceivable that heterogeneous reactions are also contributing to mercury oxidation in coal combustion systems. It must be stressed, however, that with the observed sensitivity of mercury conversion to Cl_2 concentrations, and the high level of uncertainty associated with field measurements of oxidized mercury at the low concentrations of stack gases, homogeneous pathways alone may be important.

Acknowledgements

This work was supported by the United States Department of Energy, National Energy Technology Laboratory (DE-AC22-95PC95101) and by the Electric Power Research Institute. Dr. Terry Rawlins of Physical Sciences is gratefully acknowledged for valuable discussion on kinetics.

References

- [1] M.H. Keating, et al., Mercury Study Report to Congress, Vol. I: Executive Summary, EPA-452/R-97-003, December 1997.
- [2] E.D. Stein, Y. Cohen, A.M. Winer, Environmental distribution and transformation of mercury compounds, *Crit. Rev. Environ. Sci. Technol.* 26 (1996) 1–43.
- [3] P. Pai, P. Karamchandani, C. Seigneur, Uncertainties in Modeling Long-Range Transport and Fate of Mercury Emissions in North America, presented at EPRI Managing Hazardous Air Pollutants, Fourth International Conference, Washington, DC, November 12–14, 1997.
- [4] E.M. Prestbo, N.S. Bloom, Mercury Speciation Adsorption (MESA) method for combustion flue gas: methodology, artifacts, intercomparison, and atmospheric implications, *Water, Air, Soil Pollut.* 80 (1995) 145–158.
- [5] J. Fahlke, A. Bursik, Impact of the state-of-the-art flue gas cleaning on mercury species emissions from coal-fired steam generators, *Water, Air, Soil Pollut.* 80 (1995) 209–215.
- [6] R. Meij, Trace element behavior in coal-fired power plants, *Fuel Process. Technol.* 39 (1994) 199–217.
- [7] F. Fransden, K. Dam-Johansen, P.R. Rasmussen, Trace elements from combustion and gasification of coal: an equilibrium approach, *Prog. Energy Combust. Sci.* 20 (1994) 115–138.
- [8] G. Ericksson, E. Rosen, Thermodynamic studies of high temperature equilibria: VIII. General equations for the calculation of equilibria in multi-phase systems, *Chem. Scr.* 19 (1973) 193–194.
- [9] HSC Chemistry for Windows, Version 3.0, Outokumpo Research Oy, P.O. Box 60, FIN-28101, Pori, Finland.
- [10] R.C. Flagan, J.H. Seinfeld, *Fundamentals of Air Pollution Engineering*, Prentice-Hall, Englewood Cliffs, NJ, 1988, pp. 217–219.
- [11] T.R. Carey, O.W. Hargrove, T.D. Brown, R.G. Rhudy, Enhanced Control of Mercury in Wet FGD Systems, Paper 96-P64B.02, presented at 89th Annual AWMA Meeting, June, 1996, Nashville, TN.
- [12] P.R. Tumati, M.S. DeVito, Partitioning Behavior of Mercury During Coal Combustion, ASME Paper 93-JPGC-EC-8, presented at the Joint ASME/IEEE Power Generation Conference, Kansas City, 1993.
- [13] Radian, A Study of Toxic Emissions from a Coal-Fired Power Plant Utilizing and ESP While Demonstrating the ICCT CT-121 FGD Project, Final Report on Contract DE-AC22-93PC93253, 1994.
- [14] Southern Research Institute, Characterizing Toxic Emissions from a Coal-Fired Power Plant Demonstrating the AFGD ICCT Project and a Plant Utilizing a Dry Scrubber/Baghouse System, Final Report on Contract DE-AC22-93PC93254, 1994.
- [15] Roy F. Weston, Toxic Assessment Report Illinois Power Company Baldwin Power Station, Unit 2, Final Report on Contract DE-AC22-93PC93255, 1994.
- [16] Electric Power Research Institute, Electric Utility Trace Substances Synthesis Report, Report No. EPRI TR-104614, Project 3081, 1994.
- [17] M.S. DeVito, W.A. Rosenhoover, Flue Gas Mercury and Speciation Studies at Coal-Fired Utilities Equipped with Wet Scrubbers, presented at 15th International Pittsburgh Coal Conference, Pittsburgh, PA, September 15–17, 1998.
- [18] C.J. Zygarlicke, J.H. Pavlish, Partitioning of Trace Element Species in Coal Combustion Systems and Impacts on Control, presented at 22nd International Technical Conference on Coal Utilization and Fuel Systems, Clearwater, FL, March 16–19, 1997.
- [19] B. Hall, P. Schager, O. Lindqvist, Chemical reactions of mercury on combustion flue gases, *Water, Air, Soil Pollut.* 56 (1991) 3–14.

- [20] J.A. Gaspar, N.C. Widmer, J.A. Cole, W.R. Seeker, Study of Mercury Speciation in a Simulated Municipal Waste Incinerator Flue Gas, Proceedings of 1997 International Conference on Incineration and Thermal Treatment Technologies, Oakland, CA, May 12–16, 1997.
- [21] P. Schager, The Behavior of Mercury in Flue Gases, Department of Inorganic Chemistry, University of Göteborg, Report OOK 90:07, Göteborg, Sweden, 1990.
- [22] S.B. Ghorishi, Fundamentals of Mercury Speciation and Control in Coal-Fired Boilers, EPA-600/R-98-014, February, 1998.
- [23] S.M. Miller, S.R. Ness, G.F. Weber, T.A. Erickson, D.J. Hassett, S.B. Hawthorne, K.A. Katrinak, P.K.K. Louie, A Comprehensive Assessment of Toxic Emissions from Coal-Fired Power Plants: Phase I Results from the U.S. Department of Energy Study, Energy and Environmental Research Center, University of North Dakota, Final Report on Contract DE-FC21-93MC30097, September 1996.
- [24] C.L. Senior, et al., Toxic Substances from Coal Combustion — A Comprehensive Assessment, Phase I Final Report, DOE Contract DE-AC22-95PC95101, September 1997.
- [25] B. Hall, O. Lindqvist, E. Ljungstrom, Mercury chemistry in simulated flue gases related to waste incineration conditions, Environ. Sci. Technol. 24 (1) (1990) 108–111.
- [26] W.H. Schroeder, G. Yarwood, H. Niki, Transformation processes involving mercury species in the atmosphere — results from a literature survey, Water, Air, Soil Pollut. 56 (1991) 653–666.
- [27] J.C. Kramlich, R.N. Sliger, D.J. Going, Reduction of Inherent Mercury Emissions in Pulverized Coal Combustion, DOE Grant DE-FG22-95PC95216, presentation at DOE University Coal Research Contractor's Meeting, Pittsburgh, June 1997.
- [28] D.G. Horne, R. Gosavi, O.P. Strausz, Reactions of metal atoms: I. The combination of mercury and chlorine atoms and the dimerization of HgCl, J. Chem. Phys. 48 (10) (1968) 4758–4764.

Massachusetts Institute of Technology, Cambridge, MA 02139, USA

University of Kentucky, Lexington, KY 40546, USA

US Geological Survey, Reston, VA 20192, USA

Received 9 March 1999; received in revised form 18 September 1999; accepted 20 September 1999

Abstract

Trace elements in coal have diverse modes of occurrence that will greatly influence their behavior in many coal utilization processes. Mode of occurrence is important in determining the partitioning during coal cleaning by conventional processes, the susceptibility to oxidation upon exposure to air, as well as the changes in physical properties upon heating. In this study, three complementary methods were used to determine the concentrations and chemical states of trace elements in pulverized samples of four US coals: Pittsburgh, Wilcox No. 6, Silvertown and Harlow, and Wyodak coals. Neutron Activation Analysis (NAA) was used to measure the absolute concentration of elements in the parent coals and in the size- and density-fractionated samples. Chemical leaching and X-ray absorption fine structure (XAFS) spectroscopy were used to provide information on the form of occurrence of an element in the parent coals. The composition differences between size-segregated coal samples of different density mainly reflect the large density difference between minerals, especially pyrite, and the organic portion of the coal. The heavy density fractions are therefore enriched in pyrite and the elements associated with pyrite, as also shown by the leaching and XAFS methods. Nearly all the As is associated with pyrite in the

Corresponding author. Fax: +1 925 897 3312; e-mail: senior@pkeywp.com

Present address: Department of Mechanical Engineering, UCLA, Los Angeles, CA

Present address: Department of Chemical Engineering, University of Utah, Salt Lake City, UT

EXHIBIT D

Radisav, Vidic 5/20/25

VOLS. 65-66
Completing vols. 65-66

JUNE 2000

ISSN 0378-3820



Fuel Processing Technology

Special Issue

Air Quality:
Mercury, Trace Elements
and Particulate Matter



www.elsevier.com/locate/fuproc

Radisav, Vidic 5/20/25

UNIVERSITY OF PITTSBURGH

JUN 23 2000

BEVIER ENGINEERING LIBRARY

FUEL PROCESSING TECHNOLOGY

FUEL PROCESSING TECHNOLOGY

An international journal devoted to the processing and beneficiation of coal, petroleum, oil shale, tar sands and peat

An international journal devoted to all aspects of processing and beneficiation of coal, petroleum, oil shale, tar sands and peat

Volumes 65-66 (2000)

Editor

David P. Huffman,
Lexington, KY, USA

Regional Editor for Europe

A. M. Mahto,
Zagreb, Croatia

Regional Editor for the Far East

Peng Chen,
Beijing, P.R. China

Honorary Editor

Larry L. Anderson,
St. George, UT, USA

Editorial Board

S.A. Benson, Grand Forks, ND, USA

J.C. Grigg, Cambridge, U.K., USA

E. Ersoz, Istanbul, Turkey

R.A. Gatz, New York, NY, USA

W.R. Jackson, Darwin, VIC, Australia

Z. Jin, Beijing, P.R. China

J.A. Karim, Karamona, Nepal

B. Li, Tianjin, P.R. China

R. Maruszewski, Des Plaines, IL, USA

A. Marzec, Gliwice, Poland

T.C. Min, Ann Arbor, MI, USA

Y. Niizuma, Osaka, Japan

M. Nomura, Osaka, Japan

Y. Sano, Tokushima, Japan

H.H. Schenck, University Park, PA, USA

H. Schulz, Karlsruhe, Germany

A. Tamura, Sendai, Japan

I. Wender, Pittsburgh, PA, USA

W.H. White, Salt Lake City, UT, USA

K.-C. Yu, Taiyuan, P.R. China

Y. Yilmaz, Ankara, Turkey

Volumes 65-66 (2000)



ELSEVIER

Amsterdam - Lausanne - New York - Oxford - Sharjah - Tokyo



ELSEVIER

Fuel Processing Technology 65–66 (2000) 289–310

FUEL
PROCESSING
TECHNOLOGY

www.elsevier.com/locate/fuproc

Mercury transformations in coal combustion flue gas

Kevin C. Galbreath^{*}, Christopher J. Zygarlicke

Energy and Environmental Research Center, University of North Dakota, Grand Forks, ND 58202-9018, USA

Received 12 February 1999; accepted 12 May 1999

Abstract

Mercury chlorination [i.e., formation of $\text{HgCl}_2(\text{g})$] is generally assumed to be the dominant mercury-transformation mechanism in coal combustion flue gas. Other potential mechanisms involve mercury interactions with ash particle surfaces where reactive chemical species, oxidation catalysts, and active sorption sites are available to transform $\text{Hg}^0(\text{g})$ to $\text{Hg}^{2+}\text{X}(\text{g})$ (e.g., where X is Cl_2 or O) as well as $\text{Hg}^0(\text{g})$ and $\text{HgCl}_2(\text{g})$ to particulate mercury, $\text{Hg}(\text{p})$. Results from an investigation of $\text{Hg}^0(\text{g})\text{-O}_2(\text{g})\text{-HCl}(\text{g})$ and $\text{Hg}^{0,2+}(\text{g})\text{-HCl}(\text{g})\text{-CaO}(\text{s})\text{-fly ash}$ interactions in a 42-MJ/h combustion system are consistent with the following mechanisms: mercury chlorination, catalysis of mercury oxidation by $\text{Al}_2\text{O}_3(\text{s})$ and/or $\text{TiO}_2(\text{s})$, and mercury sorption on a calcium-rich (25.0 wt.% CaO) subbituminous coal fly ash. Additions of 50 and 100 ppmv of $\text{HCl}(\text{g})$ and ≈ 12.6 wt.% of $\text{CaO}(\text{s})$ to the subbituminous coal combustion environment inhibited $\text{Hg}(\text{p})$ formation, primarily via a change in ash surface chemistry and a decrease in particle surface area, respectively. © 2000 Elsevier Science B.V. All rights reserved.

Keywords: Mercury; Speciation; Transformations; Air toxics; Hazardous air pollutants; Coal; Combustion

1. Introduction

According to the Mercury Study Report to Congress, coal combustion is the primary source of anthropogenic mercury emissions in the United States, accounting for 72 of the 158 tons/yr of total point-source mercury emissions [1]. Knowledge of mercury physical and chemical transformations in coal combustion flue gas is imperative for understanding the transport and fate of mercury released into air pollution control

^{*} Corresponding author. Tel.: +1-701-777-5127; fax: +1-701-777-5181; e-mail: kgalbreath@eerc.und.nodak.edu

systems and the atmosphere. The current knowledge of mercury transformations in coal combustion flue gas is based largely on thermodynamic modeling and experimental investigations of mercury reactions in simulated flue gases and, to a limited extent, on the interpretations of field test data [2,3]. Mercury exists primarily as gaseous (g) elemental mercury, $\text{Hg}^0(\text{g})$, and as gaseous or solid (s) inorganic mercuric compounds, Hg^{2+}X [e.g., where X is $\text{Cl}_2(\text{g})$, $\text{SO}_4(\text{s})$, $\text{O}(\text{s,g})$, $\text{S}(\text{s})$], in coal combustion flue gas. Mercury emissions from coal-fired boilers can be empirically classified, based on the capabilities of currently available analytical methods for determining mercury speciation, into three main forms: $\text{Hg}^0(\text{g})$, $\text{Hg}^{2+}\text{X}(\text{g})$, and particulate mercury, $\text{Hg}(\text{p})$. Mercury concentrations in coal combustion flue gas generally range from 5 to 10 $\mu\text{g}/\text{m}^3$, with a large range in the relative proportions of $\text{Hg}^0(\text{g})$, $\text{Hg}^{2+}\text{X}(\text{g})$, and $\text{Hg}(\text{p})$.

During combustion, $\text{Hg}^0(\text{g})$ is liberated from coal. A significant fraction of the $\text{Hg}^0(\text{g})$, however, is generally transformed to $\text{Hg}^{2+}\text{X}(\text{g})$ and $\text{Hg}(\text{p})$ in the postcombustion environment of a coal-fired boiler. $\text{Hg}^0(\text{g})$ is the most abundant and persistent (residence time of 0.5 to 2 years) form of mercury in the atmosphere [4–7]. Relative to $\text{Hg}^0(\text{g})$, $\text{Hg}^{2+}\text{X}(\text{g})$ and $\text{Hg}(\text{p})$ are more effectively captured in conventional pollution control systems (wet scrubbers and fabric filters) and are more apt to deposit locally or regionally [2,6,8,9]. Mercury emission control efficiencies and transport/deposition models for coal-fired boilers can be improved by identifying the fundamental mechanisms involved in mercury–flue gas interactions that transform $\text{Hg}^0(\text{g})$ to $\text{Hg}^{2+}\text{X}(\text{g})$ and $\text{Hg}(\text{p})$.

Mercury interactions with inorganic and carbonaceous ash particles entrained in coal combustion flue gas (i.e., fly ash), especially at the gas–particulate surface interface, are important to consider in understanding mercury transformations. Reactive chemical species and oxidation catalysts on fly ash particles can convert $\text{Hg}^0(\text{g})$ to $\text{Hg}^{2+}\text{X}(\text{g})$. Fly ash particle surfaces may also host active sites for mercury adsorption. Measurements by Otani et al. [10], Schager et al. [11], Hall et al. [12], and Carey et al. [13] indicate that some fly ashes actually adsorb mercury at rates greater than various sorbents, including activated carbon. Brown [14] reviewed mercury speciation analysis results and identified several coals that produce significant concentrations of $\text{Hg}^{2+}\text{X}(\text{g})$ and/or $\text{Hg}(\text{p})$ in the postcombustion environment of pilot- and full-scale utility boilers. Apparently the flue gases and/or fly ashes produced from certain coals possess intrinsic properties that promote mercury oxidation and/or mercury–ash sorption. Mercury sorption by fly ash can occur via physical adsorption, chemisorption, chemical reaction, or a combination of these processes. Although it is well established that fly ash particles capture mercury species, the nature of mercury–fly ash interactions is not well understood.

In this paper, information that pertains primarily to mercury–fly ash interactions is reviewed to identify the fundamental mechanisms involved in mercury combustion transformations. This review supplements those by Galbreath and Zygarlicke [2] and Laudal et al. [Section 2 in Ref. [3]] that focus on potential interactions between mercury species and gaseous flue gas components. Results from an on-going investigation of mercury transformations using a laboratory-scale (42-MJ/h) combustion system are also presented. Preliminary observations and conclusions from this investigation corroborate the importance of particulate–surface interactions in controlling high-temperature ($\geq 250^\circ\text{C}$) mercury transformations.

2. Overview of mercury coal combustion transformations

Plausible physical and chemical transformations that mercury undergoes during coal combustion and subsequently in the resulting flue gas are summarized in Fig. 1. Mercury is associated primarily with the inorganic mineral components of coal, although an association with the organic maceral components of coal as organomercuric compounds has been suggested [15–17]. Mercury is classified geochemically as a chalcophile element [18]. Accordingly, pyrite (FeS_2) and cinnabar (HgS) are the dominant mineral hosts for mercury in coal. As the mineral and possibly organomercuric hosts of mercury decompose during combustion ($> 1400^\circ\text{C}$), mercury is liberated as $\text{Hg}^0(\text{g})$ (boiling point of 357°C at 1 atm, vapor pressure of 0.180 Pa at 20°C). In contrast to the nonvolatile and semivolatile trace elements in coal, the mode of occurrence of mercury (i.e., mineral or maceral association) does not affect this initial combustion transformation mechanism.

In the chemically complex postcombustion environment and with decreasing temperature, $\text{Hg}^0(\text{g})$ may remain as a monatomic species or react to form inorganic mercurous (Hg_2^{2+}) and Hg^{2+} compounds. The principal oxidized forms of mercury in coal combustion flue gas are assumed to be Hg^{2+} compounds because of the instability of Hg_2^{2+} compounds at low concentrations (i.e., in dilute solutions) [19]. Mercury chlorination, the reaction of $\text{Hg}^0(\text{g})$ with $\text{HCl}(\text{g})$ or $\text{Cl}_2(\text{g})$ to form $\text{HgCl}_2(\text{g})$, is generally

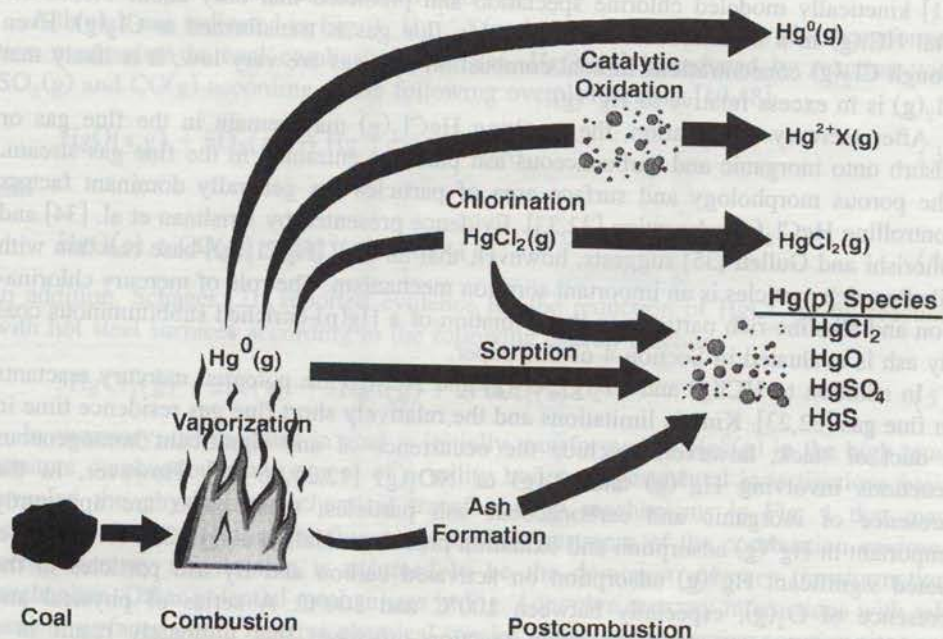


Fig. 1. Potential mercury transformations during coal combustion and subsequently in the resulting flue gas.

e. The current knowledge of mercury transformations in coal is based largely on thermodynamic modeling and experimental reactions in simulated flue gases and, to a limited extent, on test data [2,3]. Mercury exists primarily as gaseous (g), and as gaseous or solid (s) inorganic mercuric compounds, $\text{Cl}_2(\text{g})$, $\text{SO}_4(\text{s})$, $\text{O}(\text{s,g})$, $\text{S}(\text{s})$, in coal combustion flue gas. Coal-fired boilers can be empirically classified, based on the available analytical methods for determining mercury species: $\text{Hg}^0(\text{g})$, $\text{Hg}^{2+}\text{X}(\text{g})$, and particulate mercury, $\text{Hg}(\text{p})$. Mercury concentrations in coal combustion flue gas generally range from 5 to 10 $\mu\text{g}/\text{m}^3$ in the relative proportions of $\text{Hg}^0(\text{g})$, $\text{Hg}^{2+}\text{X}(\text{g})$, and $\text{Hg}(\text{p})$. $\text{Hg}^0(\text{g})$ is liberated from coal. A significant fraction of the $\text{Hg}^0(\text{g})$ is transformed to $\text{Hg}^{2+}\text{X}(\text{g})$ and $\text{Hg}(\text{p})$ in the postcombustion environment. $\text{Hg}^0(\text{g})$ is the most abundant and persistent form of mercury in the atmosphere [4-7]. Relative to $\text{Hg}(\text{p})$ are more effectively captured in conventional pollution control devices (scrubbers and fabric filters) and are more apt to deposit locally or regionally. Mercury emission control efficiencies and transport/deposition characteristics can be improved by identifying the fundamental mechanisms of mercury-flue gas interactions that transform $\text{Hg}^0(\text{g})$ to $\text{Hg}^{2+}\text{X}(\text{g})$ and $\text{Hg}(\text{p})$.

Inorganic and carbonaceous ash particles entrained in coal combustion flue gas, especially at the gas-particulate surface interface, are important in understanding mercury transformations. Reactive chemical species on fly ash particles can convert $\text{Hg}^0(\text{g})$ to $\text{Hg}^{2+}\text{X}(\text{g})$. Fly ash particles also host active sites for mercury adsorption. Measurements by Carey et al. [11], Hall et al. [12], and Carey et al. [13] indicate that fly ash can capture mercury at rates greater than various sorbents, including activated carbon. A reviewed mercury speciation analysis results and identified significant concentrations of $\text{Hg}^{2+}\text{X}(\text{g})$ and/or $\text{Hg}(\text{p})$ in the flue gas from pilot- and full-scale utility boilers. Apparently the flue gas from certain coals possess intrinsic properties that enhance mercury sorption and/or mercury-ash sorption. Mercury sorption by fly ash particles, chemisorption, chemical reaction, or a combination of these processes is well established that fly ash particles capture mercury from the flue gas. Mercury-flue gas interactions is not well understood.

One of the primary mechanisms that pertains primarily to mercury-fly ash interactions is the chemical reaction. Fundamental mechanisms involved in mercury combustion transformations are supplemented by Galbreath and Zygarlicke [2] and Carey et al. [3] that focus on potential interactions between mercury and fly ash components. Results from an on-going investigation of mercury transformations in a laboratory-scale (42-MJ/h) combustion system are also presented. Conclusions from this investigation corroborate the importance of surface interactions in controlling high-temperature (> 1000°C) mercury transformations.

2. Overview of mercury coal combustion transformations

Plausible physical and chemical transformations that mercury undergoes during coal combustion and subsequently in the resulting flue gas are summarized in Fig. 1. Mercury is associated primarily with the inorganic mineral components of coal, although an association with the organic maceral components of coal as organomercuric compounds has been suggested [15-17]. Mercury is classified geochemically as a chalcophile element [18]. Accordingly, pyrite (FeS_2) and cinnabar (HgS) are the dominant mineral hosts for mercury in coal. As the mineral and possibly organomercuric hosts of mercury decompose during combustion (> 1400°C), mercury is liberated as $\text{Hg}^0(\text{g})$ (boiling point of 357°C at 1 atm, vapor pressure of 0.180 Pa at 20°C). In contrast to the nonvolatile and semivolatile trace elements in coal, the mode of occurrence of mercury (i.e., mineral or maceral association) does not affect this initial combustion transformation mechanism.

In the chemically complex postcombustion environment and with decreasing temperature, $\text{Hg}^0(\text{g})$ may remain as a monatomic species or react to form inorganic mercurous (Hg_2^{2+}) and Hg^{2+} compounds. The principal oxidized forms of mercury in coal combustion flue gas are assumed to be Hg^{2+} compounds because of the instability of Hg_2^{2+} compounds at low concentrations (i.e., in dilute solutions) [19]. Mercury chlorination, the reaction of $\text{Hg}^0(\text{g})$ with $\text{HCl}(\text{g})$ or $\text{Cl}_2(\text{g})$ to form $\text{HgCl}_2(\text{g})$, is generally

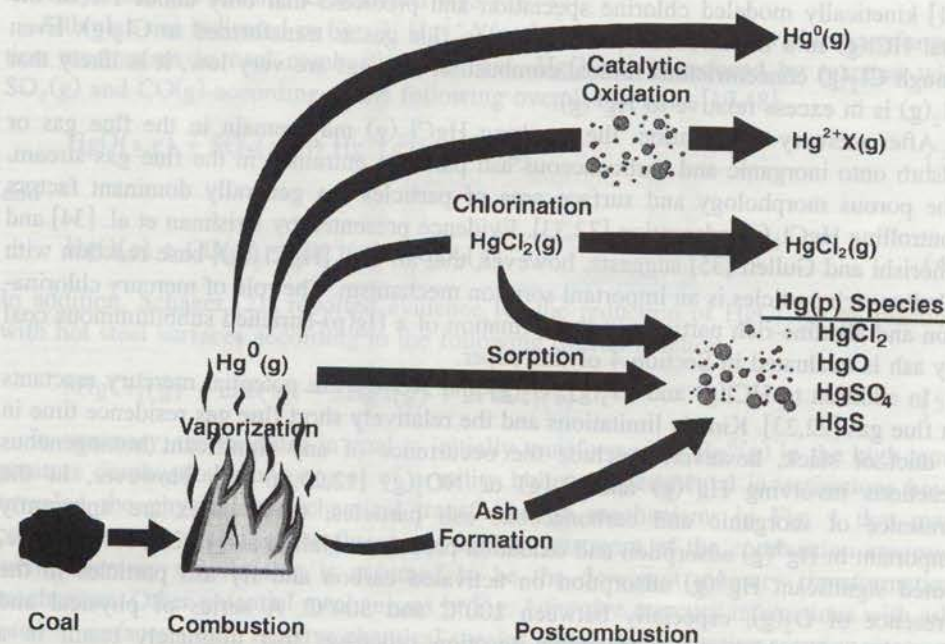
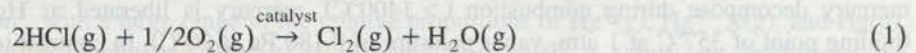
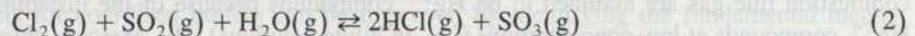


Fig. 1. Potential mercury transformations during coal combustion and subsequently in the resulting flue gas.

considered to be the dominant mercury transformation mechanism in coal combustion flue gas, even though $\text{HgCl}_2(\text{g})$ has never been directly measured. $\text{HCl}(\text{g})$ concentrations in coal combustion flue gas range from about 25 to 150 mg/m^3 [20]. Theoretical and experimental investigations indicate that although $\text{HCl}(\text{g})$ will react with $\text{Hg}^0(\text{g})$, $\text{Cl}_2(\text{g})$ is a much more active mercury-chlorinating agent [21–25]. Consequently, chlorine speciation is an important factor to consider in understanding flue gas mercury transformations. Chlorine is evolved from coal during combustion primarily as $\text{HCl}(\text{g})$ [26]. In the postcombustion environment, $\text{Cl}_2(\text{g})$ is presumably formed according to the following Deacon process reaction [27]:



Although the Deacon reaction is thermodynamically favorable at relatively low temperatures (430–475°C), it proceeds only in the presence of metal catalyst species [28]. Experimental investigations indicate that the presence of $\text{SO}_2(\text{g})$ in combustion flue gas can inhibit the formation of chlorinated compounds by depleting $\text{Cl}_2(\text{g})$ concentrations according to the following net overall reaction:



or by reducing the catalytic activity of fly ash [29,30]. Consequently, a high sulfur–chlorine ratio inhibits the formation of $\text{Cl}_2(\text{g})$ and subsequently of $\text{HgCl}_2(\text{g})$. Realizing that the formation of $\text{Cl}_2(\text{g})$ is not governed by thermochemical equilibrium, Senior et al. [31] kinetically modeled chlorine speciation and predicted that only about 1% of the total $\text{HCl}(\text{g})$ in a bituminous coal combustion flue gas is transformed to $\text{Cl}_2(\text{g})$. Even though $\text{Cl}_2(\text{g})$ concentrations in coal combustion flue gas are very low, it is likely that $\text{Cl}_2(\text{g})$ is in excess relative to $\text{Hg}^0(\text{g})$.

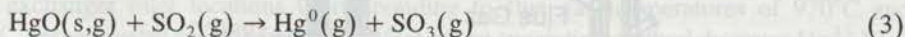
After mercury chlorination, the resulting $\text{HgCl}_2(\text{g})$ may remain in the flue gas or adsorb onto inorganic and carbonaceous ash particles entrained in the flue gas stream. The porous morphology and surface area of particles are generally dominant factors controlling $\text{HgCl}_2(\text{g})$ adsorption [32,33]. Evidence presented by Krishnan et al. [34] and Ghorishi and Gullett [35] suggests, however, that an acid [$\text{HgCl}_2(\text{g})$]-base reaction with alkaline-rich particles is an important sorption mechanism. The role of mercury chlorination and alkaline-rich particles in the formation of a $\text{Hg}(\text{p})$ -enriched subbituminous coal fly ash is evaluated in Section 4 of this paper.

In addition to $\text{HCl}(\text{g})$ and $\text{Cl}_2(\text{g})$, $\text{O}_2(\text{g})$ and $\text{NO}_2(\text{g})$ are potential mercury reactants in flue gas [22,23]. Kinetic limitations and the relatively short flue gas residence time in a duct or stack, however, preclude the occurrence of any significant homogeneous reactions involving $\text{Hg}^0(\text{g})$ and $\text{O}_2(\text{g})$ or $\text{NO}_2(\text{g})$ [12,25,36–38]. However, in the presence of inorganic and carbonaceous ash particles, these gases are apparently important in $\text{Hg}^0(\text{g})$ adsorption and oxidation processes. Hall et al. [12,23], for example, noted significant $\text{Hg}^0(\text{g})$ adsorption on activated carbon and fly ash particles in the presence of $\text{O}_2(\text{g})$, especially between 100°C and 300°C. A series of physical and chemical adsorption and dissociation reaction processes that ultimately result in a reaction between $\text{Hg}^0(\text{g})$ and atomic oxygen to form $\text{HgO}(\text{s})$ on particle surfaces was

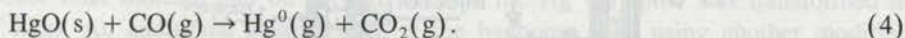
proposed to explain mercury adsorption. During an investigation of the effects of flue gas components (O_2 , CO_2 , H_2O , N_2 , SO_2 , HCl , NO , NO_2 , HF , Cl_2) on $Hg^0(g)$ –fly ash and $Hg^0(g)$ –carbon sorbent interactions in heated ($< 200^\circ C$) simulated flue gases, Laudal et al. [38] and Miller et al. [39] found that the presence of $NO_2(g)$ inhibits $Hg^0(g)$ adsorption but promotes the formation of $Hg^{2+}X(g)$. This effect was noted for $NO_2(g)$ concentrations as low as 20 ppmv [39]. Carey et al. [13] also showed that in a heated ($\leq 370^\circ C$) simulated flue gas, the presence of fly ash and certain ash components (iron and alumina compounds) promotes the conversion of $Hg^0(g)$ to $Hg^{2+}X(g)$. The presence of oxygenated and nitrogenated species and oxidation catalysts on fly ash particle surfaces appears to be an important factor controlling the transformation of $Hg^0(g)$ to $Hg(p)$ and $Hg^{2+}X(g)$.

Sulfur-rich ash particles entrained in coal combustion flue gas are potential reactants and sorbents for $Hg^0(g)$. During combustion, sulfur is released from coal as $SO_2(g)$. A fraction of the $SO_2(g)$, generally 1–3% [40], is oxidized to $SO_3(g)$. The formation of $SO_3(g)$ is catalyzed by transition metal oxide (e.g., Fe_2O_3) components of submicrometer ash but is neutralized by alkali and alkaline-earth metals in ash [41]. $SO_3(g)$ reacts with $H_2O(g)$ in flue gas to form $H_2SO_4(g)$. At temperatures below the sulfuric acid dew point, $H_2SO_4(l)$ condenses on ash particle surfaces and mercury species may absorb in $H_2SO_4(l)$ [42]. Mercury sulfation products resulting from $HgO(s)$ – $SO_2(g)$ – $O_2(g)$ – $H_2O(l)$ interactions have been identified by Shashkov et al. [43] and Zacharewski et al. [44]. In addition to $H_2SO_4(l)$ condensation on particle surfaces, the chemisorption of sulfur compounds onto particle surfaces may create active mercury sorption sites. Indeed, chemisorption is used to create sulfur-impregnated sorbents for removing mercury from gas streams as adsorbed HgS [45–47].

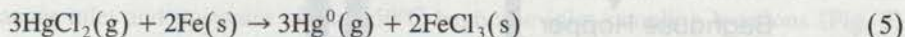
Although not indicated in Fig. 1, $Hg^{2+}X(s,g)$ reduction may be a viable transformation mechanism in coal combustion flue gas. $HgO(s,g)$ is reduced by reaction with $SO_2(g)$ and $CO(g)$ according to the following overall reactions [19,48]:



and



In addition, Schager [21] reported evidence for the reduction of $HgCl_2(g)$ by reaction with hot steel surfaces according to the following overall reaction:



In summary, the mercury in coal is initially transformed to $Hg^0(g)$ in the high-temperature combustion environment of a utility boiler. Experimental investigations have revealed the physical and chemical transformation mechanisms in Fig. 1 that may control mercury speciation as flue gases cool downstream of the combustion environment. Mercury chlorination is assumed to be the dominant mercury transformation mechanism. Other potential mechanisms in Fig. 1 involve mercury interactions with ash particle surfaces where reactive chemical species, catalysts, and active sorption sites are available to convert $Hg^0(g)$ to $Hg^{2+}X(g)$ as well as $Hg^0(g)$ and $HgCl_2(g)$ to $Hg(p)$.

3. Mercury–oxygen–chlorine interactions in a laboratory combustion system

Tests involving the injection of $10 \mu\text{g}/\text{m}^3 \text{Hg}^0(\text{g})$ and $100 \text{ppmv HCl}(\text{g})$ into a simple gas mixture of $8.5 \text{mol}\% \text{O}_2$ and $\approx 91.5 \text{mol}\% \text{N}_2$ were performed using a 42-MJ/h combustion system. Although these tests were originally intended for evaluating quality control [$\text{Hg}^0(\text{g})$ and $\text{HCl}(\text{g})$ spike recoveries], test results revealed significant $\text{Hg}^0\text{--O}_2\text{--Cl}$ interactions with insulating components of the combustor. These interactions may be relevant to mercury–fly ash interactions because the chemical and mineralogical compositions of the insulation are similar to the composition of coal fly ash.

3.1. Experimental

A schematic of the 42-MJ/h combustion system is presented in Fig. 2. Internal components of the system are composed primarily of Alumina 998 ceramic and Narcast 60 refractory materials to minimize contamination from metal surfaces. Sampling and $\text{HCl}(\text{g})$ and $\text{Hg}^0(\text{g})$ injection locations, as well as gas temperatures at these locations, are indicated in Fig. 2. A cylinder of working-standard-grade $\text{HCl}(\text{g})$ ($10,290 \pm 510 \text{ppmv HCl}$ in N_2) and a permeation device (VICI Metronics) were used as sources of $\text{HCl}(\text{g})$ and $\text{Hg}^0(\text{g})$, respectively. The concentration of $\text{HCl}(\text{g})$ was controlled using a calibrated

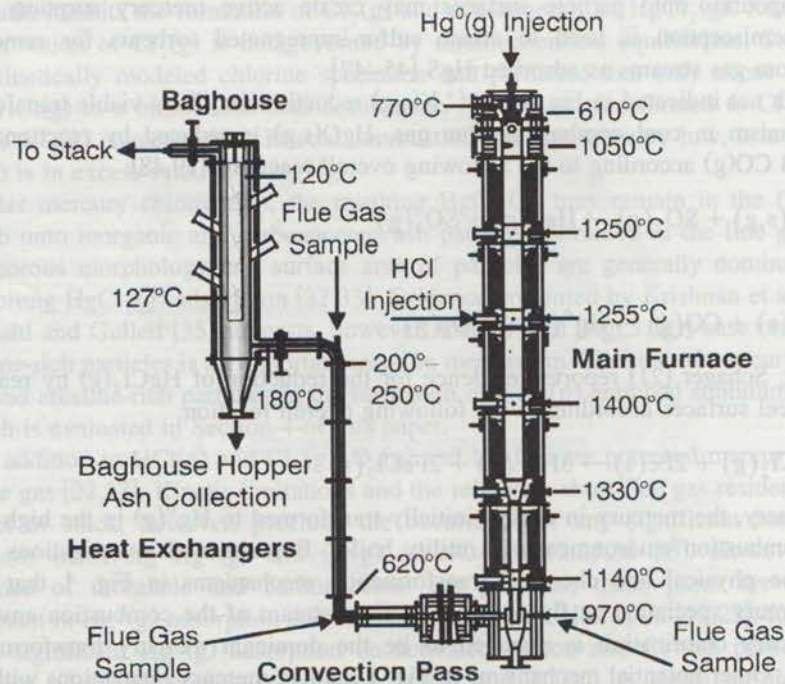


Fig. 2. Schematic of the 42-MJ/h downfired combustor showing the sampling and spiking locations as well as flue gas temperatures resulting from the heating of a gas mixture ($8.5\% \text{O}_2$, $91.5\% \text{N}_2$).

flowmeter. $\text{Hg}^0(\text{g})$ concentration was controlled by varying the temperature of the permeation tube and the gas flow rate of a N_2 carrier gas. An on-line mercury analyzer (Semtech Hg 2000 or P.S. Analytical, Sir Galahad) was used to verify $\text{Hg}^0(\text{g})$ spike concentration. Residence time of injected $\text{Hg}^0(\text{g})$ in the combustor was approximately 2.5 s. Concentrations of major flue gas components [e.g., $\text{O}_2(\text{g})$ and $\text{NO}_x(\text{g})$] were measured in the combustor using on-line analyzers (Beckman Instruments). The system was maintained at the temperatures indicated in Fig. 2 overnight prior to each test to minimize cross-contamination of mercury. Mercury speciation analyses were conducted using a modified U.S. Environmental Protection Agency (EPA) Method 29 developed by Radian International at the furnace outlet, heat exchanger inlet, and baghouse inlet corresponding to flue gas temperatures of 970°, 620°, and 250°C, respectively. An additional mercury speciation measurement was performed at the baghouse inlet using a modified EPA Method 29 developed by Ontario Hydro Technologies [49]. The mercury emission and speciation measurement capabilities of these modified EPA methods have been demonstrated through dynamic spike tests and method intercomparisons on bench- and pilot-scale flue gas systems [3,50–52]. Chlorine emissions and speciation were measured during the tests using EPA Method 26A and an on-line $\text{HCl}(\text{g})$ analyzer (Thermo Environmental Instruments, Model 15C). X-ray diffraction (XRD) analysis of materials was conducted to identify crystalline phases.

3.2. Mercury–oxygen interactions

During the first test, $10 \mu\text{g}/\text{m}^3$ of $\text{Hg}^0(\text{g})$ was injected into a simple heated (maximum of 1400°C) gas mixture (8.5 mol% O_2 , 91.5 mol% N_2). Duplicate mercury speciation measurements at the furnace outlet and heat exchanger inlet, presented in Fig. 3, indicate average $\text{Hg}^0(\text{g})$ spike recoveries of 102% and 92%, respectively. The very low concentrations ($< 1.7 \mu\text{g}/\text{m}^3$) of $\text{Hg}^{2+}\text{X}(\text{g})$ measured at the furnace outlet and heat exchanger inlet locations (corresponding to flue gas temperatures of 970°C and 620°C, respectively) are probably an artifact of the speciation method, because $\text{Hg}^{2+}\text{X}(\text{g})$ species are generally unstable at $\geq 620^\circ\text{C}$. Four mercury speciation analyses at the baghouse inlet indicate that on average 55% of the $\text{Hg}^0(\text{g})$ spike was transformed to $\text{Hg}^{2+}\text{X}(\text{g})$. An additional measurement at the baghouse inlet using another modified EPA Method 29 developed by Ontario Hydro Technologies indicates that 63% of the $\text{Hg}^0(\text{g})$ spike was converted to $\text{Hg}^{2+}\text{X}(\text{g})$. The formation of $\text{Hg}^{2+}\text{X}(\text{g})$ occurs within a 1.85-m-long, refractory-lined section of the combustor downstream of the 620°C heat exchanger inlet and upstream of the 250°C baghouse inlet sampling locations (Fig. 2). Flue gas residence time in this section is estimated to be < 0.1 s. On-line analyzers indicate that the only gaseous components available to react with $\text{Hg}^0(\text{g})$ were 8.5 mol% O_2 and 30 ppmv NO_x . Apparently NO_x was produced from heating the $\text{O}_2(\text{g})$ – $\text{N}_2(\text{g})$ mixture. Kinetic limitations and the short residence time precluded any significant homogeneous $\text{Hg}^0(\text{g})$ – $\text{O}_2(\text{g})$ or $\text{Hg}^0(\text{g})$ – $\text{NO}_2(\text{g})$ reactions to account for the formation of $\text{Hg}^{2+}\text{X}(\text{g})$ [12,25,36–38]. The formation of $\text{Hg}^{2+}\text{X}(\text{g})$ must therefore involve a heterogeneous or catalytic reaction on refractory surfaces in the heat exchanger section of the combustor. Possible reaction products in the $\text{Hg}^0(\text{g})$ – $\text{NO}_2(\text{g})$ system include mercury nitrite and nitrate compounds, but they are generally unstable at flue gas

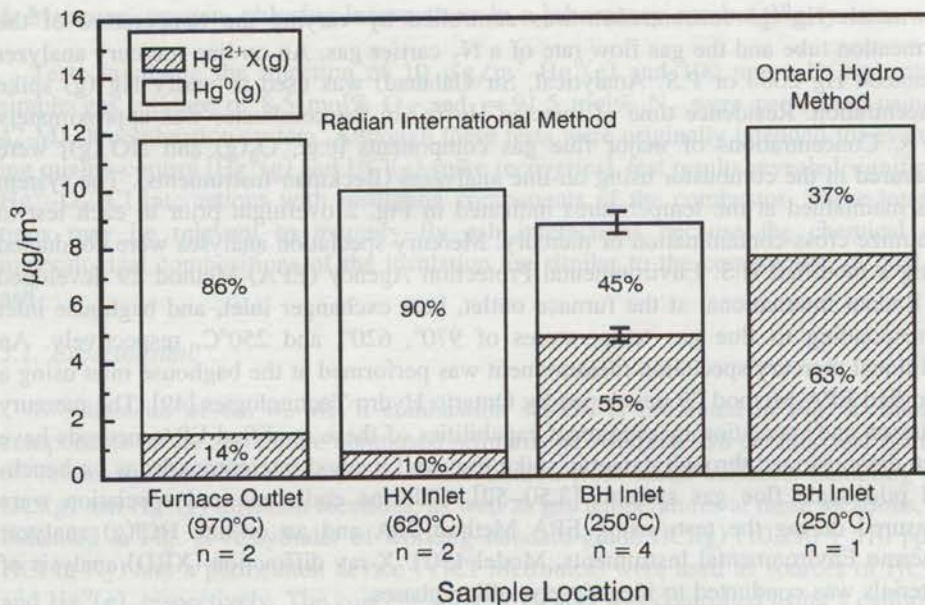
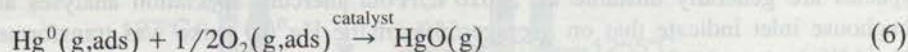


Fig. 3. Mercury speciation results for the $10\text{-}\mu\text{g}/\text{m}^3$ $\text{Hg}^0(\text{g})$ baseline spike test. The relative proportions of different mercury species are indicated within each bar as a percent of the total mercury. Error bar represents 95% confidence limits based on four modified (Radian International) EPA Method 29 measurements. Abbreviations: n = number of speciation measurements performed, BH = baghouse, and HX = heat exchanger.

temperatures upstream of the sampling location, $> 250^\circ\text{C}$ [19]. Alternatively, the oxidation of $\text{Hg}^0(\text{g})$ could involve a heterogeneous reaction with adsorbed (ads) Hg^0 or O_2 on surfaces or a catalyzed $\text{Hg}^0(\text{g})\text{-O}_2(\text{g})$ reaction resulting in $\text{HgO}(\text{g})$ (decomposes at 500°C) as the reaction product. The most plausible overall reaction is



although mercury nitrite or nitrate species could be an intermediate. Chemical and mineralogical (i.e., XRD) analyses indicate that mullite ($\text{Al}_6\text{Si}_2\text{O}_{13}$), dicalcium silicate (Ca_2SiO_4), and the known catalysts corundum (Al_2O_3) and rutile (TiO_2) compose the refractory. Testing by Carey et al. [13] at $\leq 370^\circ\text{C}$ demonstrated that $\text{Al}_2\text{O}_3(\text{s})$ and $\text{TiO}_2(\text{s})$ are $\text{Hg}^0(\text{g})$ oxidation catalysts in a simulated coal combustion flue gas. However, in a real coal combustion flue gas, the catalysts are poisoned, possibly because of the presence of fly ash [13].

3.3. Mercury–chlorine interactions

Tests involving the injection of $10\ \mu\text{g}/\text{m}^3$ $\text{Hg}^0(\text{g})$ and 100 ppmv $\text{HCl}(\text{g})$ into a simple gas mixture of 8.5 mol% $\text{O}_2(\text{g})$ and ≈ 91.5 mol% $\text{N}_2(\text{g})$ were also performed in the 42-MJ/h combustion system. The purpose of these tests was to determine 100-ppmv

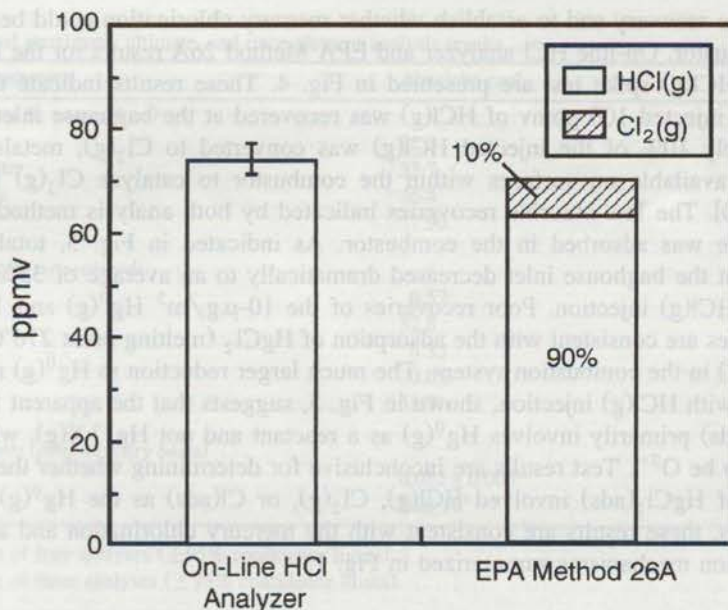


Fig. 4. On-line and EPA Method 26A chlorine analysis results for the 10- $\mu\text{g}/\text{m}^3$ $\text{Hg}^0(\text{g})$ +100-ppmv $\text{HCl}(\text{g})$ spike test. Error bar represents 95% confidence limits based on three HCl measurements.

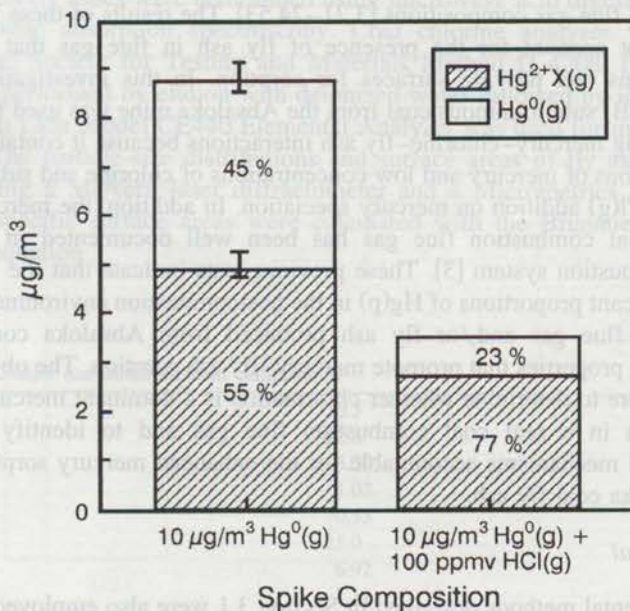


Fig. 5. Mercury speciation results for the 10- $\mu\text{g}/\text{m}^3$ $\text{Hg}^0(\text{g})$ baseline spike and 10- $\mu\text{g}/\text{m}^3$ $\text{Hg}^0(\text{g})$ +100-ppmv $\text{HCl}(\text{g})$ spike tests. The relative proportions of different mercury species are indicated within each bar as a percent of the total mercury.

HCl(g) spike recovery and to establish whether mercury chlorination could be achieved in the combustor. On-line HCl analyzer and EPA Method 26A results for the $\text{Hg}^0(\text{g}) + 100\text{-ppmv HCl}(\text{g})$ spike test are presented in Fig. 4. These results indicate that about 70% of the injected 100 ppmv of HCl(g) was recovered at the baghouse inlet and that approximately 10% of the injected HCl(g) was converted to $\text{Cl}_2(\text{g})$; metals such as Al_2O_3 are available on surfaces within the combustor to catalyze $\text{Cl}_2(\text{g})$ formation [reaction (1)]. The low chlorine recoveries indicated by both analysis methods suggest that chlorine was adsorbed in the combustor. As indicated in Fig. 5, total mercury recoveries at the baghouse inlet decreased dramatically to an average of 35% with the 100-ppmv HCl(g) injection. Poor recoveries of the $10\text{-}\mu\text{g}/\text{m}^3 \text{Hg}^0(\text{g})$ and 100-ppmv HCl(g) spikes are consistent with the adsorption of HgCl_2 (melting point 276°C , boiling point 302°C) in the combustion system. The much larger reduction in $\text{Hg}^0(\text{g})$ relative to $\text{Hg}^{2+}\text{X}(\text{g})$ with HCl(g) injection, shown in Fig. 5, suggests that the apparent formation of $\text{HgCl}_2(\text{ads})$ primarily involves $\text{Hg}^0(\text{g})$ as a reactant and not $\text{Hg}^{2+}\text{X}(\text{g})$, where X is suspected to be O^{2-} . Test results are inconclusive for determining whether the apparent formation of $\text{HgCl}_2(\text{ads})$ involved HCl(g), $\text{Cl}_2(\text{g})$, or Cl(ads) as the $\text{Hg}^0(\text{g})$ reactant. Nevertheless, these results are consistent with the mercury chlorination and adsorption transformation mechanisms summarized in Fig. 1.

4. Mercury–chlorine–fly ash interactions in a coal combustion flue gas

Mercury–chlorine interactions have been investigated experimentally using simulated coal combustion flue gas compositions [3,21–24,53]. The results of these investigations, however, do not account for the presence of fly ash in flue gas that may catalyze mercury reactions and provide surfaces for sorption. In this investigation, a Powder River Basin (PRB) subbituminous coal from the Absaloka mine was used for experimentally investigating mercury–chlorine–fly ash interactions because it contains sufficiently high concentrations of mercury and low concentrations of chlorine and sulfur to quantify the effect of HCl(g) addition on mercury speciation. In addition, the mercury speciation of Absaloka coal combustion flue gas has been well documented in tests using a 580-MJ/h combustion system [3]. These previous tests indicate that the Absaloka coal produces significant proportions of Hg(p) in the postcombustion environment ($\approx 180^\circ\text{C}$). Apparently the flue gas and/or fly ash produced from Absaloka coal combustion possess intrinsic properties that promote mercury–fly ash sorption. The objectives of this investigation were to determine whether chlorination is a dominant mercury transformation mechanism in a real coal combustion flue gas and to identify the flue gas components and mechanisms accountable for the enhanced mercury sorption characteristics of Absaloka coal fly ash.

4.1. Experimental

The experimental methods described in Section 3.1 were also employed in investigating mercury–chlorine–fly ash interactions. HCl(g) was injected at concentrations of 50 and 100 ppmv into the combustion region of the 42-MJ/h combustor shown in Fig. 2 while Absaloka coal was being burned. Most of the temperatures in Fig. 2 generally

Table 1
Absaloka coal proximate, ultimate, and trace element analysis results

Analysis parameters	Absaloka coal
<i>Proximate (wt.%, as-received)</i>	
Moisture	22.0
Volatile matter	33.7
Fixed carbon	36.4
Ash	7.90
<i>Ultimate (wt.%, as-received)</i>	
Sulfur	0.57
Carbon	52.8
Hydrogen	6.33
Nitrogen	0.65
Oxygen	31.7
<i>Trace elements (ppm on a dry basis)</i>	
Mercury	0.052 ± 0.005 ^a
Chlorine	50 ± 10 ^b

^aAverage of four analyses (±95% confidence limits).

^bAverage of three analyses (±95% confidence limits).

increased by 50°C during the combustion of Absaloka coal. Fly ash was sampled from the baghouse and analyzed for mercury and chlorine after each test. Mercury concentrations in coal and fly ashes were determined using microwave acid digestion followed by cold-vapor atomic absorption spectroscopy. Coal chlorine analyses were conducted using American Society for Testing and Materials Method D 4208. Fly ash chlorine analyses were performed by elution with deionized water followed by ion chromatography. A Leeman Labs Model CE440 Elemental Analyzer was used for measuring carbon in fly ashes. The particle-size distributions and surface areas of fly ash samples were determined using a Malvern laser diffractometer and a Micrometrics Flowsorb 2300, respectively. Specific surface areas were calculated with the Brunauer, Emmett, and Teller (BET) equation.

Table 2
Absaloka coal ash major and minor element composition

SiO ₂	36.3
Al ₂ O ₃	22.6
Fe ₂ O ₃	3.30
TiO ₂	1.02
P ₂ O ₅	0.53
CaO	25.0
MgO	6.92
Na ₂ O	1.11
K ₂ O	0.52
SO ₃	1.70
Total	99.0

Table 3
Absaloka coal combustion flue gas compositions

Component	Baseline	50-ppmv HCl spike	100-ppmv HCl spike
Excess O ₂ (mol%)	8.48	8.69	8.22
CO ₂ (mol%)	10.6	10.7	10.9
CO (ppmv)	390	580	1540
SO ₂ (ppmv)	410	380	420
NO _x (ppmv)	960	1110	1030
HCl (ppmv) ^a	3	46	105

^aCalculated value.

4.2. Results

Proximate, ultimate, and major, minor, and trace element analysis results for the sample of Absaloka coal selected for this investigation are presented in Tables 1 and 2. HCl(g) was injected at concentrations of 50 and 100 ppmv into the combustion region of the combustor while Absaloka coal was being burned. Presented in Table 3 are flue gas compositions for the Absaloka coal combustion tests. The flue gas compositions are similar except for a relatively high CO(g) concentration during the 100-ppmv HCl spike test. Chlorine speciation results for the Absaloka combustion tests are presented in Fig. 6. As expected, chlorine was not detected with EPA Method 26A for the baseline test

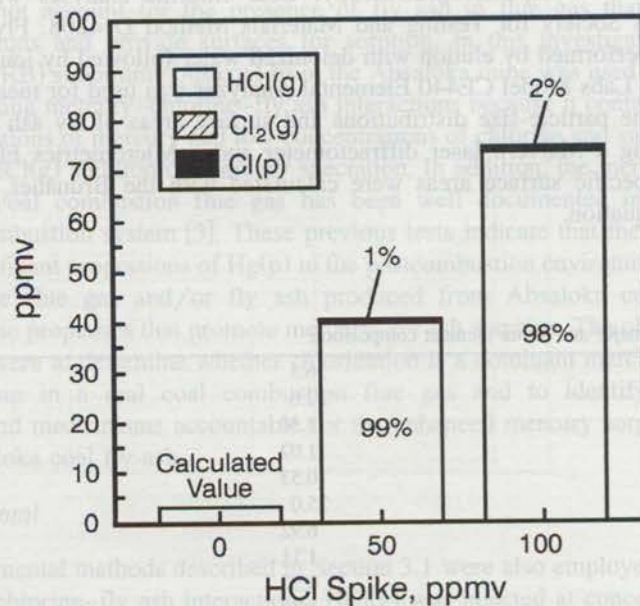


Fig. 6. Chlorine speciation results for the 50- and 100-ppmv HCl(g) injections during Absaloka coal combustion tests.

because of the low chlorine content of Absaloka coal (Table 1). The chlorine speciation result for the baseline test in Fig. 6 is actually a calculated value based on coal chlorine content and assuming 100% HCl(g) speciation. Recoveries of the 50- and 100-ppmv HCl(g) spikes are similar at 82% and 73%, respectively. These HCl(g) recoveries are also similar to those determined for the 10- $\mu\text{g}/\text{m}^3$ Hg⁰(g) + 100-ppmv HCl(g) spike test (refer to Fig. 4). Analogous to the Hg⁰(g)–HCl(g) spike test, the relatively low HCl(g) spike recoveries are consistent with the adsorption of chlorine in the combustor. Chlorine speciation results for the 50- and 100-ppmv HCl(g) spikes are very similar. In contrast to the Hg⁰(g)–HCl(g) spike testing, however, Cl₂(g) was not detected and particulate chlorine [Cl(p)] composes $\leq 2\%$ of the total chlorine measured.

Mercury speciation results for the Absaloka coal baseline and 100-ppmv HCl(g) injection tests are presented in Table 4 and Fig. 7. Results of the 50-ppmv HCl(g) injection test are not presented because of a lack in repeatability among the three mercury speciation measurements. The mercury mass balance closures in Table 4 provide an indication of data quality and the possibility of mercury retention in the combustor. As shown in Fig. 7, baseline testing of the Absaloka coal indicates that on average 41%, 19%, and 40% of the total mercury in the flue gas was present as Hg(p), Hg²⁺X(g), and Hg⁰(g), respectively. In comparison, mercury speciation of the 100-ppmv HCl(g) spiked flue gas was 14% Hg(p), 29% Hg²⁺X(g), and 57% Hg⁰(g). Similarly to the Hg⁰(g)–HCl(g) spike testing (Fig. 5), total mercury recovery decreased as a result of the 100-ppmv HCl injection. The results in Table 4 indicate that Hg²⁺X(g) and Hg⁰(g) concentrations remained constant, within analytical uncertainty, during the baseline and 100-ppmv HCl(g) spike tests, but Hg(p) was significantly depleted as a result of the 100-ppmv HCl(g) injection. The depletion of Hg(p) suggests that the injected HCl(g) reacted with Hg(p), causing mercury adsorption in the combustor, possibly as HgCl₂.

Additional evidence for the depletion of Hg(p) as a result of fly ash–HCl(g) interaction is presented in Fig. 8, where baghouse ash chlorine and mercury concentrations are plotted for the three Absaloka coal tests. The results in Fig. 8 indicate that even though the ash scavenged chlorine during the 50- and 100-ppmv HCl(g) injections, the Hg(p) content decreased relative to the baseline Absaloka coal test. A similar plot for ash carbon content is shown in Fig. 9. The significant increase in residual carbon content of the ash produced during the 100-ppmv HCl(g) injection test is reflected by the much higher CO(g) concentration in the flue gas (Table 3). The results in Fig. 9 indicate that

Table 4
Mercury speciation results for absaloka coal tests (mean \pm 95% confidence limits)

	Baseline ($\mu\text{g}/\text{m}^3$)	100-ppmv HCl spike ($\mu\text{g}/\text{m}^3$)
Hg ⁰ (g)	2.22 \pm 0.28	2.40 \pm 0.52
Hg ²⁺ X(g)	1.06 \pm 0.05	1.21 \pm 0.11
Hg(p)	2.26 \pm 0.37	0.60 \pm 0.41
Total Hg	5.53 \pm 0.65	4.21 \pm 0.53
Number of measurements	4	3
Hg mass balance closure	110 \pm 17%	82 \pm 13%

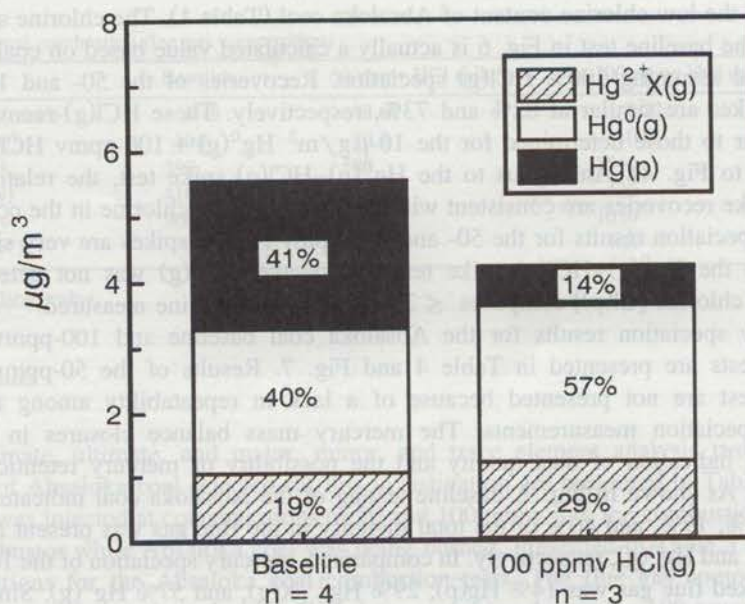


Fig. 7. Average mercury speciation results for the Absaloka baseline and 100-ppmv HCl spike tests. The relative proportions of different mercury species are indicated within each bar as a percent of the total mercury.

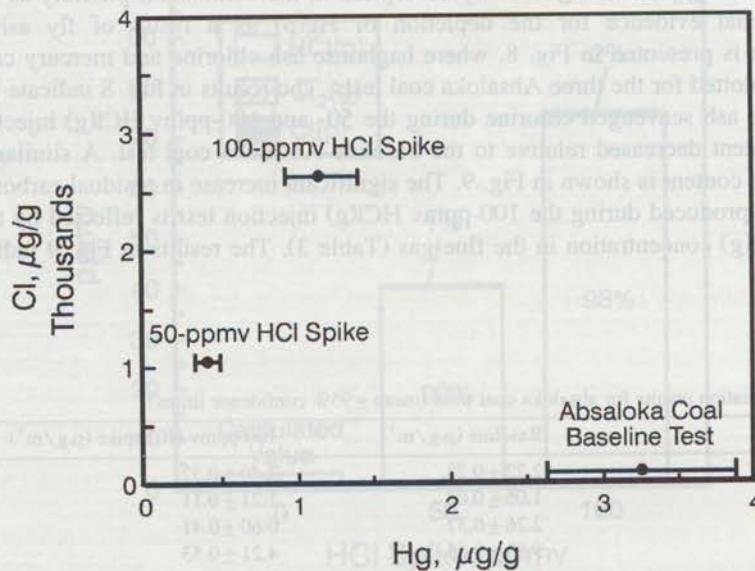


Fig. 8. Chlorine versus mercury concentrations for the Absaloka coal fly ash. Error bars represent 95% confidence limits based on three mercury measurements.

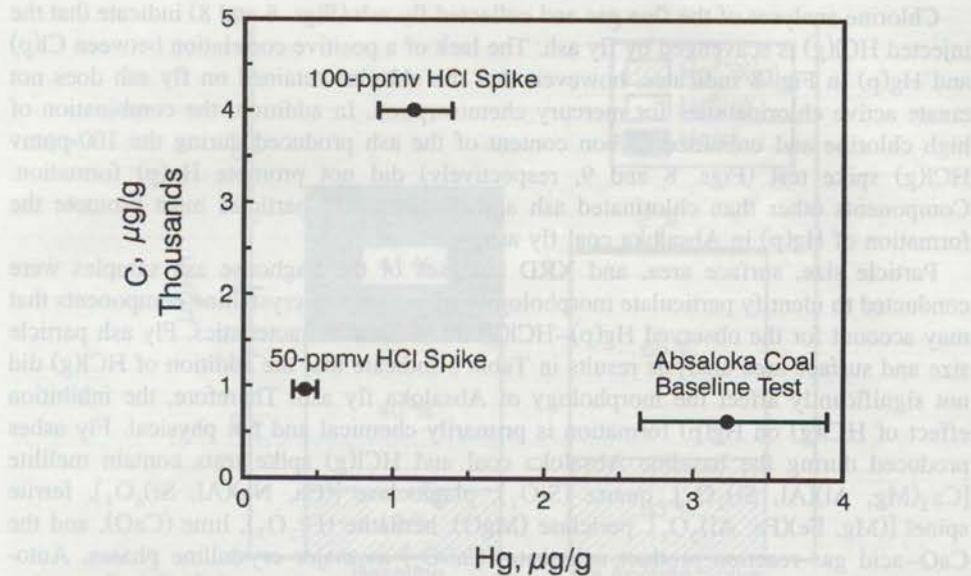


Fig. 9. Carbon versus mercury concentrations for the Absaloka coal fly ash. Error bars represent 95% confidence limits based on three mercury measurements.

an increase in carbon, a potential mercury sorbent, did not correspond to an increase in Hg(p).

4.3. Discussion

Mercury speciation results for the baseline Absaloka coal test, shown in Fig. 7, are very similar to results obtained from burning the pulverized Absaloka coal in a much larger pilot-scale (580-MJ/h) combustion system and measuring mercury speciation using several different methods (Fig. 7–28 in Ref. [3]). Test results from both combustion systems indicate that Absaloka coal combustion flue gas and/or entrained fly ash possess intrinsic properties that promote mercury sorption, as evidenced by relatively high proportions of Hg(p). The similarity in mercury speciation results suggests that the Hg⁰(g) oxidation mechanism postulated to occur on refractory surfaces within the 42-MJ/h combustor did not significantly affect the mercury speciation of Absaloka coal combustion flue gas. Apparently the presence of other flue gas components, including ash, impedes reaction (6) from occurring.

A significant depletion in Hg(p) during HCl(g) injection tests, resulting in a relatively low mercury mass balance closure (Table 4), provides indirect evidence for the adsorption of HgCl₂ on surfaces within the 42-MJ/h combustor. Based on chlorine mass balance and speciation results (Fig. 6), the apparent formation of HgCl₂(ads) involves Cl(ads), HCl(g), or Cl(p) as a reactant. Test results, however, are inconclusive for deciphering the reaction mechanism(s) responsible for the apparent formation of HgCl₂(ads).

Chlorine analyses of the flue gas and collected fly ash (Figs. 6 and 8) indicate that the injected HCl(g) is scavenged by fly ash. The lack of a positive correlation between Cl(p) and Hg(p) in Fig. 8 indicates, however, that the chlorine retained on fly ash does not create active chlorine sites for mercury chemisorption. In addition, the combination of high chlorine and unburned carbon content of the ash produced during the 100-ppmv HCl(g) spike test (Figs. 8 and 9, respectively) did not promote Hg(p) formation. Components other than chlorinated ash and carbonaceous particles must promote the formation of Hg(p) in Absaloka coal fly ash.

Particle size, surface area, and XRD analyses of the baghouse ash samples were conducted to identify particulate morphology parameters and crystalline components that may account for the observed Hg(p)–HCl(g) interaction characteristics. Fly ash particle size and surface area analysis results in Table 5 indicate that the addition of HCl(g) did not significantly affect the morphology of Absaloka fly ash. Therefore, the inhibition effect of HCl(g) on Hg(p) formation is primarily chemical and not physical. Fly ashes produced during the baseline Absaloka coal and HCl(g) spike tests contain melilite [$\text{Ca}_2(\text{Mg}, \text{Al})(\text{Al}, \text{Si})_2\text{O}_7$], quartz (SiO_2), plagioclase [$(\text{Ca}, \text{Na})(\text{Al}, \text{Si})_4\text{O}_8$], ferrite spinel [$(\text{Mg}, \text{Fe})(\text{Fe}, \text{Al})_2\text{O}_4$], periclase (MgO), hematite (Fe_2O_3), lime (CaO), and the CaO–acid gas reaction product anhydrite (CaSO_4) as major crystalline phases. Automated scanning electron microscopy analyses by Galbreath et al. [54] indicate that CaO(s) is generally a major component of the fine ash fractions ($< 2 \mu\text{m}$ in diameter) of PRB subbituminous coal fly ashes. CaO(s) and portlandite [$\text{Ca}(\text{OH})_2(\text{s})$], a hydration product of CaO(s), are effective $\text{HgCl}_2(\text{g})$ and HCl(g) sorbents [35,55,56]. In bench-scale experiments, Ghorishi and Gullett [35] found that the presence of HCl(g) inhibits the adsorption of $\text{HgCl}_2(\text{g})$ by $\text{Ca}(\text{OH})_2(\text{s})$. They hypothesized that this inhibition effect was a result of reactive competition between the acidic gases for the available alkaline sites. The inverse relationship between Hg(p) and Cl(p) documented in this investigation is consistent with the hypothesis of Ghorishi and Gullett [35], thus implying that CaO(s) is an important mercury sorption component of Absaloka fly ash.

The hypothesis that CaO(s) is a dominant mercury sorption component of Absaloka fly ash was investigated by adding calcium acetate monohydrate [$\text{Ca}(\text{C}_2\text{H}_3\text{O}_2)_2 \cdot \text{H}_2\text{O}$] to the Absaloka coal to enhance the liberation of organically bound CaO during combustion. The CaO concentration of the Absaloka coal ash increased from 25.0 to 37.6 wt.%, and XRD indicated a significant increase in CaO(s) content as a result of $\text{Ca}(\text{C}_2\text{H}_3\text{O}_2)_2 \cdot \text{H}_2\text{O}$ addition. Mercury speciation measurements in Fig. 10 indicate, however, that the relative proportion of Hg(p) was reduced from 41% of the total mercury in the baseline combustion flue gas to only 2% as a result of CaO(s) addition. Mercury analyses of ashes collected from the baghouse also indicated a reduction from

Table 5
Absaloka fly ash morphological properties

Sample	D_{50} (μm)	BET surface area (m^2/g)
Baseline	5.3	2.67
50-ppmv HCl spike	4.1	2.18
100-ppmv HCl spike	5.7	3.05

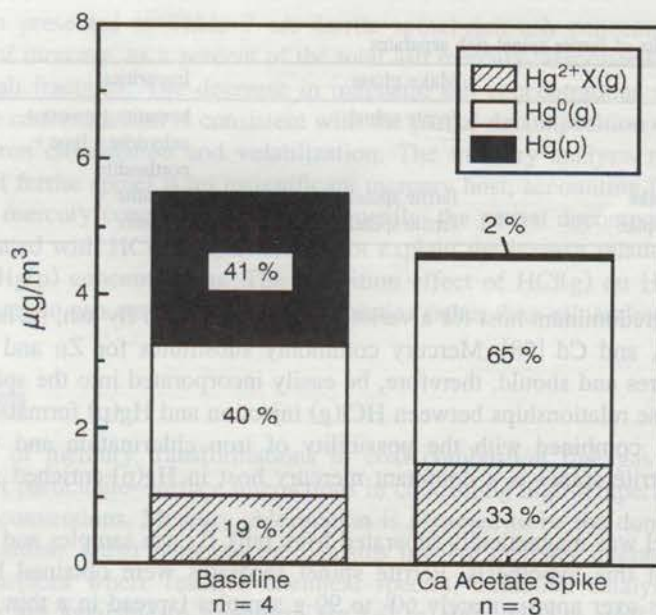


Fig. 10. Average mercury speciation results for the baseline and $\text{Ca}(\text{C}_2\text{H}_3\text{O}_2)_2 \cdot \text{H}_2\text{O}$ -spiked Absaloka coal combustion flue gases. The relative proportions of different mercury species are indicated within each bar as a percent of the total mercury.

$3.26 \pm 1.26 \mu\text{g/g}$ in the baseline Absaloka fly ash to $0.085 \pm 0.044 \mu\text{g/g}$ in the $\text{CaO}(\text{s})$ -spiked ash. Contrary to the hypothesized $\text{Hg}-\text{CaO}(\text{s})$ adsorption effect, the presence of additional $\text{CaO}(\text{s})$ inhibited $\text{Hg}(\text{p})$ formation. The added $\text{CaO}(\text{s})$ apparently interacted with a gaseous or fly ash component of the flue gas that promotes $\text{Hg}(\text{p})$ formation. Alternatively, $\text{CaO}(\text{s})$ addition may have affected ash particle morphology.

On-line gas, XRD, particle-size, and surface area analyses indicate that the addition of $\text{CaO}(\text{s})$ did not significantly affect the baseline flue gas composition (Table 3), but did affect fly ash mineralogy and morphology. $\text{CaO}(\text{s})$ addition promoted the formation of merwinite $[\text{Ca}_3\text{Mg}(\text{SiO}_4)_2]$ at the expense of melilite and plagioclase. The addition of $\text{CaO}(\text{s})$ also significantly increased the D_{50} of the baseline Absaloka fly ash from 5.3 to 10.5 μm and decreased BET surface area from 2.67 to 1.60 m^2/g . Based on crystal chemical considerations (e.g., ionic radii, chemical bonding characteristics, cation-site occupancies), the decomposition of melilite and plagioclase cannot account for the inverse relationship between $\text{CaO}(\text{s})$ addition and $\text{Hg}(\text{p})$ concentration. However, the reduction in particulate surface area and possibly a change in ash surface chemistry are consistent with the decline in $\text{Hg}(\text{p})$.

In addition to $\text{CaO}(\text{s})$ chlorination, experimental testing by Shimada et al. [57] indicates that iron is readily chlorinated by $\text{HCl}(\text{g})$ and then vaporized from coal fly ash. The addition of 50- and 100-ppmv $\text{HCl}(\text{g})$ may have resulted in the partial decomposition of ferrite spinel and hematite, the major iron-bearing minerals in the Absaloka fly ashes. In contrast to hematite, ferrite spinel (a thermal decomposition product of pyrite

Table 6
XRD analysis results of ferrite spinel-rich separates

Sample	Major phase	Impurities
Baseline	ferrite spinel	hematite + quartz + anhydrite + lime + portlandite
50-ppmv HCl(g) spike	ferrite spinel	hematite
100-ppmv HCl(g) spike	ferrite spinel	hematite

in coal) is the predominant host for a variety of trace metals in fly ash, including Cu, Cr, Co, Ni, V, Zn, and Cd [58]. Mercury commonly substitutes for Zn and Cd in other mineral structures and should, therefore, be easily incorporated into the spinel structure [59]. The inverse relationships between HCl(g) injection and Hg(p) formation, shown in Figs. 7 and 8, combined with the possibility of iron chlorination and volatilization suggest that ferrite spinel is a dominant mercury host in Hg(p)-enriched Absaloka fly ash.

Ferrite spinel was magnetically separated from bulk fly ash samples and analyzed for mercury to test this hypothesis. Ferrite spinel separates were obtained by passing a canister magnet over approximately 60- to 90-g samples (spread in a thin layer) of the Absaloka baseline and chlorine-enriched ashes. The ashes were agitated numerous times, and the magnetic separation process was repeated until magnetic particles could no longer be collected. Relatively small samples (0.06–0.3 g) of ferrite spinel-rich ash were recovered from the fly ashes using this magnetic separation procedure. XRD analysis results, presented in Table 6, indicate that hematite is a ubiquitous impurity in the ferrite spinel-rich separates. The separate from the baseline Absaloka fly ash also contains quartz, anhydrite, lime, and portlandite as impurities.

Mercury analysis results for the Absaloka bulk fly ash, magnetic ferrite spinel-rich separates, and nonmagnetic ash fractions are presented in Table 7. Mercury analyses of the separates could not be repeated because of the small sample amounts involved. As a quality control measure, a National Institute of Standards and Technology (NIST) Standard Reference Material 1633b subbituminous coal fly ash (0.141 $\mu\text{g/g}$ Hg) was analyzed for mercury in the same manner as the separates. Agreement between the measured and certified mercury values was acceptable, with a relative difference of 11%. The mercury mass balance closures in Table 7 also provide an indication of data

Table 7
Hg analysis results for Absaloka bulk fly ash and magnetic and nonmagnetic fly ash fractions

	Baseline	50-ppmv HCl spike	100-ppmv HCl spike
Bulk ash Hg ($\mu\text{g/g}$)	3.26 \pm 1.26	0.406 \pm 0.105	1.16 \pm 0.56
Magnetic ash fraction Hg ($\mu\text{g/g}$)	0.513	0.122	0.627
Magnetic ash fraction (wt.%)	0.35	0.19	0.08
Magnetic ash fraction Hg (%)	0.05	0.06	0.04
Nonmagnetic ash fraction Hg ($\mu\text{g/g}$)	1.18 \pm 0.07	0.438 \pm 0.008	1.09 \pm 0.04
Hg mass balance closure (%)	36	108	94

quality. Also presented in Table 7 are ferrite spinel-rich ash concentrations and the proportions of mercury, as a percent of the total ash mercury, associated with the ferrite spinel-rich ash fractions. The decrease in magnetic ash concentrations with increasing HCl(g) spike concentrations is consistent with the partial decomposition of ferrite spinel because of iron chlorination and volatilization. The mercury analysis results indicate, however, that ferrite spinel is an insignificant mercury host, accounting for $\leq 0.06\%$ of the total ash mercury concentrations. Consequently, the partial decomposition of ferrite spinel associated with HCl(g) injection cannot explain the inverse relationship between HCl(g) and Hg(p) concentrations. The inhibition effect of HCl(g) on Hg(p) formation probably relates to ash surface chemical properties rather than mineralogical properties.

5. Conclusions

A review of mercury transformations in coal combustion flue gas highlights the importance of particulate–surface interactions in controlling high-temperature Hg⁰(g) to Hg²⁺X(s,g) conversions. Mercury chlorination is assumed to be the dominant transformation mechanism. Other potential mechanisms involve mercury interactions with ash particulate surfaces where reactive chemical species, oxidation catalysts, and active sorption sites are available to transform Hg⁰(g) to Hg²⁺X(g) as well as Hg⁰(g) and HgCl₂(g) to Hg(p). The following observations and conclusions from an investigation of Hg⁰(g)–O₂(g)–HCl(g) and Hg^{0.2+}(g)–HCl(g)–CaO(s)–fly ash interactions in a 42-MJ/h combustor support the proposed mechanisms:

- Approximately 60% of a 10- $\mu\text{g}/\text{m}^3$ Hg⁰(g) spike injected into a simple heated (maximum of 1400°C) gas mixture (8.5 vol% O₂, 30 ppmv NO_x, ≈ 91.5 vol% N₂) was transformed rapidly (< 0.1 s) to Hg²⁺X(g) within a 1.85-m-long refractory-lined section of the combustor where gas temperatures decrease from 620°C to 250°C. A Hg⁰(g)–O₂(g) reaction catalyzed by Al₂O₃(s) and/or TiO₂(s) components of the refractory is postulated. HgO(g) is the suspected reaction product, although mercury nitrite or nitrate species could be an intermediate.
- On average, 41% of the total mercury ($5.5 \pm 0.6 \mu\text{g}/\text{m}^3$) in a 250°C PRB subbituminous coal combustion flue gas is present as Hg(p). The addition of HCl(g) or CaO(s) into the PRB coal combustion environment, however, inhibits Hg(p) formation in the resulting fly ash. The inhibition effects of HCl(g) and CaO(s) on Hg(p) formation are primarily chemical and physical (i.e., decrease in particulate surface area), respectively.
- Low recoveries of mercury during 100-ppmv HCl(g) injections into a simple gas mixture and PRB coal combustion flue gas suggest that HgCl₂ was formed and sorbed onto insulating components of the combustor.

Acknowledgements

We are greatly indebted to Richard Schulz, Carolyn Lillemoen, Kristi Schmalenberg, and Grant Dunham for their sampling and analysis efforts. Although the research described in this article has been funded in part by United States Environmental

Protection Agency (EPA) through Grant No. R 824854-01-0 to the University of North Dakota, it has not been subjected to the Agency's required peer and policy review and therefore does not necessarily reflect the views of the Agency and no official endorsement should be inferred.

References

- [1] U.S. Environmental Protection Agency, Mercury Study Report to Congress, Volume I: Executive Summary, Office of Air Quality Planning and Standards and Office of Research and Development, EPA-452/R-97-003, December 1997.
- [2] K.C. Galbreath, C.J. Zygarlicke, Mercury speciation in coal combustion and gasification flue gases, *Environ. Sci. Technol.* 30 (1996) 2421–2426.
- [3] D.L. Laudal, K.C. Galbreath, M.K. Heidt, A state-of-the-art review of flue gas mercury speciation methods, Electric Power Research Institute, Palo Alto, CA, November 1996, EPRI Report No. TR-107080.
- [4] O. Lindqvist, H. Rodhe, Atmospheric mercury — a review, *Tellus* 37B (1985) 136–159.
- [5] F. Slemr, W.J. Seiler, G. Schuster, Distribution, speciation, and budget of atmospheric mercury, *J. Atmos. Chem.* 3 (1985) 407–434.
- [6] O. Lindqvist, K. Johansson, M. Aastrup, A. Anderson, L. Bringmark, G. Hovsenius, L. Håkanson, Å. Iverfeldt, M. Meili, B. Timm, Mercury in the Swedish environment — recent research on causes, consequences, and corrective methods, *Water Air Soil Pollut.* 55 (1991) 1–261.
- [7] B. Hall, The gas phase oxidation of elemental mercury by ozone, *Water Air Soil Pollut.* 80 (1995) 301–315.
- [8] O.W. Hargrove, Jr., J.R. Peterson, D.M. Seeger, R.C. Skarupa, R.E. Moser, Update of EPRI wet FGD pilot-scale mercury emissions control research, EPRI-DOE International Conference on Managing Hazardous and Particulate Air Pollutants, Toronto, Ontario, Canada, August 1995.
- [9] W.H. Schroeder, J. Munthe, Atmospheric mercury — an overview, *Atmos. Environ.* 32 (1998) 809–822.
- [10] Y. Otani, C. Kanaoka, C. Usui, S. Matsui, H. Emi, Adsorption of mercury vapor on particles, *Environ. Sci. Technol.* 20 (1986) 735–738.
- [11] P. Schager, B. Hall, O. Lindqvist, Retention of gaseous mercury on fly ashes, Second International Conference on Mercury as a Global Pollutant, Monterey, CA, June 1992.
- [12] B. Hall, P. Schager, J. Weesmaa, The homogeneous gas phase reaction of mercury with oxygen, and the corresponding heterogeneous reactions in the presence of activated carbon and fly ash, *Chemosphere* 30 (1995) 611–627.
- [13] T.R. Carey, R.C. Skarupa, O.W. Hargrove Jr., Enhanced control of mercury and other HAPs by innovative modifications to wet FGD processes, Phase I Report for the U.S. Department of Energy, Contract DE-AC22-95PC95260, August 28, 1998.
- [14] T. Brown, DOE control technology R&D, Managing Hazardous Air Pollutants Fourth International Conference, Washington, DC, November 12–14, 1997.
- [15] D.J. Swaine, *Trace Elements in Coal*, Butterworths, London, 1990, p. 292.
- [16] J.C. Groen, J.R. Craig, The inorganic geochemistry of coal, petroleum, and their gasification/combustion products, *Fuel Process. Technol.* 40 (1994) 15–48.
- [17] R.B. Finkelman, Modes of occurrence of potentially hazardous elements in coal: levels of confidence, *Fuel Process. Technol.* 39 (1994) 21–34.
- [18] V.M. Goldschmidt, *Geochemistry*, Oxford Univ. Press, Fair Lawn, NJ, 1954.
- [19] B.J. Ayllett, *The chemistry of zinc, cadmium, and mercury*, Pergamon Texts in Inorganic Chemistry, Vol. 18, Pergamon, 1975.
- [20] R. Meij, The fate of mercury in coal-fired power plants and the influence of wet flue-gas desulphurization, *Water Air Soil Pollut.* 56 (1991) 21–33.
- [21] P. Schager, The behaviour of mercury in flue gases, Statens energiverk, National Energy Administration, Sweden, Report FBT-91-20, 1990, p. 59.

- [22] B. Hall, O. Lindqvist, E. Ljungström *et al.*, Mercury chemistry in simulated flue gases related to waste incineration conditions, *Environ. Sci. Technol.* 24 (1990) 108–111.
- [23] B. Hall, P. Schager, O. Lindqvist, Chemical reactions of mercury in combustion flue gases, *Water Air Soil Pollut.* 56 (1991) 3–14.
- [24] D.L. Laudal, K.C. Galbreath, C.J. Zygarlicke, Experimental investigation of mercury speciation in coal combustion flue gases, Fourth International Conference on Mercury as a Global Pollutant, Hamburg, Germany, August 1996.
- [25] A. Fontijn, Reaction kinetics of toxic metals, The Fifth International Congress on Toxic Combustion Byproducts, Management of Risk from Combustion Sources, Program and Abstracts, University of Dayton, Dayton, OH, June 25–27, 1997, p. 86.
- [26] D. Shao, W. Pan, Behavior of chlorine and sulfur during coal combustion, in: K.H. Michaelian (Ed.), International Conference on Coal Science, Banff, Alberta, Canada, September 12–17, 1993, Conference Proceedings, Vol. 1, pp. 656–659.
- [27] H. Deacon, U.S. Patent 165 802, July 1875; U.S. Patent 85 370, December 1868; U.S. Patent 118 209, August 1871; U.S. Patent 141 333, July 1875.
- [28] H.Y. Pan, R.G. Minet, S.W. Benson, T.T. Tsotsis, Process for converting hydrogen chloride to chlorine, *Ind. Eng. Chem. Res.* 33 (1994) 2996–3003.
- [29] R.L. Lindbauer, F. Wurst, T. Prey, Combustion dioxin suppression in municipal solid waste incineration with sulfur additives, *Chemosphere* 25 (1992) 1409.
- [30] K. Raghunathan, B.K. Gullett, Role of sulfur in reducing PCDD and PCDF formation, *Environ. Sci. Technol.* 30 (1996) 1827–1834.
- [31] C.L. Senior, L.E. Bool III, G.P. Huffman, F.E. Huggins, N. Shah, A.F. Sarofim, I. Olmez, T. Zeng, A fundamental study of mercury partitioning in coal fired power plant flue gas, Air and Waste Management Association's 90th Annual Meeting and Exhibition, Toronto, Ontario, Canada, June 8–13, 1997, Paper 97-WP72B.08.
- [32] C.L. Senior, J.R. Morency, G.P. Huffman, F.E. Huggins, N. Shah, T. Peterson, F. Shadman, B. Wu, Interactions between vapor-phase mercury and coal fly ash under simulated utility power plant flue gas conditions, Air and Waste Management Association's 91st Annual Meeting and Exhibition, June 14–18, 1998, Paper 98-RA79B.04.
- [33] S.V. Krishnan, B.K. Gullett, W. Jozewicz, Mercury control in municipal waste combustors and coal-fired utilities, *Environ. Prog.* 16 (1997) 47–53.
- [34] S.V. Krishnan, B.K. Gullett, W. Jozewicz, Control of mercury emissions from coal combustors, EPRI-DOE International Conference on Managing Hazardous and Particulate Air Pollutants, Toronto, Ontario, Canada, August 15–17, 1995.
- [35] B. Ghorishi, B.K. Gullett, Fixed-bed control of mercury: role of acid gases and a comparison between carbon-based, calcium-based, and coal fly ash sorbents, EPRI-DOE-EPA Combined Utility Air Pollutant Control Symposium, Washington, DC, August 25–29, 1997, EPRI Report TR-108683-V3, p. 15.
- [36] B. Hall, P. Schager, E. Ljungström, An experimental study of the rate of reaction between mercury vapour and gaseous nitrogen dioxide, *Water Air Soil Pollut.* 81 (1995) 121–134.
- [37] C.-Y. Wu, E. Arar, P. Biswas, Mercury capture by aerosol transformation in combustion environments, 89th Annual Meeting of the Air and Waste Management Association, Nashville, TN, June 1996, Paper 96-MP2.02.
- [38] D. Laudal, T. Brown, B. Nott, P. Chu, Bench-scale studies to determine the effects of flue gas constituents on mercury speciation, Conference on Air Quality: Mercury, Trace Elements, and Particulate Matter, McLean, VA, December 1–4, 1998.
- [39] S.J. Miller, E.S. Olson, G.E. Dunham, R.K. Sharma, Preparation methods and test protocol for mercury sorbents, Air and Waste Management Association's 91st Annual Meeting and Exhibition, San Diego, CA, June 14–18, 1998, Paper 98-RA79B.07.
- [40] J.D. Singer (Ed.), *Combustion fossil power systems*, Combustion Engineering, 3rd edn., Windsor, CT, 1981.
- [41] K.A. Graham, A.F. Sarofim, Inorganic aerosols and their role in catalyzing sulfuric acid production in furnaces, *J. Air Waste Manage. Assoc.* 48 (1998) 106–112.
- [42] L.L. Zhao, G.T. Rochelle, Mercury absorption in aqueous oxidants catalyzed by mercury(II), *Ind. Eng. Chem. Res.* 37 (1998) 380–387.

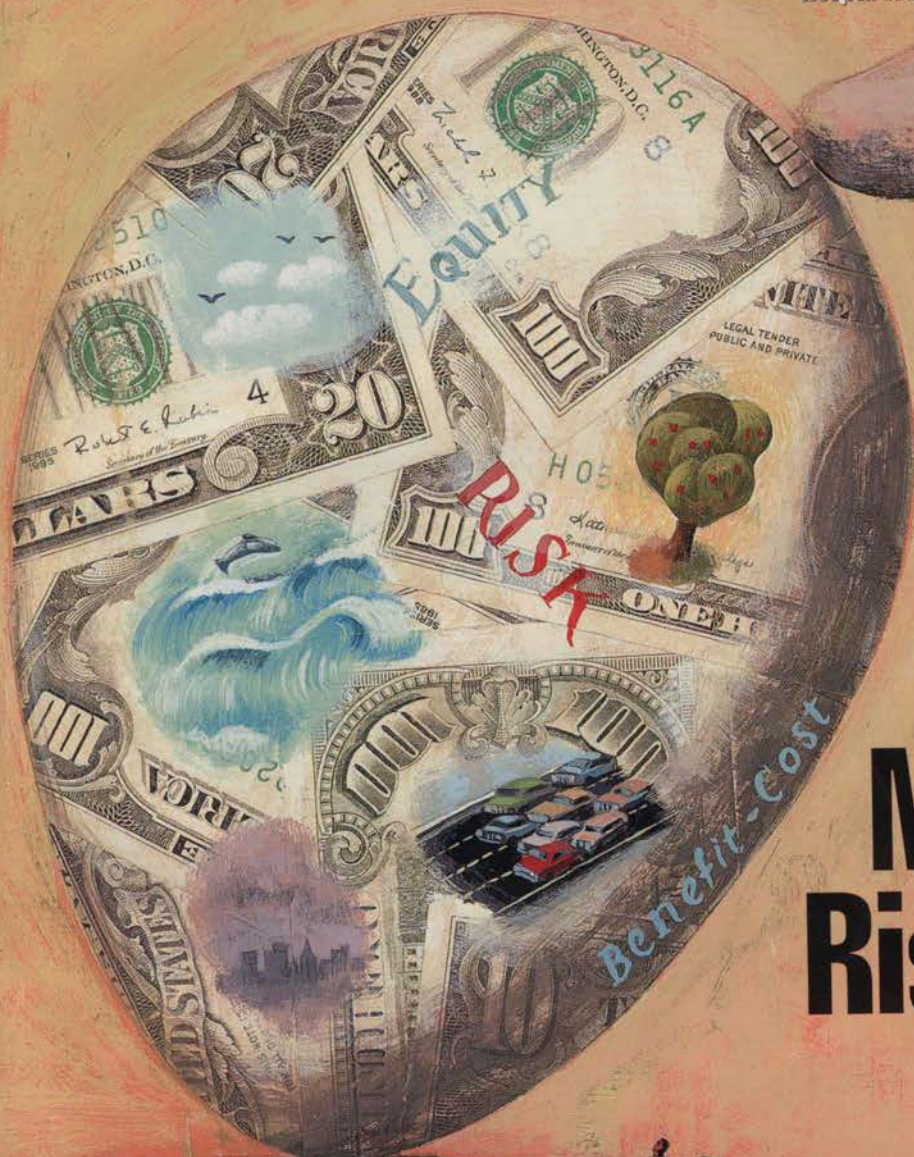
- [43] V.I. Shashkov, I.P. Mukhlenov, E.Ya. Beñiyash, V.I. Ostanina, M.M. Shokarev, F.I. Vershinina, Effect of mercury vapors on the oxidation of sulfur dioxide in a fluidized bed of vanadium catalyst, *Khim. Prom-st. (Moscow)* 47 (1971) 288–290.
- [44] T.R. Zacharewski, E.A. Cherniak, W.H. Schroeder, FTIR investigation of the heterogeneous reaction of $\text{HgO}(s)$ with $\text{SO}_2(g)$ at ambient temperature, *Atmos. Environ.* 21 (1987) 2327–2332.
- [45] J.A. Korpziel, R.D. Vidic, Effect of sulfur impregnation method on activated carbon uptake of gas-phase mercury, *Environ. Sci. Technol.* 31 (1997) 2319–2325.
- [46] W. Liu, R.D. Vidić, T.D. Brown, Optimization of sulfur impregnation protocol for fixed-bed application of activated carbon-based sorbents for gas-phase mercury removal, *Environ. Sci. Technol.* 32 (1998) 531–538.
- [47] M.I. Guijarro, S. Mendioroz, V. Muñoz, Effect of morphology of sulfurized materials in the retention of mercury from gas streams, *Ind. Eng. Chem. Res.* 37 (1998) 1088–1094.
- [48] W.H. Schroeder, G. Yarwood, H. Niki, Transformation processes involving mercury species in the atmosphere — results from a literature survey, *Water Air Soil Pollut.* 56 (1991) 653–666.
- [49] K.E. Curtis, K.E. Eagleson, Speciation of mercury emissions from Ontario Hydro's coal-fired generating stations, Report No. A-F-95-22-Con, Ontario Hydro Technologies, Toronto, Ontario, Canada, March 1995, p. 30.
- [50] D.L. Laudal, M.K. Heidt, B.R. Nott, T.D. Brown, Recommended methods for mercury speciation measurements in coal combustion systems, *Managing Hazardous Air Pollutants Fourth International Conference*, Washington, DC, November 12–14, 1997.
- [51] D.L. Laudal, M.K. Heidt, Evaluation of flue gas mercury speciation methods, *Electric Power Research Institute Report No. TR-108988*, December 1997.
- [52] D. Laudal, B. Nott, T. Brown, R. Roberson, Mercury speciation methods for utility flue gas, *Fresenius' J. Anal. Chem.* 358 (1997) 397–400.
- [53] N.C. Widmer, J.A. Cole, W.R. Seeker, J.A. Gaspar, Practical limitation of mercury speciation in simulated municipal waste incinerator flue gases, *The Fifth International Congress on Toxic Combustion By-products, Management of Risk from Combustion Sources, Program and Abstracts*, Dayton, OH, June 25–27 1997, p. 66.
- [54] K.C. Galbreath, C.J. Zygarlicke, D.P. McCollor, D.L. Toman, Development of a stack-plume opacity index for subbituminous coal-fired utility boilers, in: S.-H. Chiang (Ed.), *Proceedings of the 12th Annual International Pittsburgh Coal Conference, Coal — Energy and the Environment*, September 11–15 1995, pp. 19–26.
- [55] A. Lancia, D. Musmarra, F. Pepe, G. Volpicelli, Adsorption of mercuric chloride vapours from incinerator flue gases on calcium hydroxide particles, *Combust. Sci. Technol.* 93 (1993) 277–289.
- [56] W. Jozewicz, B.K. Gullett, Reaction mechanisms of dry Ca-based sorbents with gaseous HCl, *Ind. Eng. Chem. Res.* 34 (1995) 607–612.
- [57] T. Shimada, T. Kajinami, T. Kumagai, S. Takeda, J. Hayashi, T. Chiba, Characteristics of vaporization of coal ash minerals chlorinated by gaseous hydrogen chloride, *Ind. Eng. Chem. Res.* 37 (1998) 894–900.
- [58] R.J. Lauf, Characterization of the mineralogy and microchemistry of fly ash, *Nucl. Chem. Waste Manage.* 5 (1985) 231–236.
- [59] D. Grdenić, G. Tunell, J.J. Rytuba, in: K.H. Wedepohl (Ed.), *Handbook of Geochemistry: Elements La (57) to U (92)*, chap. 80, Vol. II/5, Springer, Heidelberg, 1978.

EXHIBIT E

January 1, 2000

ENVIRONMENTAL Science & Technology

<http://www.acs.org/est>



Managing Risk: *A Delicate Balancing Act*

AMEREN UE EXHIBIT 1082
Page 68

PUBLISHED BY
THE AMERICAN
CHEMICAL SOCIETY

Governments are a speed bump to smart growth • 13A

The public decisively supports smart-growth initiatives, but solutions for controlling suburban development continue to elude state planners.

Scientists discover complexities of algal production • 14A

Although nitrogen and phosphorus are a cause of excess algal production, scientists caution against overlooking the significant role played by other nutrients, such as silicon and iron.

Defense Department environmental liability weakened by appropriations loophole • 14A

Thanks to a controversial rider, this year's Defense Appropriations Act requires the Pentagon to gain congressional approval before paying for any environmental violations.

Plant geneticist wins Volvo Environment Prize • 15A

Monkombu Sambasivan Swaminathan believes that genetic engineering may play a key role in helping developing nations like his native India feed their people.

UNEP Prize winner to study megacities in developing world • 16A

Nobel Laureate Mario J. Molina, the winner of the 1999 UNEP Sasakawa Prize, continues his pioneering research on the earth's atmosphere.

News Briefs • 17A

Breast cancer link with pollutants suggested • Shrinking the dead zone • Water pricing • Wind energy potential • Increased humidity due to global warming • Rise in sea level not tied to global warming • Eastern European environmental compliance • Starvation threat in sub-Saharan Africa



34(1) 1A-56A/1-224
ISSN 0013 936X

Departments**Comment • 7A**

The new millennium

EPA Watch • 19A

Chemicals used in children's products • Shortcomings in drinking water research • Environmental justice at U.S.-Mexican border • NRC wetland mitigation review • Fuel efficiency slipping

Technology Update • 36A

Technologies cut electric power impacts • Detoxifying anti-NO_x technology

Research Watch • 38A

Chlorinated hydrocarbon destruction • *Cryptosporidium parvum* transport

Online/In Print • 40A

Web sites and new books

Meeting Calendar • 41A

New events through April 2000

Buyer's Guide • 42A

Environmental products and services

2000 Advisory Board • 43A

Introducing editors and board members for 2000

Editorial Policy for 2000 • 44A

Author guidelines

Ethical Guidelines • 51A

Guidelines for authors, editors, and reviewers

Classifieds • 54A

Environmental career opportunities • Advertiser index

Research at a Glance

Aerosols, behavior, 71
Aerosols, detection, 211
Air quality, metals, 27
Algal blooms, sediments, 107
Ammonia, volatilization, 199
Arsenic, in plants, 22
Atrazine, in precipitation, 55
Chlorocarbons, in groundwater, 149
Chlorocarbons, reduction, 173
Chlorothalonil, soil, 120, 125
Chromium, in soils, 112
Colloids, measurements, 187
Cryptosporidium, soil, 62
Dichloroethene, mineralization, 221
Dioxins, destruction, 143
Disinfectants, drinking water, 83
Fly ash, degradation, 130, 137
Hexafluorobenzene, sorption, 204
Lead, deposition, 12
Mercury, emissions control, 154
Metals, sediments, 91
Mine waste, spectroscopy, 47
Minerals, microbial reduction, 100
Minerals, partitioning, 192
PCBs, in atmosphere, 78
PCNs, in environment, 33
Perchlorate, in fertilizer, 224
Sewage, water quality, 39
Surfactants, remediation, 160
VOCs, adsorption, 1
Wastewater, life cycle, 180
Wastewater, textiles, 167

The table of contents of research papers in this issue begins on page 5A.



Cover: Granger Morgan questions current one-size-fits-all risk management practices and suggests that an innovative strategy for accomplishing both benefit-cost and equity objectives should be explored. (Artwork by Curtis Parker)

Impact of Flue Gas Conditions on Mercury Uptake by Sulfur-Impregnated Activated Carbon

WEI LIU AND RADISAV D. VIDIC*

Department of Civil and Environmental Engineering,
943 Benedum Hall, University of Pittsburgh,
Pittsburgh, Pennsylvania 15261-2294

THOMAS D. BROWN

U.S. Department of Energy, Federal Energy Technology Center,
P.O. Box 10940, Pittsburgh, Pennsylvania 15236-0940

Novel sulfur-impregnated activated carbons (SIACs) have shown excellent mercury uptake capacity when pure nitrogen was used as a carrier gas. This study investigated the impact of various gas constituents found in a real flue gas on the performance of SIACs. Fixed-bed adsorber tests showed that CO₂ (up to 15%) had no impact on mercury uptake by SIAC, while the presence of O₂ (up to 9%) increased the adsorptive capacity up to 30%. Increase in the amount of oxygen-containing acidic surface functional groups had no impact on mercury uptake, and it is postulated that the enhanced performance was due to the formation of HgO catalyzed by SIAC. Moisture presence (up to 10%) can decrease SIAC's capacity for mercury uptake by as much as 25% due to competitive adsorption and additional internal mass transfer resistance. SO₂ (1600 ppm) and NO (500 ppm) exhibited no impact on mercury uptake by SIAC even in the presence of 10% moisture. Adsorptive capacity of SIAC decreased significantly when the reaction temperature increased from 140 to 250 and 400 °C due to the pronounced exothermic nature of HgS formation, but increasing the empty-bed contact time can partially offset this loss of capacity.

Introduction

Since the Clean Air Act Amendments were enacted in 1990, the U.S. Environmental Protection Agency (EPA) has been focused on evaluating and implementing new regulatory standards to control air toxic metal emissions. Mercury attracted significant attention due to its toxicity (1-3). The EPA's draft mercury report to Congress in 1995 showed that coal-fired power plants, municipal waste combustors, and medical waste incinerators account for 216 ton/yr of the overall 253 ton/yr of total anthropogenic mercury emissions in the United States (4). The EPA's final mercury report released in 1997 (5) showed that the total mercury emission from point-sources was lowered to 158 ton/yr. However, coal-fired power plants, municipal waste combustors, and medical waste incinerators still accounted for 75% of the total emission.

Prompted by the possibility of more stringent regulations on mercury, much work has been done or is under way to develop more efficient processes to reduce mercury emissions

from point-sources. Traditional pollution control techniques, such as baghouses, ESPs, and wet scrubbers, are able to capture oxidized forms of mercury to some extent (6-8). However, these devices showed low efficiency for the control of elemental mercury emissions. As a result, a significant amount of elemental mercury leaves the stacks. Researchers (9-11) have found that solid sorbents, especially chemically impregnated activated carbons, showed greatly improved efficiency for elemental mercury removal that was strongly related to sorbent characteristics (e.g., surface area, chemical composition) and operating conditions (e.g., temperature, residence time, flue gas composition).

Previous studies (11, 12) investigated mercury removal efficiency of sulfur-impregnated activated carbons (SIAC) produced at elevated temperatures using pure nitrogen as a carrier gas. These novel adsorbents showed enhanced adsorptive capacity when compared to commercially available products because of a higher content of active sulfur molecules and a larger surface area.

Although using pure nitrogen in these studies was helpful to understand the baseline performance of these sorbents, the real coal-fired power plant flue gas contains other gas constituents such as carbon dioxide (10-15%), oxygen (3-7%), moisture (8-10%), and trace amounts of SO₂ (100-3000 ppm), NO_x (200-600 ppm), and HCl (0-50 ppm) (8, 13, 14). It is therefore necessary to investigate the impact of these flue gas constituents on the performance of these novel SIAC adsorbents. A systematic approach was used in this study to evaluate the influence of one gas constituent at a time because the coexistence of several gas components could have compounding impacts and preclude fundamental understanding of their possible effects on mercury uptake. For example, a particular gas constituent may improve the performance of the carbon, while another may deteriorate it, but their simultaneous presence in the carrier gas stream would not allow such observations. Furthermore, certain gases may react with others if they are mixed together, and byproducts may affect the adsorptive capacity of the adsorbent. It is crucial to understand the behavior and impact of each individual gas component. The resulting performance of the sorbent can then be discussed based on the possible molecular interactions among different gas constituents, mercury, sulfur, and activated carbon surface.

Experimental Methods

Column runs for these newly developed SIAC adsorbents were conducted in a fixed-bed reactor charged with 100 mg of 60 × 80 U.S. Mesh size virgin (BPL) or sulfur-impregnated activated carbon (SIAC) and operated at 140 °C using the carrier gas flow rate of 1.0 L/min (unless otherwise noted). Detailed description of sorbent preparation and experimental parameters for column tests is given elsewhere (11, 12) and will not be repeated here.

The first step to ensure quality control in this study was to check if any gas constituent interfered with elemental mercury detection by atomic absorption spectrophotometer (AAS). It was determined that CO₂, O₂, and NO had no impact on mercury measurements by AAS. Since water vapor affected the AAS reading, the effluent gas was first passed through a Nafion dryer (Perma Pure, Inc., Toms River, NJ) to eliminate this interference. The gas lines from the moisture generator to the dryer (including the first foot of the dryer tube) were heated to prevent moisture condensation. A hygrometer, Testo 610 (Testo Inc., Flanders, NJ), was used to monitor relative humidity of the carrier gas. The Nafion dryer was able to remove the moisture from the gas stream without

* Corresponding author phone: (412)624-1307; fax: (412)624-0135; e-mail: vidic@engrng.pitt.edu.

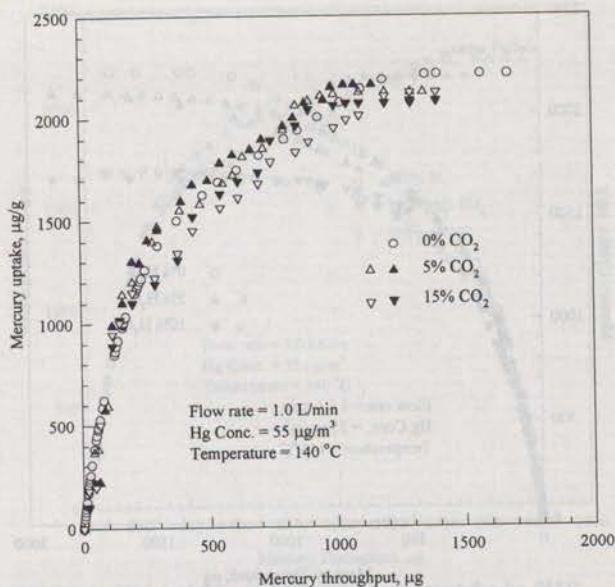


FIGURE 1. Impact of CO₂ on mercury uptake by SIAC.

any impact on mercury concentration or speciation in the vapor phase.

It was also observed that SO₂ affected the AAS detection capability, and 0.1 M NaOH solution in a gas-washing bottle was used to scrub SO₂ from the gas stream. It was then also necessary to use the Nafion dryer to remove water vapor entrained in the gas-washing bottle to ensure that AAS adequately detected elemental mercury concentration in the carrier gas.

Additional quality control testing was performed to determine if any of the gas constituents would react with elemental mercury in the gas phase in the absence of carbon surface. Nitrogen flow at 1.0 L/min was first used as a carrier gas, and the empty column was connected to the system. The oven temperature was maintained at 140 °C, and all system parameters were adjusted until the AAS reading indicated an elemental mercury concentration of 55 µg/m³. Then, nitrogen was replaced with 1.0 L/min of carrier gas containing one of the major or trace components that will be used in this study. The AAS was monitored continuously for the variation in instrument reading, and impinger trains (11, 12) were used to collect the mercury-laden gas for 1 h. The results of the liquid-phase mercury analysis and AAS monitoring confirmed that the elemental mercury concentration in the carrier gas remained at 55 µg/m³ for all carrier gas compositions evaluated in this study. For each column run, periodic collection of the effluent by liquid impingers (11, 12) was used to verify that no interaction between mercury and different carrier gas constituents occurred even in the presence of the sorbent surface, while combustion of spent sorbents (12) was used to verify the mass balance for mercury.

Results and Discussions

Impact of Carbon Dioxide. The results described in the Experimental Section showed that CO₂ did not interfere with elemental mercury measurements and did not react with vapor-phase mercury. Effect of CO₂ on the performance of SIAC was tested at two different concentrations, namely, 5% and 15% (both tests were performed in duplicate), while the remainder was pure N₂ gas.

Figure 1 compares mercury uptake by SIAC in the presence of different CO₂ concentrations. As can be seen from this figure, the adsorptive capacity of SIAC was virtually unchanged regardless of the presence of CO₂. This result

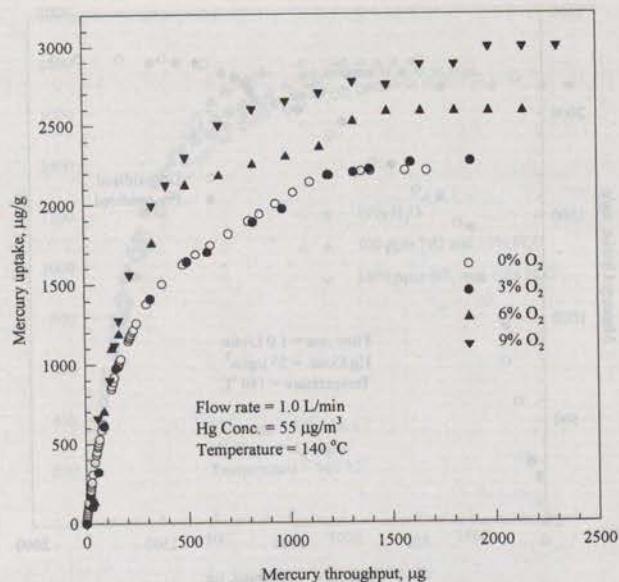


FIGURE 2. Effect of oxygen on mercury uptake by SIAC.

indicated that CO₂ behaves like an inert gas during the course of the experiment and does not affect the performance of SIAC.

Impact of Oxygen. The concentration of O₂ in the carrier gas was varied from 0 to 9%, and the resulting mercury uptake is shown in Figure 2. When the concentration of O₂ was increased from 0% to 3%, the mercury uptake capacity of SIAC remained almost unchanged. The overall mercury removal capacity increased by 16 and 33% as the O₂ concentration increased to 6% and 9%, respectively.

Since oxygen is readily chemisorbed by activated carbons to form carbon-oxygen complexes that are important in determining surface reactions and adsorptive behavior (15), it was necessary to study the possibility of carbon-oxygen complexes formation during the column tests conducted in the presence of oxygen and their impact on mercury removal.

Both virgin carbon (BPL) and SIAC were tested for the formation of acidic oxygen complexes upon exposure to oxygen using the procedure described by Tessmer et al. (16). Preoxidized samples are those prepared by contacting 2 g of the unoxidized samples with a stream of air (flow rate of 1.0 L/min) in a ceramic boat at 140 °C for a period of 7 days. Total acidic surface oxygen content of virgin BPL increased from 445 ± 15 to 578 ± 8 µequiv/g (based on triplicate measurements) as a result of air treatment, while that increase was more pronounced for SIAC (from 130 ± 20 to 620 ± 5 µequiv/g). Lower acidic surface functional group content of unoxidized SIAC as compared to BPL can be explained by outgassing effects during exposure of BPL carbon to a temperature of 600 °C (16). The finding that carbon-oxygen complexes formed on SIAC after exposure to oxygen are equal to those formed on preoxidized BPL carbon suggests that a significant portion of the original surface area of BPL carbon remained reactive even after impregnation with sulfur. Sulfur analysis of the SIAC showed that a negligible amount of sulfur (less than 1% of impregnated sulfur) was lost during 7 days of contact with air stream at 140 °C.

Column tests were performed using these unoxidized and preoxidized carbons with pure N₂ as a carrier gas. The breakthrough curves depicted in Figure 3 clearly show that air pretreatment had no impact on the performance of SIAC. Identical observation was made in the case of BPL carbon. In addition, 1% sulfur loss did not reduce the adsorptive capacity of SIAC. These results indicate that air can oxidize carbon surface and increase its acidic surface

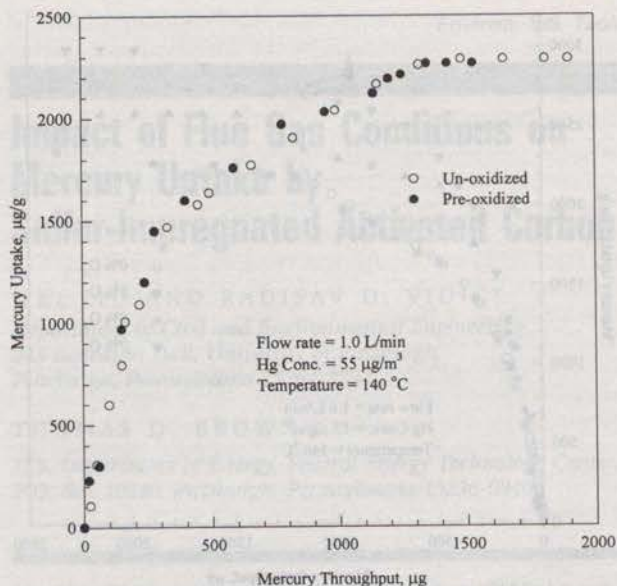


FIGURE 3. Mercury uptake by SIAC before and after oxidation with air.

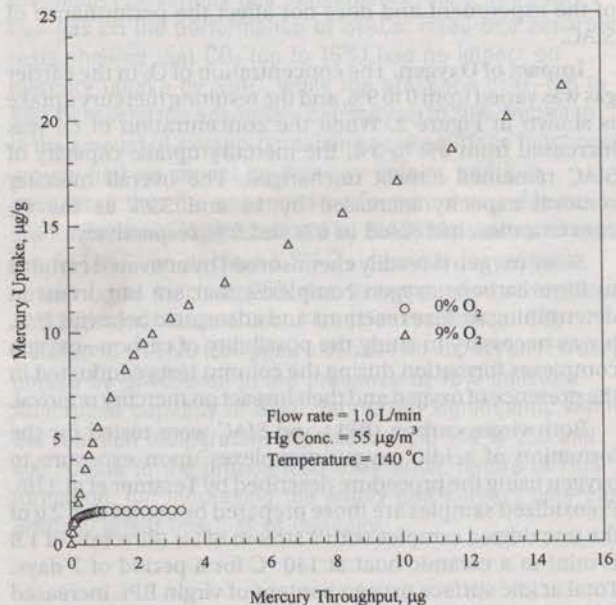


FIGURE 4. Catalysis of mercury and oxygen reaction by BPL.

functional group content, but these changes have no impact on the performance of activated carbon for mercury removal.

It is reasonable to assume that the reaction between O_2 and mercury that is catalyzed by activated carbon surface (17) is responsible for the enhanced performance of SIAC in the presence of oxygen (Figure 2), since oxidized mercury is much more adsorbable than elemental mercury. Virgin BPL was tested for mercury uptake using a carrier gas containing 9% oxygen to test this hypothesis. Figure 4 illustrates that virgin carbon showed much higher capacity for mercury uptake (20 μg of Hg/g of carbon) after 4 h of contact in 9% O_2 than in the absence of oxygen (1.5 μg of Hg/g of carbon at saturation). Since virgin BPL can only remove 1.5 μg of Hg/g of carbon in the absence of oxygen, the additional capacity for mercury removal in the presence of oxygen can only be explained by the conversion of mercury to mercuric oxide as there was no reaction between oxygen and mercury in the absence of activated carbon surface.

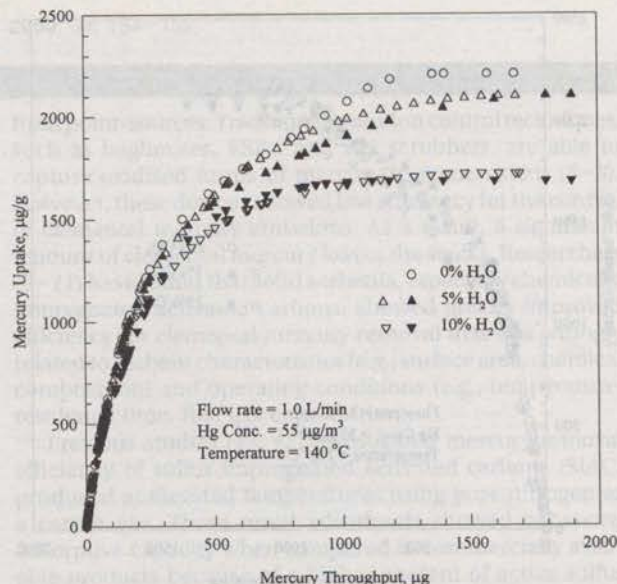


FIGURE 5. Effect of moisture content on mercury uptake by SIAC.

Although, the virgin activated carbon acted as a catalyst for mercury oxidation, it is possible that its catalytic effect could decrease due to the loss of surface area resulting from sulfur impregnation. Surface area of activated carbon covered with sulfur molecules for SIAC would be about 7% of the initial surface area of virgin BPL of 900 m^2/g if it is assumed that sulfur molecules (diameter, $D = 2.08 \times 10^{-10}$ m) (18) are impregnated onto the carbon surface in a monolayer. The actual available activated carbon surface area should be higher since the sulfur molecules may form multiple layers on the carbon surface, and it is reasonable to assume that SIAC still has enough active sites to catalyze the reaction between mercury and oxygen as seen for virgin activated carbon.

Impact of Moisture. Figure 5 shows the impact of carrier gas moisture content on mercury uptake by SIAC. The total mercury uptake capacity did not change significantly when 5% moisture was introduced in the carrier gas (based on duplicate test). However, carbon adsorptive capacity decreased as much as 25% when the moisture content increased to 10% (based on duplicate test). Since the adsorptive capacity of carbon did not change at low moisture content, it can be concluded that moisture does not affect the reaction between sulfur and mercury. Therefore, it is postulated that the effect of moisture is related to the adsorption of water by the carbon surface. The carbon surface can bind water molecules to form hydrogen bonds with other molecules (19). Higher vapor pressure will increase the amount of adsorbed water. For the 5% moisture in the carrier gas, the capillary condensation may be the dominant process. As the water vapor pressure increased to 10%, water molecules were able to fill the micropores so that isolated water zones merged to block the access to some active sites on the carbon surface and active sulfur molecules, thereby creating additional mass transfer resistance for the adsorption of elemental mercury.

Another factor that could influence the carbon performance is the hydrogen formation due to the dissociation of water induced by carbon. It was reported that hydrogen and CO can be formed if sufficient water vapor pressure is present above the carbon surface in the temperature range used in this study and that hydrogen is preferentially retained by the carbon (15). Due to extremely small size, hydrogen molecules can easily reach different size carbon pores to form strong hydrogen-carbon complexes. As a result, the available surface area in the mesoporous region is decreased, and mercury is unable to react with sulfur retained in those pores.

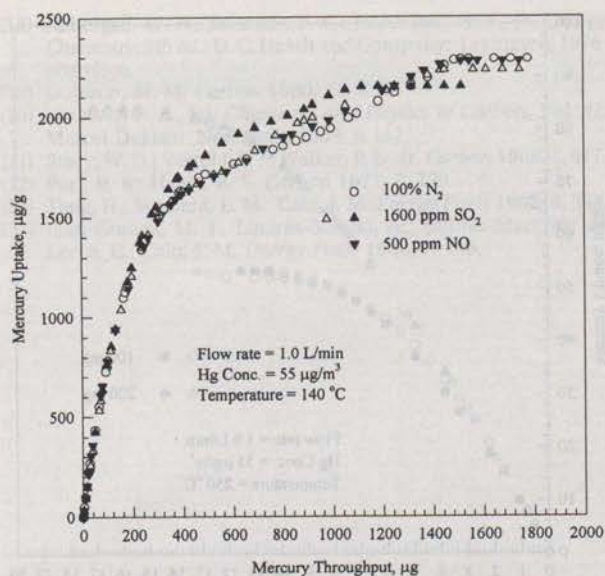
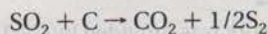


FIGURE 6. Effect of SO₂ and NO on mercury uptake by SIAC.

Impact of Sulfur Dioxide. Figure 6 compares mercury uptake by SIAC in pure N₂ and in 1600 ppm SO₂/N₂ mixture. This test indicated that the mercury uptake capacity of SIAC was not affected by the presence of SO₂. Identical observation was made for virgin BPL (data not shown).

It is well-known that SO₂ could interact with activated carbon via physisorption or chemisorption at relatively high temperatures (>500 °C) and high concentrations (20–22) according to the following overall reaction:



Thermogravimetric analysis (TGA) used to investigate the potential impact of SO₂ on virgin BPL and SIAC revealed that the weight of BPL and SIAC samples remained unchanged even after 5 h of exposure to 3000 ppm SO₂ at 140 °C (data not shown). From the overall reaction, every mole of SO₂ would consume 1 mol of carbon and deposit 0.5 mol of S₂, thereby increasing the net weight of carbon by about 20 g/mol of SO₂ reacted. Based on the experimental conditions used in the TGA test (100 mL/min of 3000 ppm SO₂ in N₂ at 140 °C), the weight increase that could have been observed for the 5-h period was estimated at 3.54 mg. The TGA instrument used in this study would have registered even if only 1/3500 of SO₂ reacted with carbon since the detection limit is 0.001 mg. The results of TGA tests suggest that SO₂ did not react with virgin carbon surface or with impregnated sulfur. This behavior is most likely due to low SO₂ concentration and low reaction temperature that retarded possible reactions.

Impact of Nitric Oxide. Figure 6 indicates that the performance of SIAC did not exhibit a significant change as the carrier gas was switched from pure N₂ to NO/N₂ mixture. Identical observation was made for virgin BPL carbon (data not shown). TGA tests showed that the weight of both BPL and SIAC samples remained unchanged upon exposure to 100 mL/min of 400 ppm NO in N₂ after 5 h of exposure at 140 °C (data not shown).

On the basis of the experimental conditions used in TGA tests, the amount of NO passed through the system in 5 h was about 11.59 mg. Since the detection limit of the TGA instrument used in this study is 0.001 mg, it would have registered if only 1/10000 of NO had been adsorbed by the carbon. Since this was not observed, it is postulated that NO was not adsorbed by the carbon at the test conditions employed.

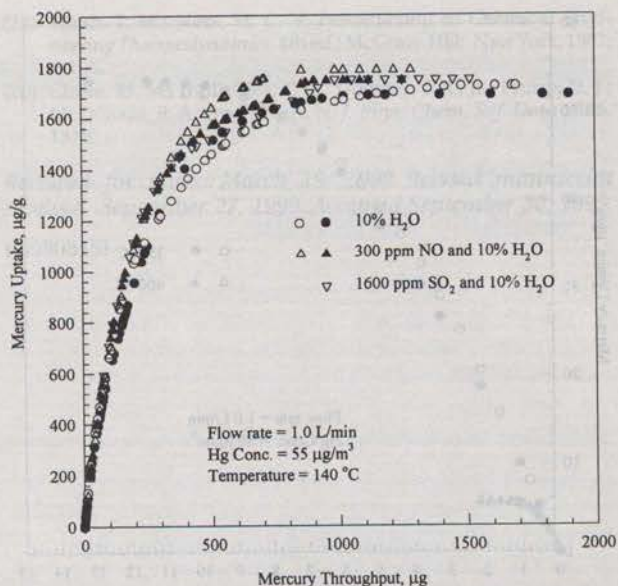
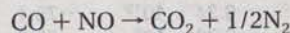
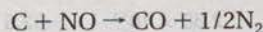


FIGURE 7. Effect of SO₂/H₂O and NO/H₂O on mercury uptake by SIAC.

Several studies found that NO could react with carbon to form various gas products (23, 24) based on the following reactions:



According to these reactions, carbon weight loss could occur due to gasification. However, this was not observed under the experimental conditions used in this study. One possibility is that the concentration of NO in this study was extremely low (0.0004%) as compared to 1–10% NO used in other studies. Low temperature was another reason for the lack of gasification that was shown to occur at 500–800 °C (23, 24). Since the SIAC did not experience any weight loss in the presence of NO, it can be concluded that there was no reaction between NO and elemental sulfur.

Impact of Gas Mixture. Preliminary studies were performed to investigate the combined effects of SO₂ and water vapor and NO and water vapor. Figure 7 shows that the performance of SIAC in the presence of SO₂ (1600 ppm) and 10% moisture or NO (300 ppm) and 10% moisture did not differ very much from the tests conducted in the presence of 10% moisture alone. Even if weak acids (H₂SO₃ or HNO₂) did form on the carbon surface, the low concentration of the acid resulting from the low concentration of SO₂ and NO did not have a major impact on the performance of SIAC, and moisture was the dominant factor influencing the adsorptive capacity of this sorbent.

Impact of Flue Gas Temperature. Mercury uptake by SIAC was evaluated at 250 and 400 °C in order to obtain preliminary information on the performance of this sorbent if it is injected upstream of the air heat exchanger where the flue gas temperatures can be as high as 400 °C. The main advantage of moving the point of sorbent injection further upstream is that it increases the contact time to as much as 4 s. To accomplish these temperatures in the fixed-bed adsorber, a tube furnace was used as the heating section for the column instead of an oven. Also, stainless steel tubing, which can tolerate high temperatures, was used for the inlet and outlet connections for the reactor in lieu of Teflon tubing. Due to the existence of heat transfer resistance between the

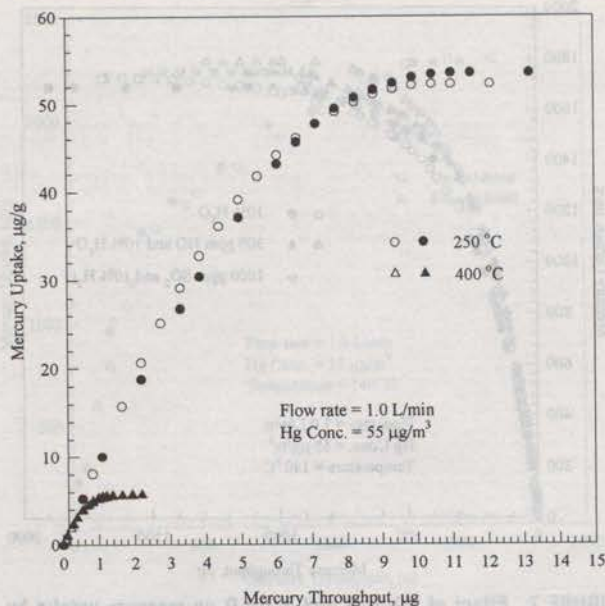


FIGURE 8. Impact of temperature on mercury uptake by SIAC.

TABLE 1. Thermodynamic Parameters of the Reaction between Mercury and Sulfur

temp (°C)	S(l) + Hg(g) → HgS(s)		S(s) + Hg(g) → HgS(s)	
	ΔG (kJ/mol)	K	ΔG (J/mol)	K
25	-82.5	2.88×10^{14}	-82.5	2.83×10^{14}
50	-79.6	7.45×10^{12}	-79.6	7.35×10^{12}
90	-75.1	6.34×10^{10}	-75.1	6.31×10^{10}
140	-69.6	6.30×10^8	-69.6	6.32×10^8
250	-57.9	6.17×10^5	-58.1	6.38×10^5
400	-42.7	2.07×10^3	-43.6	2.41×10^3

heating element and the gas stream, the actual temperature inside the reactor was monitored by a thermocouple. Pure N₂ rather than a mixture of gases was used as the carrier gas so that the results can be compared with previous runs at 140 °C, while the other experimental conditions were the same as before.

Figure 8 shows the rate of mercury uptake by SIAC at 250 and 400 °C. As can be seen from this figure, the performance of SIAC significantly deteriorated at 250 (53.5 µg/g) and 400 °C (5.68 µg/g) as compared to the performance at 140 °C (2600 µg/g). Thermodynamic calculations shown in Table 1 (25, 26) indicate that the reaction between mercury and sulfur is highly exothermic and irreversible regardless of the form of sulfur participating in the reaction and that the possibility of HgS decomposition can be ignored. Another important observation is that the ΔG values for the solid and liquid sulfur are almost identical at a given temperature. Therefore, the state change of sulfur does not affect the tendency of the reaction. The values of the equilibrium constant, K, show a drastic decrease with an increase in temperature so that much less HgS can be created at higher temperatures. Since K value at 140 °C is several orders of magnitude higher than K at 250 and 400 °C, significantly larger amount of HgS can be formed at 140 °C, which explains the difference in SIAC performance shown in Figure 8.

Figure 9 shows the impact of empty-bed contact time on SIAC performance at 250 °C. It can be seen that the mercury uptake capacity of this carbon was increased by about 60% when the empty-bed contact time was doubled from 0.011 to 0.022 s. Such behavior suggests that the longer contact time in a fixed bed could at least partially offset the loss of capacity due to the increase in the reaction temperature.

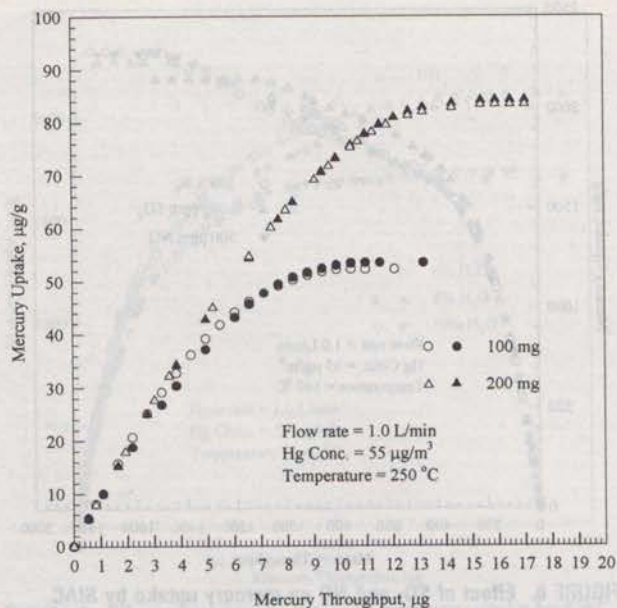


FIGURE 9. Impact of empty-bed contact time on mercury uptake by SIAC at 250 °C.

However, due to the fact that the initial rates of mercury uptake (slope of the mercury uptake curve at the beginning of the run) are almost identical in both experiments, the impact of longer contact time facilitated by the injection of powdered sorbent upstream of the heat exchanger may be quite limited.

Acknowledgments

Funding for this work was provided by the U.S. Department of Energy (Grant DE-FG22-96PC96212). The views expressed are entirely those of authors and do not necessarily reflect the views of the agency. Mention of trade names or commercial products does not constitute endorsement or recommendation for use.

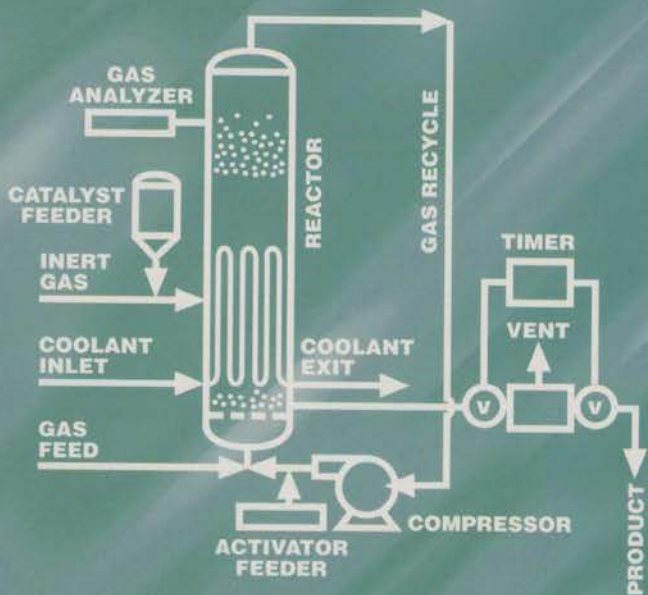
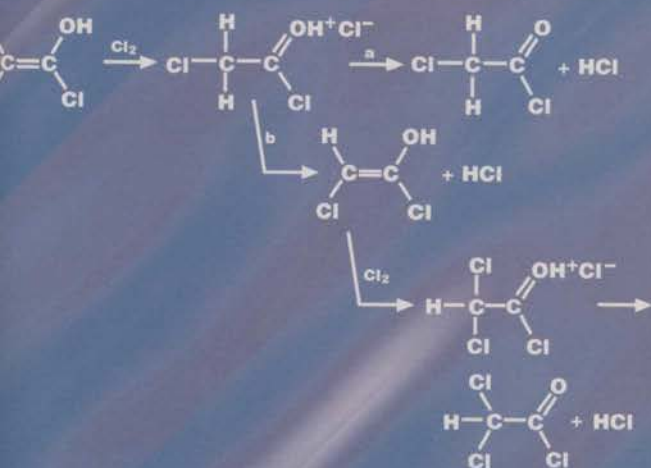
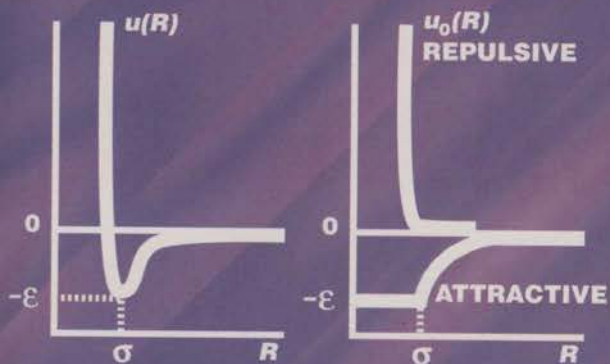
Literature Cited

- (1) Elvers, B.; Hawkins, S.; Schulz, G., Eds. *Ullmann's Encyclopedia of Industrial Chemistry*, Vol. A16, Magnetic Materials to Mutagenic Agents; VCH Publishers: New York, 1990; p 269.
- (2) Corneliussen, P. E., *Pestic. Monit. J.* **1969**, *2*, 140.
- (3) McFarland, R. B.; Reigel, H. J. *Occup. Med.* **1978**, *20*, 532.
- (4) Johnson, J. *Environ. Sci. Technol.* **1997**, *31*, 218A.
- (5) U.S. Environmental Protection Agency. *Mercury Study Report to Congress*, Vol. VIII; EPA-452/R-97-004; U.S. Government Printing Office: Washington, DC, December 1997.
- (6) Chu, P.; Porcella, D. B. *Water, Air Soil Pollut.* **1995**, *80*, 135.
- (7) Meij, R. *Water, Air, Soil Pollut.* **1991**, *56*, 21.
- (8) Chang, R.; Offen, G. *Power Eng.* **1995**, *99* (11), 51.
- (9) Krishnan, S. V.; Gullet, B. K.; Jozewicz, W. *Environ. Sci. Technol.* **1994**, *28*, 1506.
- (10) Matsumura, Y. *Atmos. Environ.* **1974**, *8*, 1321.
- (11) Liu, W.; Vidic, R. D.; Brown, T. D. *Environ. Sci. Technol.* **1998**, *32*, 531.
- (12) Korpel, J. A.; Vidic, R. D. *Environ. Sci. Technol.* **1997**, *31*, 2319.
- (13) Laudal, D. L.; Heidt, M. K.; Galbreath, K. C.; Nott, B. R.; Brown, T. D. Presented at the AWMA 90th Annual Meeting and Exhibition, Toronto, Ontario, Canada, June 8-13, 1997; Paper 97-WA72A.04.
- (14) Evans, A. P.; Nevitt, K. D. Presented at the AWMA 90th Annual Meeting and Exhibition, Toronto, Ontario, Canada, June 8-13, 1997; Paper 97-WP72B.07.
- (15) Walker, P. L., Jr., Ed. *Chemistry and Physics of Carbon*, Vol. 6; Marcel Dekker: New York, 1970; p 264.
- (16) Tessmer, C. H.; Vidic, R. D.; Uranowski, L. J. *Environ. Sci. Technol.* **1997**, *31*, 1872.
- (17) Hall, B.; Schager, P.; Lindqvist, O. *Water, Air, Soil Pollut.* **1991**, *56*, 3.

EXHIBIT F

INDUSTRIAL & ENGINEERING CHEMISTRY RESEARCH

A PUBLICATION OF THE AMERICAN CHEMICAL SOCIETY FOR APPLIED CHEMISTRY & CHEMICAL ENGINEERING



INDUSTRIAL & ENGINEERING CHEMISTRY RESEARCH

UNIVERSITY OF PITTSBURGH

APR 1 1 2000

COMPUTER SCIENCE LIBRARY

EDITOR

DONALD R. PAUL

Department of Chemical Engineering, University of Texas at Austin
Austin, Texas 78712-1062

(512) 471-5392; Fax (512) 471-0542

E-mail iecr@che.utexas.edu

ASSOCIATE EDITORS

Spiro D. Alexandratos
University of Tennessee

Lorenz T. Biegler
Carnegie-Mellon University

David T. Allen
University of Texas at Austin

Milorad P. Dudukovic
Washington University

John L. Anderson
Carnegie-Mellon University

Babatunde A. Ogunnaike
DuPont Central Research & Development

ADVISORY BOARD

Joan F. Brennecke
University of Notre Dame

Massimo Morbidelli
ETH Zürich

Joseph M. DeSimone
University of North Carolina—
Chapel Hill

K. J. L. Paciorek
Corona Del Mar, California

Christodoulos A. Floudas
Princeton University

Richard J. Quann
Mobil Technology Company

David S. Hacker
Highland Park, Illinois

G. V. Reklaitis
Purdue University

Bal K. Kaul
ExxonMobil Research &
Engineering Company

Steven F. Rice
Sandia National Laboratories

M. J. Lockett
Praxair, Inc.

Dominique Richon
Ecole des Mines de Paris,
France

William L. Luyben
Lehigh University

Robin D. Rogers
The University of Alabama

Paul Mathias
Aspen Technology, Inc.

Shivaji Sircar
Air Products

Patrick L. Mills
DuPont Company

P. R. Westmoreland
University of Massachusetts


**AMERICAN
CHEMICAL SOCIETY**

Science That Matters.

Quick...what
alerts you to
ACS Web Edition
Articles ASAP*?

[ASAP Alerts]

↑
It's Free!

Sign up today—it's FREE!

1. Go to <http://pubs.acs.org>
2. Click on the ASAP Alerts icon.
3. Complete the registration form.

*Articles ASAP[™] (As Soon As Publishable) delivers fully accepted articles within 48 hours of final author approval—in both HTML and PDF full-text formats—weeks before appearing in print—only from ACS.

ACS  WEB EDITIONS

Know it Now!

<http://pubs.acs.org>

SEPARATIONS

Novel Sorbents for Mercury Removal from Flue Gas

Evan J. Granite,* Henry W. Pennline, and Richard A. Hargis

National Energy Technology Laboratory, United States Department of Energy, P.O. Box 10940, Pittsburgh, Pennsylvania 15236-0940

A laboratory-scale packed-bed reactor system is used to screen sorbents for their capability to remove elemental mercury from various carrier gases. When the carrier gas is argon, an on-line atomic fluorescence spectrophotometer (AFS), used in a continuous mode, monitors the elemental mercury concentration in the inlet and outlet streams of the packed-bed reactor. The mercury concentration in the reactor inlet gas and the reactor temperature are held constant during a test. For more complex carrier gases, the capacity is determined off-line by analyzing the spent sorbent with either a cold vapor atomic absorption spectrophotometer (CVAAS) or an inductively coupled argon plasma atomic emission spectrophotometer (ICP-AES). The capacities and breakthrough times of several commercially available activated carbons as well as novel sorbents were determined as a function of various parameters. The mechanisms of mercury removal by the sorbents are suggested by combining the results of the packed-bed testing with various analytical results.

Introduction

Over 32% of anthropogenic mercury emissions in the United States are from coal-burning utilities. This percentage will increase over the next few years because of the mandated control of mercury emissions from municipal solid waste and medical waste incinerators. A low concentration of mercury, on the order of 1 ppbv, exists in flue gas when coal is burned. The primary forms in the flue gas are elemental mercury and mercuric chloride.¹

Control technologies for removing mercury from flue gas include scrubbing solutions and activated carbon sorbents. Mercuric chloride is soluble in water; elemental mercury is not. Dry sorbents have the potential to remove both elemental and oxidized forms of mercury. Activated carbons have been successfully applied for the control of mercury emissions from incinerators.^{1,2}

Several sorbents, such as activated carbons, can remove mercury from flue gas produced by the combustion of coal. However, there are problems associated with the use of activated carbons for mercury removal from flue gas. Activated carbons are general adsorbents; most of the components of flue gas will adsorb on carbon, with some in competition with mercury. Carbon sorbents operate effectively over a limited temperature range, typically working best at temperatures well below 300 °F. The projected annual costs for an activated carbon cleanup process are high, not only because of the high cost of the sorbent but also because of its poor utilization/selectivity for mercury. Carbon-to-mercury weight ratios of 3000:1 to 100 000:1 have been projected.^{1,3-5} In addition, activated carbons can only be regenerated a few times before they exhibit unac-

ceptably low activity for mercury removal. Therefore, the development of improved activated carbons as well as novel sorbents merits further research.

A sorbent can capture mercury via amalgamation, physical adsorption, chemical adsorption, and/or chemical reaction. The noble metal sorbents⁶⁻¹⁴ can capture mercury via amalgamation. Unpromoted activated carbons and aluminosilicates¹⁵ physisorb elemental mercury. Both amalgamation and physisorption are low-temperature processes, typically occurring below 300 °F. Chemically promoted (with sulfur, iodine, or chlorine) activated carbons,¹⁶⁻²¹ selenium,^{22,23} and manganese dioxide or hopcalite^{24,25} are examples of sorbents which chemisorb or chemically react with mercury. Chemisorption and chemical reaction can occur over a wider range of temperatures than physical adsorption and amalgamation. The enthalpy and activation energies of chemisorption/chemical reaction are typically larger than those for physical adsorption.

In this work, which is sponsored by the Advanced Research and Environmental Technology Power Subprogram of the U.S. Department of Energy's Fossil Energy Program, various sorbents were examined for the removal of elemental mercury from argon. It was realized that elemental mercury in flue gas would be more difficult to remove than oxidized mercury, and thus the thrust was to initially identify sorbents that could remove the less reactive elemental mercury. Very few techniques can be used to make an on-line and continuous determination of elemental mercury down to ppb levels, and the exact mechanism by which most sorbents remove mercury is unresolved. The atomic fluorescence spectrophotometer can be used to measure the concentration of elemental mercury in argon on a continuous basis²⁶ and was used in determining the breakthrough curves of sorbents in a packed bed. When more complex carrier gases were used, the capacity was

* To whom correspondence should be addressed. Tel.: (412) 386-4607. Fax: (412) 386-6004. E-mail: evan.granite@netl.doe.gov.

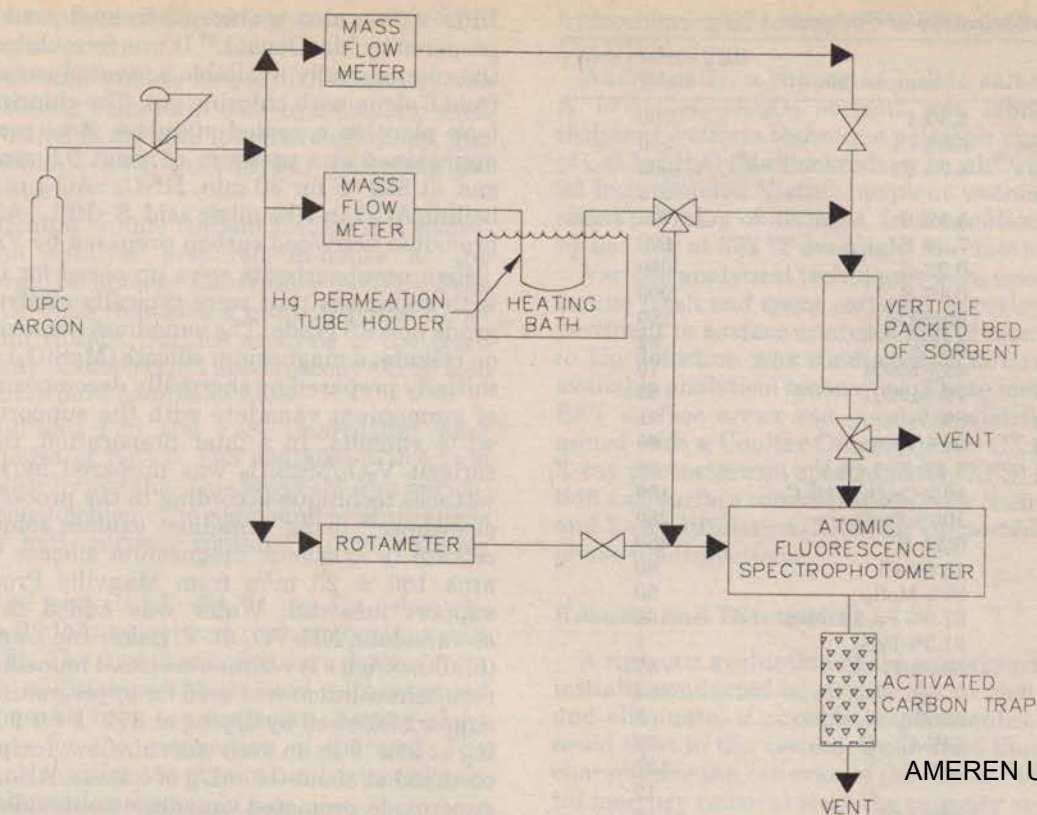


Figure 1. Schematic of sorbent screening unit.

determined off-line via ICP-AES or CVAAS. The capacities of several commercially available activated carbons, metal oxides, a halide salt, metal sulfides, silicates, chlorinated sorbents, a noble metal, and fly ashes were determined.

Experimental Procedures

The assembly used for measuring sorbent capacities consists of an elemental mercury permeation tube, a packed-bed reactor, an on-line atomic fluorescence spectrophotometer, and a data acquisition system. The reactor scheme is shown in Figure 1. A certified Dynacal permeation tube from VICI Metronics is used as the source of elemental mercury. The permeation tube has been certified by the manufacturer to release 144 ng of Hg/min at 212 °F. The permeation tube is located at the bottom of a Dynacal glass U-tube, which is maintained at 212 ± 1.6 °F at all times by immersing it in a Hacke L oil bath. A flow (30 mL/min) of ultra-high-purity carrier-grade (99.999%) argon gas passes over the permeation tube and is maintained at all times with a thermal conductivity mass flow controller. The output of the permeation tube and the flow rate of argon yields a calculated concentration of mercury in argon of 585 ppb. The mercury output of the tube has been verified on a monthly basis via weight loss measurement and has been found to be consistent (155 ng of Hg/min) with the certified release. After a year in service, the output of the permeation tube dropped to 139 ng of Hg/min and was replaced with a second certified tube rated for 119 ng of Hg/min. The output of this tube has also been verified by weight loss measurement and has been found to be consistent (107 ng/min) with the certified release. Sorbent capacities have all been normalized to reflect the output of the original permeation tube.

The reactor (adsorber) is a quartz tube (20 in. in length with an outer diameter of $\frac{1}{4}$ in. and inner

diameter of $\frac{1}{6}$ in.) held in a vertical position. All of the plumbing and valves which come into contact with mercury are constructed from either stainless steel or Teflon. These materials have been demonstrated to have good chemical resistance and inertness toward mercury. The packed bed of sorbent is surrounded by a large clam-shell furnace. A Self-tune Plus 300 PID controller is used to maintain the bed at the desired temperature. The temperature at the top of the bed has been determined to be within 1.8 °F of the temperature at the bottom of the bed.

The detector for elemental mercury is a Brooks Rand CVAFS-2 cold vapor atomic fluorescence spectrophotometer (AFS). When used as a continuous on-line monitor for elemental mercury in argon, the detection limit is below 0.1 ppb. The AFS is an ultraviolet (UV) detector for elemental mercury; mercury atoms absorb 253.7-nm light and re-emit (fluoresce) this wavelength. A mercury bulb serves as the UV source, and a photomultiplier tube serves as the UV fluorescence detector. Any gas can be used as a carrier, although sensitivity varies dramatically with inertness, because of quenching of the excited Hg atoms by collisions with polyatomic species. Maximum sensitivity (ppt) is achieved with high-purity argon or helium carrier gases. When the AFS was used as an on-line detector for elemental mercury, argon was used as the carrier gas. For the more complex carrier gases, the sorbent capacity was determined off-line by analyzing the spent sorbent with ICP-AES or CVAAS. The ICP-AES is a Perkin-Elmer Optima 3000 radial view spectrometer. The CVAAS is a Cetac M-6000A unit dedicated for the analysis of elemental mercury.

Key process parameters were recorded with a data acquisition system. This on-line data acquisition system was used to take and store the various voltage signals

Table 1. Characterization of Sorbents

sorbent	composition	BET surface area (m ² /g)
I-AC	3.5% I	750
Cl-AC-1	6.0% Cl	550
Cl-BPL-AC	6.7% Cl	1000
HNO ₃ -AC-1		575
S-BPL-AC	5.9% S	790
S-AC	7.6% S	690
AC-1	0.9% S	650
AC-2	0.4% S	900
celkate	MgSiO ₃	160
alumina	Al ₂ O ₃	82
MoO ₃ /MgSiO ₃	46% MoO ₃	70
MnO ₂ /Al ₂ O ₃	7% MnO ₂	65
V ₂ O ₅ -MgSiO ₃ -1	8% V ₂ O ₅	91
V ₂ O ₅ -MgSiO ₃ -2	50% V ₂ O ₅	60
KO ₂ -V ₂ O ₅	3.4% K, 1.4% V	85
Cr ₂ O ₃ /Al ₂ O ₃	13% Cr ₂ O ₃ , 11% C	156
Fe ₂ O ₃	100% Fe ₂ O ₃	250
TS-7	3.5% S	450
Cl-celkate	15.0% Cl	80
MoS ₂	87% MoS ₂	50
FeS	57.8% Fe, 22.6% S	32
FeS ₂	81.3% FeS ₂	1
CERF-FA-#2	59.3% C	37
CERF-FA-#4	37% C	24
FA-1	5% C	5
WCFA-1	64% C	32
WCFA-1-air-750F	50% C	127
Cl-WCFA-1		12
DCFA-1	29% LOI	16
DCFA-2	52% LOI	25
DCFA-3	82% LOI	34
CaCl ₂ /Al ₂ O ₃	10% CaCl ₂	41
Pt/wool	40% Pt	20

from the thermocouples, flowmeters, and the atomic fluorescence spectrophotometer. Data logging occurred every 15 s.

Typically, 10 milligram (mg) of 200/325-mesh (45–75- μ m) sorbent is placed in the center of the tube and is supported by about 50 mg of quartz wool. The quartz wool and reactor tube have been demonstrated to be inert toward elemental mercury. Separate argon gas streams flow through the bed and through the permeation tube holder. The latter flow is sent to the AFS to determine a baseline for the mercury concentration. Once thermal stability is reached in the reactor, the mercury/argon mixture is diverted to flow through the reactor. Breakthrough curves were generated by plotting the atomic fluorescence spectrophotometer voltage signal at the reactor exit versus time. Sorbent capacities were determined by integration under the breakthrough curve.

Sorbent Preparation

The sorbents examined in this study and their characterization are listed in Table 1. The sorbents I-AC, S-AC, AC-1, and AC-2 are commercially available activated carbons. I-AC is an iodine-promoted activated carbon, containing both elemental iodine and potassium iodide. S-AC is a sulfur-promoted activated carbon. AC-1 and AC-2 are unpromoted carbons from Calgon and CarboChem, respectively. Some typical mercury control applications for AC-1 include municipal waste combustors, hazardous waste combustors, and hospital waste incinerators.² AC-2 is a food-grade activated carbon used commercially for decolorizing corn syrup.

Cl-AC-1 is a chlorine-promoted activated carbon, prepared by boiling AC-1 in 37% hydrochloric acid. Cl-

BPL-AC is also a chlorine-treated activated carbon prepared by MacDonald.²⁷ It was formulated by treating the commercially available activated carbon BPL-AC from Calgon with chlorine gas. The chlorine treatment took place in a sealed stainless steel reaction vessel maintained at a pressure of about 0.5 atm of chlorine gas, at 330 °F for 30 min. HNO₃-AC-1 is prepared by boiling AC-1 in 70% nitric acid. S-BPL-AC is a sulfur-promoted activated carbon prepared by Vidic.¹⁷

Five novel sorbents were prepared for investigation with chemicals that were typically analytical reagent grade or ACS grade. The vanadium pentoxide dispersed on celkate, a magnesium silicate (MgSiO₃) support, was initially prepared by thermally decomposing a mixture of ammonium vanadate with the support to obtain 8 wt % vanadia. In a later preparation, the supported sorbent V₂O₅/MgSiO₃ was prepared by the incipient wetness technique according to the procedure outlined elsewhere²⁸ using vanadium oxalate solution and the celkate (a synthetic magnesium silicate with surface area 180 \pm 25 m²/g from Manville Products Corp.) support material. Water was added to ammonium *m*-vanadate, NH₄VO₃ (J. T. Baker Inc.), and oxalic acid (Mallinckrodt). A reaction occurred immediately and the resultant solution was used for impregnating the celkate support followed by drying at 572 °F for 2 h and calcining at 932 °F in an oven with air flow. Incipient wetness occurred at about 0.9 mL/g of celkate. Also, a potassium superoxide-promoted vanadium pentoxide (KO₂-V₂O₅) celkate-supported sorbent, whose preparation was similar to the preceding sorbent, was fabricated as well.

The supported sorbent MoO₃/MgSiO₃ was prepared by the incipient wetness technique by dissolution of ammonium molybdate, (NH₄)₆Mo₇O₂₄·4H₂O (Fisher Scientific Co.), with ammonium hydroxide in distilled water, and then contact with the celkate. The solution pH was 8. Impregnation was followed by drying at 248 °F for 24 h and then calcination at 932 °F for 6 h.²⁹

The alumina-supported MnO₂ sorbent was prepared by the incipient wetness technique using an aqueous solution of manganese nitrate, Mn(NO₃)₂·4H₂O (Sigma Chemical Corp.), with alumina, Al₂O₃ (Catalox SCFA 90 with surface area 82 \pm 25 m²/g from Condea Vista). Incipient wetness occurred at about 0.6 mL/g of alumina. Impregnation was followed by the thermal decomposition of manganese nitrate in air at 261 °F as outlined elsewhere.³⁰ Preliminary X-ray diffraction data did not show a MnO₂ diffraction pattern, indicating that the MnO₂ phase was well-dispersed over the alumina and that the crystallite size was below 5 nm.

The chromium oxide sorbent Cr₂O₃/Al₂O₃ that was obtained from Cadus was prepared by impregnation of alumina by chromic acid at room temperature for 30 min.³¹ Immediately after impregnation, the sorbent was dried overnight to 122 °F in a vacuum oven and then calcined at 1202 °F in air for 7 h.

MACH I Inc. supplied the ferric oxide sorbent Fe₂O₃. It was the Nanocat superfine iron oxide, which is a dark brown amorphous powder. The particle size is 3 nm.

The platinum sorbent Pt/wool was prepared by deposition of Engelhard metallo organic platinum ink upon quartz wool. The ink was fired in air at red heat to form a platinum film.

Pacific Northwest National Laboratory provided a novel self-assembled monolayer thiol-promoted aluminosilicate sorbent (TS-7). The sorbent was successfully applied to purify mercury-contaminated water streams.

This sorbent has a high BET surface area and is 3.5% sulfur by weight.

A chlorine-treated celkate sorbent (Cl-celkate) was prepared by boiling celkate in 37% hydrochloric acid. The slurry is boiled in air until it is thoroughly dry. The boiling hydrochloric acid turns green, indicating the evolution of chlorine.

The molybdenum sulfide sorbent (MoS_2) is a hydrodesulfurization catalyst prepared in-house at the National Energy Technology Laboratory (NETL). Bulk analysis by ICP-AES indicates a composition of 87 wt % molybdenum sulfide. Surface analysis of the fresh sorbent by X-ray photoelectron spectroscopy (XPS) also indicates a fairly pure sample of MoS_2 .

The iron sulfides FeS and FeS_2 (marcasite) were prepared in-house at NETL. FeS contains 57.8% iron and 22.6% sulfur by weight. This suggests iron enrichment as in a nonstoichiometric compound or multiphase mixture. The FeS_2 sorbent contains 81.3% FeS_2 by weight.

CERF-FA-#2 and CERF-FA-#4 are fly ashes obtained from a 35 lb/h pulverized coal combustion unit located at NETL. The fly ash samples were derived from the combustion of Pittsburgh #8 coal and were extracted from the furnace at high temperatures, having short residence times for the combustion of the coal. The resulting fly ash samples are atypical and extraordinarily high in unburned carbon.

Sorbents were prepared from fly ash in an effort to utilize unburned carbon from the fly ash. The starting material, FA-1, is fly ash obtained from the combustion of Blacksville coal in the 500 lb/h pilot-scale coal combustion unit located at NETL. FA-1 contains 5% carbon and has a BET surface area of $5 \text{ m}^2/\text{g}$. WCFA-1 is a unburned carbon separated from fly ash obtained from the 500 lb/hr combustion unit. The carbon is concentrated from the fly ash through a wet separation technique. WCFA-1 contains 64% carbon and has a BET surface area of $32 \text{ m}^2/\text{g}$.

Cl-WCFA-1 is a chlorine-treated carbon derived from fly ash. It is prepared by soaking WCFA-1 in aqua regia for 24 h and drying in air. Also, WCFA-1-air-750F is prepared by heating the carbon WCFA-1 in air at 750°F for 2 h. This is done to increase the BET surface area of the carbon.³² Thermal oxidation in air increases the microporosity of carbon resulting from the chemical reaction. WCFA-1 has a BET surface area of $32 \text{ m}^2/\text{g}$, whereas WCFA-1-air-750F has a higher surface area of $127 \text{ m}^2/\text{g}$. The oxidation in air decreases the carbon content from the original 64% down to 50%.

DCFA-1 is a fly ash that is high in carbon content because of poor combustion at a commercial utility; DCFA-2 and DCFA-3 are unburned carbon fractions separated from the DCFA-1 fly ash. The two carbon samples are obtained from the fly ash by a dry separation method (triboelectrostatic) where the first sample is a one-pass separation and the second is a two-pass separation. The elements present in these sorbents were determined via ICP-AES and are silicon, aluminum, iron, titanium, potassium, calcium, magnesium, phosphorus, and sodium. Sulfur, chlorine, and several other elements were not determined by ICP-AES, suggesting that the mass balances obtained (near 90%) are reasonable. Silicon and aluminum accounted for 70–80 wt % of these sorbents (excluding the carbon). These carbons were subsequently treated with chlorine by soaking in

hydrochloric acid to form Cl-DCFA-1, Cl-DCFA-2, and Cl-DCFA-3.

Additionally, a supported halide salt was prepared. A 10% $\text{CaCl}_2/\text{Al}_2\text{O}_3$ sorbent was fabricated by the incipient wetness technique using an aqueous solution of $\text{CaCl}_2 \cdot 2\text{H}_2\text{O}$ (Mallinckrodt) with Al_2O_3 (Catalox SCFA 90 from Condea Vista). Incipient wetness occurred at about 0.6 mL/g of alumina. Impregnation was followed by heating at 392°F overnight to remove the moisture.

Various analytical techniques were used to characterize the fresh and spent sorbents. A review of literature pertinent to surface analyses and of reports pertaining to Hg detection was conducted to determine the best available analytical techniques. These methods included BET surface areas and pore size distributions determined with a Coulter Omnisorp 100 CX apparatus, an X-ray photoelectron spectrometer (XPS) for Hg speciation and surface concentration, bulk chemical analyses, and X-ray diffraction (XRD) for supported oxide sorbent phase identifications.

Results and Discussion

A rigorous evaluation of the experimental setup was initially conducted in an attempt to identify, quantify, and eliminate, if possible, experimental artifacts that could exist in the system. Quantities that were used to characterize the behavior of the sorbent toward elemental mercury removal were the capacity and breakpoint. The capacity was defined as the amount of elemental mercury removed by the sorbent after 350 min on stream. When the continuous on-line AFS monitor for elemental mercury was used, the breakpoint was defined as the time when the outlet concentration of mercury emerging from the reactor bed equaled 10% of the inlet mercury concentration.

The reproducibility of the experimentally determined 350-min capacity and the 10% breakpoint were determined for the baseline sorbent, iodine-promoted activated carbon. Ten milligrams of 200/325-mesh iodine-promoted activated carbon was exposed to 585 ppb of elemental mercury in a $30 \text{ cm}^3/\text{min}$ flow of argon at 350°F in order to generate the breakthrough curves. This sorbent was used in this exercise because it represented the most reactive sorbent to date. The experiment was replicated with good results. The capacity determined via the on-line AFS in argon was reproducible to within $\pm 0.2 \text{ mg/g}$ and the breakpoint time to within $\pm 25\%$.

The capacity determined with the on-line AFS was compared with the results obtained from analyzing the spent sample with cold vapor atomic absorption spectrophotometry (CVAAS) and the inductively coupled argon plasma atomic emission spectrophotometer (ICP-AES). The on-line AFS is the most reliable technique for determining sorbent capacity. Unfortunately, this technique is primarily limited to argon (or other noble gas) or nitrogen carrier gas streams.³³ The AFS also has a detection limit for mercury which is an order of magnitude less than the detection limit for the atomic absorption spectrophotometer (AAS).

CVAAS is the next most reliable method for capacity determination and is the preferred analytical technique for the quantitative determination of trace levels of mercury in solids because of the elimination of the background matrix. Great care is taken to transfer the mercury into a noble carrier gas, providing good reproducibility. In CVAAS, the solid is dissolved into solution. Mercury is reduced from solution with tin chloride,

Table 2. Sorbent Experimental Results: Argon Carrier Gas

sorbent	capacity (mg/g) ^a	breakpoint (min)	temperature (°F)
I-AC	3.1		350
I-AC	4.8	330	350
S-AC	0.4	4	350
S-AC	3.5	7	280
S-BPL-AC	1.9		280
Cl-AC-1	4.0	70	280
Cl-BPL-AC	2.6		280
HNO ₃ -AC-1	1.2	3	280
AC-1	0.37		280
AC-2	0.4	4	280
celkate	0.5	2.5	350
alumina	0.6	2.5	140
MnO ₂ /Al ₂ O ₃	2.2	3	350
MnO ₂ /Al ₂ O ₃	2.4	11	280
MnO ₂ /Al ₂ O ₃	2.4	40	140
V ₂ O ₅ -MgSiO ₃ -1	0.4	3	350
V ₂ O ₅ -MgSiO ₃ -2	0.1	2	350
MoO ₃ /MgSiO ₃	0.2	3	350
Cr ₂ O ₃ /Al ₂ O ₃	1.2	2	140
Cr ₂ O ₃ /Al ₂ O ₃	3.1		280
Cr ₂ O ₃ /Al ₂ O ₃	3.3	9	350
Fe ₂ O ₃	0.1		280
TS-7	0.01 (ICP-AES)		150
Cl-celkate	0.8	0.5	280
MoS ₂	8.8 (ICP-AES)		280
MoS ₂	3.9		280
MoS ₂	3.6	17	280
MoS ₂	4.5	194	140
FeS	cap < 0.01		280
FeS ₂	0.2		280
CERF-FA-#2	1.7	4	280
CERF-FA-#2	1.4		280
CERF-FA-#4	2.2	20	280
CERF-FA-#4	1.7		280
FA-1	0.02		280
WCFA-1	0.1		280
WCFA-1	0.04		350
Cl-WCFA-1	2.5		280
Cl-WCFA-1	0.64		350
DCFA-1	0.03		280
DCFA-2	0.12		280
DCFA-3	0.15		280
Cl-DCFA-1	0.24		280
Cl-DCFA-2	0.30		280
Cl-DCFA-3	0.41		280
Pt/wool	5.0		280
CaCl ₂ /Al ₂ O ₃	0.6	2	140

^a Capacity determined via on-line AFS when a breakpoint time is given; otherwise, the capacity was determined by CVAAS, except as noted.

aerated onto a gold trap, thermally desorbed from the gold trap, and swept into an argon stream to an ultraviolet (AAS) detector. Chemical (tin chloride reduction) and physical (amalgamation) steps are taken to separate the mercury. The detection limit of CVAAS is 10 ng/g.³⁴ The typical precision for measurement of mercury concentrations in solids is 5–10% relative standard deviation.³⁴ A comparison of capacity determinations via the on-line AFS and CVAAS shown in Tables 2 and 3 for I-AC in argon at 350 °F, MoS₂ in argon at 280 °F, CERF-FA #2 in argon at 280 °F, and CERF-FA #4 in argon at 280 °F shows a fair agreement.

The ICP-AES is the least reliable of the three techniques for trace-level mercury determinations. It can be seen from Table 2 that the ICP-AES yields capacities which are high by a factor of 2. The ICP-AES is the most versatile tool for multielement analysis, but it is not the preferred method for trace-level mercury measurements in solids. No steps are taken to separate the mercury from the other elements present in the solid sample.

Table 3. Sorbent Experimental Results: Air Carrier Gas

sorbent	capacity (mg/g)	analysis method	temperature (°F)
KO ₂ -V ₂ O ₅	0.02	CVAAS	280
KO ₂ -V ₂ O ₅	0.04	CVAAS	350
MnO ₂ /Al ₂ O ₃	3.50	CVAAS	280
TS-7	0.00	ICP-AES	140
S-BPL-AC	0.53	ICP-AES	280
S-BPL-AC	0.28	ICP-AES	350
MoS ₂	5.6	ICP-AES	140
MoS ₂	5.2	ICP-AES	280
MoS ₂	1.1	ICP-AES	350
AC-1 ^a	0.04	CVAAS	280
AC-1 ^a	0.19	AFS	280

^a 4% O₂ in N₂ carrier gas.

Other elements could interfere in the detection of mercury. For example, the cobalt emission line at 253.649 nm could interfere in the determination of mercury by the 253.652-nm emission line.³⁵ The concentration of the interfering element (in this case cobalt), monochromator slit width, and relative intensity of the shared emission line are factors in determining the extent of spectral interference. Experiments with the Perkin-Elmer Optima 3000 radial view ICP-AES confirmed that cobalt will interfere in the trace-level determination of mercury in solids. Additionally, because of their emission lines close to 253.7 nm, iron and manganese³⁶ will also interfere in the determination of mercury by ICP-AES.

The effect of intraparticle mass-transfer resistance due to the diffusion of mercury within the pores was determined by carrying out the same experiment but with various size fractions of the baseline iodine-promoted activated carbon. For a sub-400-mesh size fraction of the same carbon, the 350-min capacity was 4.9 mg of Hg/g and the breakpoint was 405 min. This is in good agreement with the data for the larger size fraction (see I-AC in Table 2), suggesting that mass-transfer resistance due to the diffusion of mercury into the sorbent at the sizes used in the testing is negligible. Calculations further indicated that bulk mass-transfer effects, heat-transfer effects, channeling, and pressure drop would not be significant in the experimentation.

Most of the experiments used a gas feed of 585 ppb elemental mercury in argon. This is dramatically different than the composition of a typical flue gas from a coal-fired utility. Most of the components in a typical flue gas (e.g., acid gases, etc.) can adsorb on an activated carbon and could possibly hinder or help the adsorption of mercury on carbon. As pointed out above, the ultra-high-purity argon carrier gas was selected to maximize the sensitivity of the AFS for elemental mercury. However, the capacity of the sorbents in argon can be quite different from the capacity in flue gas. Also, the temperatures at which sorbent capacities were typically determined are 140, 280, and 350 °F. These temperatures were chosen because of their potential relevance to coal-fired utilities. If a sorbent were contacted with the flue gas by injection into the duct work of a coal-fired utility after the air preheater but before the particulate collection device, it would experience temperatures in the range of 350–280 °F. If a sorbent was placed downstream of a wet scrubber, it would encounter a temperature near 140 °F.

The 350 min capacities and the 10% breakpoint times for the sorbents are listed in Table 2. The baseline sorbent—the iodine-promoted activated carbon—exhibited

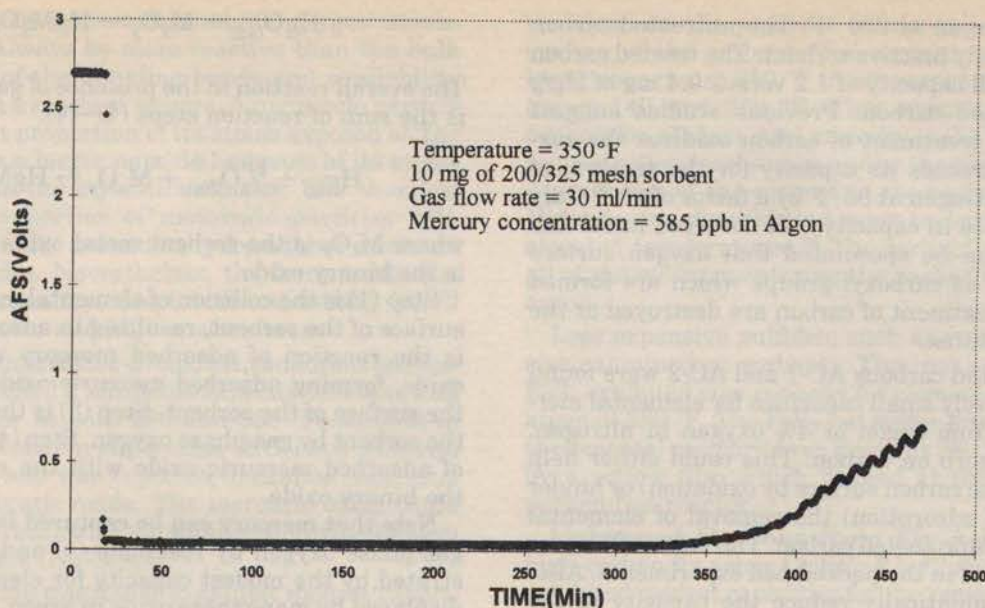


Figure 2. Breakthrough curve for I-AC using the AFS for mercury detection.

both the largest, most reliably determined (on-line AFS) capacity and longest breakpoint time. A typical breakthrough curve for the iodine-promoted activated carbon is shown in Figure 2.

Activated Carbons. With the activated carbons, the effect of the chemical promoter on the capacity for elemental mercury was determined by comparing the capacities of the commercially available unpromoted carbon with the capacities of the sulfur, iodine, chlorine, and nitric acid-treated carbons at the same temperature. The sulfur- and iodine-promoted carbons are available commercially. The carbons, when chemically promoted, exhibited a far greater capacity for elemental mercury. An unpromoted carbon primarily captures elemental mercury via physical adsorption. Chemically promoted carbons capture elemental mercury by both physical adsorption and chemisorption/chemical reaction, where mercuric sulfide, mercuric iodide, and so forth formation enables the promoted carbons to remove more elemental mercury.

Various analyses were performed on the spent baseline iodated carbon sorbent to elucidate the role of the promoter. A 3-day run in the packed bed was performed on 35 mg of iodated activated carbon so that gross differences, if any, between the fresh sorbent and spent sorbent could be differentiated by the BET surface analysis. Results indicate a reduction in surface area from 780 to 300 m²/g. Additionally, after it was determined that the vacuum treatment would not impact the mercury concentration, XPS studies with the spent iodated activated carbon showed that the Hg species on the surface was oxidized and in the form of HgI₂; no elemental Hg was detected. Potassium iodide was also detected. The total iodide concentration was 0.4% atomic and the Hg surface concentration was 0.13% atomic. Also, the capacity of the spent iodine-promoted carbon was confirmed by atomic absorption analysis. The used sorbent was digested in acid, and the concentration of mercury in the solution was measured by an atomic absorption spectrophotometer. The capacity (gaseous determination) of the iodine-promoted carbon found by integration under the breakthrough curve (4.8 mg/g)

was in reasonably good agreement with the capacity (solid determination) established by atomic absorption (3.1 mg/g).

The effect of flue gas temperature was studied by examining the breakthrough curves for the sulfur-promoted carbon S-AC at 280 and 350 °F. The capacity of this carbon at 280 °F was 3.5 versus 0.4 mg of Hg/g at 350 °F. As many studies have demonstrated, activated carbons perform much better at lower temperatures. The temperatures at which activated carbons have been reported to possess good capacities for mercury range from 70 to 500 °F.^{1-6,13,16-19,23,37-46} This suggests that physical adsorption may be the first step in the removal of mercury for both unpromoted and promoted carbons. Physical adsorption, analogous to condensation, is a low-temperature process. For a chemically promoted carbon, such as sulfur-impregnated carbon, chemisorption/reaction between the physically adsorbed mercury and sulfur promoter to form mercuric sulfide could be the second step in the mechanism of mercury removal.

The hydrochloric acid-treated activated carbon Cl-AC-1 exhibited a large capacity of 4.0 mg of Hg/g when tested in argon at 280 °F, making it one of the most active sorbents studied to date. Additionally, the chlorine gas-treated activated carbon, Cl-BPL-AC, exhibited a modest capacity for elemental mercury removal. One previous study suggests that hydrochloric acid treatment yields activated carbons which have chemisorbed chlorine.⁴⁷ Quimby demonstrated that HCl-treated activated carbon will adsorb mercuric chloride from air at 300 °F.²¹ Mercury is known to primarily form the tetrachloromercury complex HgCl₄²⁻ on the surface of activated carbons used for the removal of mercuric chloride from wastewater; little mercuric chloride was found on the surface of these carbons.⁴⁸ Other prior studies have shown that HCl treatment of silica increases its capacity for mercury. It can be speculated that elemental mercury reacts with chemisorbed chlorine to form the tetrachloromercury complex on the surface of the carbon.

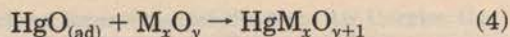
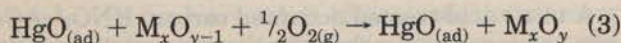
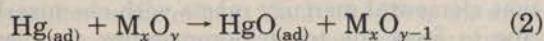
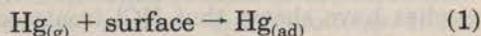
A nitric acid-treated activated carbon, HNO₃-AC-1, was examined as a sorbent for the removal of elemental

mercury from argon at 280 °F. The untreated carbon AC-1 is a relatively inactive sorbent. The treated carbon exhibited a small capacity of 1.2 versus 0.4 mg of Hg/g for the untreated carbon. Previous studies suggest that nitric acid treatment of carbon oxidizes the surface^{20,47} and increases its capacity for the removal of mercury from nitrogen at 86 °F by a factor of 20.²⁰ Only a modest increase in capacity was observed in our lab at 280 °F. It can be speculated that oxygen surface complexes such as carboxyl groups which are formed by nitric acid treatment of carbon are destroyed at the higher temperatures.

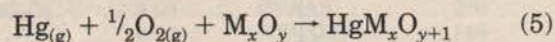
The unpromoted carbons AC-1 and AC-2 were found to possess relatively small capacities for elemental mercury, whether from argon or 4% oxygen in nitrogen. Oxygen will adsorb on carbon. This could either help (by promoting the carbon surface by oxidation) or hinder (by competitive adsorption) the removal of elemental mercury by an unpromoted carbon. The latter effect was probably observed in the packed-bed experiments. Also, oxygen may dramatically reduce the capacity of the sulfur-promoted carbon as the capacity dropped from 3.5 mg/g in argon for S-AC to 0.5 mg/g in air at 280 °F for S-BPL-AC. S-AC and S-BPL-AC both exhibit high capacities for elemental mercury from inert carrier gases.¹⁷ This suggests that oxygen competitively adsorbs on sulfur, reducing the capacity.

The results obtained from the packed-bed unit require judicious interpretation when attempting to extrapolate their relevance to activated carbon sorbent duct injection as a mercury control technique for industrial size combustors. AC-1 was also studied in the NETL 500 lb of coal/h pilot-scale combustor unit for the removal of mercury from the flue gas.⁴⁹ When introduced at a large sorbent-to-mercury ratio of around 5000:1, AC-1 used in the 500 lb/h unit achieved a high level of mercury removal. However, the used AC-1 recovered from the baghouse had mercury levels of less than 300 ppm (0.3 mg of Hg/g), but a high level of mercury removal is achieved. Unpromoted activated carbons sequester elemental mercury via physical adsorption and therefore exhibit small capacities. Duct injection at large sorbent-to-mercury ratios from 5000:1 to 100 000:1 allows them to, nevertheless, achieve high levels of removal of mercury from flue gas.

Metal Oxides. Metal oxides are proposed as novel alternatives to activated carbon sorbents. It is noted that there are many binary oxides of mercury, such as mercury vanadates, mercury molybdates, and mercury manganates.⁵⁰⁻⁵² Vanadium pentoxide, molybdenum trioxide, and manganese dioxide are all partial oxidation oxide catalysts for the oxidation of various hydrocarbons.^{26,53} In the oxidation of various hydrocarbons, lattice oxygen serves as the oxidant in a Mars-Maessen mechanism. This suggests that lattice oxygen of partial oxidation oxides could also serve as the oxidant of mercury. The reaction mechanism for the capture of mercury by oxide catalysts can be written as



The overall reaction in the presence of gas-phase oxygen is the sum of reaction steps (1)–(4):



where M_xO_y is the sorbent metal oxide and $\text{HgM}_x\text{O}_{y+1}$ is the binary oxide.

Step (1) is the collision of elemental mercury with the surface of the sorbent, resulting in adsorption. Step (2) is the reaction of adsorbed mercury with the metal oxide, forming adsorbed mercuric oxide and reducing the surface of the sorbent. Step (3) is the reoxidation of the sorbent by gas-phase oxygen. Step (4) is the reaction of adsorbed mercuric oxide with the sorbent to form the binary oxide.

Note that mercury can be captured in the absence of gas-phase oxygen by reactions (1) and (2), as demonstrated by the modest capacity for elemental mercury displayed by manganese oxide in argon, shown in Table 2. There are many potential rate-limiting factors which can impact oxide capacity for mercury, including surface area, activity of the sorbent as an oxidation catalyst, stability of lower oxides, oxygen partial pressure, and tendency to form the binary oxide. Mercury is a semi-noble metal with a standard reduction potential similar to palladium's. Mercury may not be easily oxidized by the metal oxide sorbent. An oxide's tendency to form sulfates is a critical factor for sorbent performance in flue gas because sulfur dioxide is present at concentrations orders of magnitude greater than mercury's.

Alumina (Al_2O_3) or celkate (MgSiO_3), which were used as supports for some of the novel sorbents, were examined as sorbents for the removal of elemental mercury from argon. Both exhibit small capacities, demonstrating their inertness toward elemental mercury. The role of the alumina or celkate support is to provide a high surface area substrate for maximizing the number of collisions between mercury and the sorbent.

Supported vanadium pentoxide and supported molybdenum trioxide exhibited low capacities for the removal of elemental mercury from argon at 350 °F. Preparation of the V_2O_5 -supported sorbent either via the thermal decomposition of ammonium vanadate or via incipient wetness did not impact the sorbent capacity. Manganese dioxide supported on alumina was examined as a sorbent for the removal of elemental mercury from argon at 350, 280, and 140 °F. Manganese dioxide has been reported to remove elemental mercury from both air and argon at room temperature.^{24,25} MnO_2 exhibited modest 350-min capacities of 2.2 mg of Hg/g at the higher temperature and 2.4 mg of Hg/g, at both 140 and 280 °F.

In the Mars-Maessen mechanism, gas-phase oxygen can serve to reoxidize the reduced oxide. Oxygen was absent from the gas phase in these experiments. Manganese dioxide is the most powerful oxidation catalyst⁵³ of the oxide oxidation catalysts examined and exhibited the largest capacity for mercury. A Mars-Maessen redox mechanism for the removal of mercury has been proposed above for partial oxidation oxide sorbents. The capacity of the manganese dioxide sorbent was observed to be larger in air than in argon at 280 °F (see Table 3).

Nanoscale iron oxide was examined as a sorbent for mercury removal from argon at 280 °F. Each particle

contains about 600 iron atoms and 900 oxygen atoms. A surface will always be more reactive than the bulk lattice because of the dangling bonds and availability for collision with a reactant species. A nanoscale particle has a significant proportion of its atoms exposed on the surface whereas a larger particle has most of its atoms contained within the crystalline lattice. The chemical and physical properties of nanoscale particles will, therefore, often differ dramatically from those exhibited by larger particles. Nevertheless, the ferric oxide displayed a poor capacity, despite the unusually small (3-nm) particle size and high surface area.

A potassium superoxide-promoted vanadium pentoxide sorbent exhibited a miniscule capacity for elemental mercury from air at both 280 and 350 °F, as seen in Table 3. The potassium superoxide (KO_2) is a powerful oxidizing agent and was expected to oxidize elemental mercury to mercuric oxide. The mercuric oxide could then chemisorb/react with vanadium pentoxide to form mercury vanadate (HgV_2O_6).

Chromium oxide was found to exhibit modest capacities for elemental mercury. Cr_2O_3 is a fairly strong oxidation catalyst, with a catalytic activity for the deep oxidation of methane comparable to manganese dioxide.⁵³ A crude correlation was found between the catalytic activity for deep oxidation exhibited by the oxide and the sorbent capacity for elemental mercury removal. Sorbents that are active catalysts for the deep oxidation of methane $\text{Cr}_2\text{O}_3/\text{Al}_2\text{O}_3$ and $\text{MnO}_2/\text{Al}_2\text{O}_3$ exhibit large capacities, whereas the inactive oxide catalysts Fe_2O_3 , $\text{MoO}_3/\text{Al}_2\text{O}_3$, and $\text{V}_2\text{O}_5\text{-MgSiO}_3\text{-1}$ show small capacities.

Promotion of metal oxide supports was also investigated. The chlorine-promoted magnesium silicate Cl-celkate exhibited a small capacity for the removal of elemental mercury from argon at 280 °F. Braman demonstrated that HCl-treated Chromosorb-W, a diatomite chromatographic packing, will adsorb mercuric chloride vapors at 70 °F.⁷ Additionally, the novel thiol-promoted aluminosilicate sorbent (TS-7) exhibited very small capacities for elemental mercury both in argon and in air. Thiols are the sulfur analogues of alcohols. Thiols are also called mercaptans, from the Latin, *mercurium captans*, meaning "capturing mercury".⁵⁴ Mercaptans react with mercuric ions and the ions of other heavy metals to form precipitates. The sorbent was developed for the removal of oxidized mercury from contaminated water. Elemental mercury is insoluble in water. Oxidized forms of mercury are known to react efficiently with thiols. The low decomposition temperatures of thiols as well as the lack of reactivity with elemental mercury suggest that thiols are not practical promoters for the removal of elemental mercury from flue gas.

Metal Sulfides. Molybdenum sulfide (MoS_2) displayed a large capacity for the removal of elemental mercury from argon and air. This sorbent was originally developed as a hydrodesulfurization catalyst for the conversion of thiopene and mercaptans to hydrogen sulfide and alkanes. A possible mechanism of mercury capture is chemisorption/chemical reaction to form mercuric sulfide. XPS analysis of the used sorbent run in argon at 280 °F confirms the presence of mercury on the surface. Elemental mercury was not detected on the surface of the used MoS_2 sorbent. This rules out physical adsorption of elemental mercury as the primary means of sequestration. The X-ray excited photoelectron spec-

tra suggests the presence of mercuric sulfide on the surface of the sorbent. The sorbent exhibits a much lower capacity at 350 °F in air versus the capacities in air at 140 and 280 °F. This suggests that physical adsorption of elemental mercury is the first step in the sequestration mechanism and/or the physical-chemical degradation of the sorbent at the higher temperature. Molybdenum disulfide is known to decompose in air at elevated temperatures.³⁶ The sorbent removed nearly all of the mercury entering the packed bed at 140 °F in argon.

Less expensive sulfides, such as iron sulfides, were also examined as sorbents. The iron sulfides FeS and FeS_2 exhibited poor capacity for elemental mercury from argon at 280 °F. The FeS_2 lost sulfur during the sorption of elemental mercury from argon at 280 °F, as evidenced by a yellow film which formed at the bottom of the packed-bed reactor.

Unburned Carbons from Fly Ash. The atypical high-carbon fly ashes CERF-FA-#2 and CERF-FA-#4 exhibited modest capacities for the removal of elemental mercury from argon at 280 °F. These capacities are, however, significantly higher than those exhibited by the unpromoted carbon and the alumina and celkate supports. Further characterization of these fly ash sorbents is needed to determine the mechanism of mercury capture. These carbons were extracted from the combustor at high temperatures of around 2300 °F. It is speculated that novel forms of carbon present in these samples could positively impact capacity.

The fly ash obtained from the combustion of Blacksville coal, FA-1, exhibited a miniscule capacity for elemental mercury at 280 °F. The carbon separated from this fly ash, WCFA-1, exhibited a small capacity for the removal of elemental mercury from argon at 280 °F. Nevertheless, WCFA-1 does exhibit a larger capacity than the parent fly ash, FA-1. The capacity of WCFA-1 was smaller at 350 °F, as expected. The unpromoted activated carbons show similarly low capacities. The chlorine-promoted carbon extracted from fly ash, Cl-CFA-1, exhibited a much larger capacity for elemental mercury, much like the chlorine-promoted activated carbons. The capacity was lower at the higher temperature, as expected.

DCFA-2 and DCFA-3 are carbons separated from the parent fly ash, DCFA-1, by a dry separation method and exhibit small capacities for elemental mercury. The capacity increases with increasing carbon content. The chlorine-treated materials Cl-DCFA-1, Cl-DCFA-2, and Cl-DCFA-3 showed significantly larger, but still small, capacities. The capacity again increases with increasing carbon content.

Halide salts are also proposed as an alternative to carbon sorbents. There are many binary halides of mercury such as calcium chloromercurate and potassium iodomercurate.⁵⁰ These are double salts of calcium chloride and mercuric chloride and potassium iodide and mercuric iodide, respectively. Potassium iodide is used as a chemical promoter in some of the commercially available activated carbons,^{18,19} such as the baseline sorbent in this study. However, the thermal stability of the binary halides of mercury is poor, as evidenced by their low decomposition temperatures.⁵⁰ Mercuric chloride was absent from the gas phase in these experiments. The absence of mercuric chloride could explain the small capacity exhibited by the calcium chloride sorbent. Mercuric chloride can be present in the flue gas

obtained from the combustion of coal, municipal waste, and medical waste.¹

Noble Metals. The platinum sorbent Pt/wool exhibited a large capacity for elemental mercury from argon at 280 °F. Breakthrough was not observed. After the absorption experiment, the used Pt/wool sorbent was slowly heated in argon to 770 °F over a 70-min period, with the effluent sent directly to the AFS. Over 99.4% of the mercury remained sequestered on the platinum. A minor desorption spike of mercury was observed at 320 °F, likely due to unburned carbon from the organometallic platinum paint precursor. The noble metals are often used for small-scale sampling of gases for mercury, i.e., mercury is often collected on gold, thermally desorbed, and sent to a UV detector for its analytical determination. Thermal desorption of the mercury is accomplished by heating the noble metal to 1470 °F,¹³ greater than the 770 °F maximum temperature in the desorption experiment.

Conclusions

A packed-bed reactor system was used to screen sorbents for the removal of elemental mercury from a carrier gas. An on-line atomic fluorescence spectrophotometer was used to measure elemental mercury in argon on a continuous basis. For more complex carrier gases, sorbent capacities were determined off-line via CVAAS or ICP-AES. Chemically promoted activated carbons exhibit a far greater capacity for mercury than unpromoted carbons. The activated carbons possess higher capacities at lower temperatures. Chlorine could be a cost-effective chemical promoter for carbon sorbents for the removal of mercury.

Metal oxides and sulfides are proposed as a possible alternative to activated carbon sorbents, with MnO₂, Cr₂O₃, and MoS₂ exhibiting moderate capacities for mercury removal among the candidates investigated. Unburned carbon sorbents from fly ash typically showed poor performance toward mercury removal, although promotion of these increases the activity for elemental mercury removal. Future work will concentrate on testing inexpensive chlorine-promoted carbons as well as metal oxides and sulfides in a simulated flue gas matrix which includes acid gases, oxygen, water, and mercuric chloride. Promising sorbent candidates will be further evaluated on a pilot-scale system.^{49,55}

Acknowledgment

Evan Granite acknowledges the support of a post-doctoral fellowship at the U.S. Department of Energy administered by Oak Ridge Institute For Science and Education (ORISE). George Haddad, also through the ORISE program, provided project support. Michael Hilterman, Edward Zagorski, Dennis Stanko, Sheila Hedges, John Baltrus, Mac Gray, Yee Soong, Rod Diehl, Murphy Keller, Mark Freeman, Anthony Cugini, James Hoffman, Karl Schroeder of the Department of Energy, Robert Thompson and Joseph Niedzwicki of Parsons Infrastructure, Donald Floyd of EG&G Technical Services, and Mark Wesolowski of SSI Services, Inc. provided outstanding technical assistance. Several individuals and organizations provided sorbent samples for examination by the DOE. Professor Radisav Vidic of The University of Pittsburgh supplied a sulfur-promoted carbon sorbent. Professor Jayne MacDonald of the Royal Military College of Canada provided a chlorinated carbon sample. CarboChem Inc. donated

an unpromoted activated carbon sorbent. Dr. Shas Mattigod of Pacific Northwest National Laboratory provided the thiol-promoted aluminosilicate. Professor Luis Cadus of INTEQUI Instituto de Investigaciones en Tecnologia Quimica, San Luis, Argentina supplied the chromium oxide sorbent. Dr. John Stencil of the Kentucky Center For Applied Energy Research provided carbons derived from fly ash. MACH I Inc. of King of Prussia Pennsylvania contributed the iron oxide sample.

Disclaimer

Reference in this paper to any specific commercial product, process, or service is to facilitate understanding and does not necessarily imply its endorsement by the U.S. Department of Energy.

Literature Cited

- (1) *Mercury Study Report to Congress*; EPA 452/R-97-003; U. S. Environmental Protection Agency, Office of Air Quality Planning and Standards: Washington, DC, Dec 1997.
- (2) *Flue Gas Treatment Reference Bulletin*; Calgon Carbon Corporation: Pittsburgh, PA, Nov 1994.
- (3) Ghorishi, B.; Jozewicz, W.; Gullet, B. K.; Sedman, C. B. Mercury Control: Overview of Bench-Scale Research at EPA/APPCC. Presented at the First Joint Power & Fuel Systems Contractors Conference, Pittsburgh, PA, July 1996.
- (4) Waugh, E. G.; Jensen, B. K.; Lapatnick, L. N.; Gibbons, F. X.; Haythornthwaite, S.; Sjostrom, S.; Ruhl, J.; Slye, R.; Chang, R. Mercury Control on Coal-Fired Flue Gas Using Dry Carbon-Based Sorbent Injection: Pilot-Scale Demonstration. Presented at the Fourth International Conference on Managing Hazardous Air Pollutants, Washington, DC, Nov 1997.
- (5) Brown, T. D.; Smith, D. N.; Hargis, R. A.; O'Dowd, W. J. Mercury Measurement and Its Control: What We Know, Have Learned, and Need to Further Investigate. *J. Air Waste Manage. Assoc.* **1999**, *6*, 1.
- (6) Attari, A.; Chao, S. Trace Constituents in Natural Gas; Sampling and Analysis. *Oper. Sect. Proc. Am. Gas Assoc.* **1994**, *28-32*.
- (7) Braman, R. S.; Johnson, D. L. Selective Absorption Tubes and Emission Technique for Determination of Ambient Forms of Mercury in Air. *Environ. Sci. Technol.* **1974**, *8* (12), 996.
- (8) Williston, S. H. Mercury in the Atmosphere. *J. Geophys. Res.* **1968**, *73* (22), 7051.
- (9) Henriques, A.; Isberg, J.; Kjellgren, D. Collection and Separation of Metallic Mercury and Organo-mercury Compounds in Air. *Chem. Scr.* **1973**, *4* (3), 139.
- (10) Henriques, A.; Isberg, J. A New Method for Collection and Separation of Metallic Mercury and Organomercury Compounds in Air. *Chem. Scr.* **1975**, *8* (4), 173.
- (11) Roberts, D. L.; Stewart, R. M. Novel Process for Removal and Recovery of Vapor Phase Mercury. Presented at the First Joint Power & Fuel Systems Contractors Conference, Pittsburgh, PA, July 1996.
- (12) Yan, T. Y. A Novel Process for Hg Removal from Gases. *Ind. Eng. Chem. Res.* **1994**, *33*, 3010.
- (13) Dumarey, R.; Dams, R.; Hoste, J. Comparison of the Collection and Desorption Efficiency of Activated Charcoal, Silver, and Gold for the Determination of Vapor-Phase Atmospheric Mercury. *Anal. Chem.* **1985**, *57*, 2638.
- (14) Roberts, D. Novel Process for Removal and Recovery of Vapor-Phase Mercury. Presented at the Advanced Coal-Based Power and Environmental Systems '97 Conference, Pittsburgh, PA, July 1997.
- (15) Livengood, C. D.; Huang, H. S.; Mendelsohn, M. H.; Wu, J. M. Enhancement of Mercury Control in Flue Gas Cleanup Systems. Presented at the First Joint Power & Fuel Systems Contractors Conference, Pittsburgh, PA, July 1996.
- (16) Walker, P. L.; Sinha, R. K. Removal of Mercury by Sulfurized Carbons. *Carbon* **1972**, *10*, 754.
- (17) Korpel, J.; Vidic, R. Effect of Sulfur Impregnation Method on Activated Carbon Uptake of Gas-Phase Mercury. *Environ. Sci. Technol.* **1997**, *31* (8), 2319.
- (18) *Material Safety Data Sheet for Activated Carbon 717*; Barnebey & Sutcliffe: Columbus, OH, Sept 1996.

- (19) Carbon Product Bulletin HGR-LH; Calgon Carbon Corp.: Pittsburgh, PA, Feb 1994.
- (20) Matsumura, Y. Adsorption of Mercury Vapor on the Surface of Activated Carbons Modified by Oxidation or Iodization. *Atmos. Environ.* **1974**, *8*, 1321.
- (21) Quimby, J. M. Mercury Emissions Control From Combustion Systems. Proceedings of Annual Meeting, Air Waste Management Association: Pittsburgh, PA, 1993.
- (22) Hogland, W. K. H. Usefulness of Selenium for the Reduction of Mercury Emissions From Crematoria. *J. Environ. Qual.* **1994**, *23*, 1364.
- (23) Tsuji, K.; Shiraishi, I.; Olson, D. G. EPRI Report no. TR-105258; EPRI: Palo Alto, CA, 1995; conf-950332, Vol. 3, pp 66.1-66.15.
- (24) Janssen, J.; Van Den Enk, J.; De Groot, D. Determination of Total Mercury in Air by Atomic Absorption Spectrometry After Collection on Manganese Dioxide. *Anal. Chim. Acta* **1977**, *92*, 71.
- (25) Rathje, A.; Marcero, D.; Dattilo, D. Personal Monitoring Technique for Mercury Vapor in Air and Determination by Flameless Atomic Absorption. *J. Am. Ind. Hyg. Assoc.* **1974**, *35*, 571.
- (26) Granite, E. J.; Pennline, H. W.; Hargis, R. A. Sorbents For Mercury Removal From Flue Gas. *Topical Report DOE/FETC/TR-98-01*; National Energy Technology Laboratory: Pittsburgh, PA, Jan 1998.
- (27) MacDonald, J.; Evans, M.; Halliop, E.; Liang, S. The Effect of Chlorination On Surface Properties Of Activated Carbon. *Carbon* **1998**, *36*, 6 (11), 1677.
- (28) Oyama, S. T.; Went, G. T.; Lewis, K. B.; Bell, A. T.; Somarjai, G. A. *J. Phys. Chem.* **1989**, *93*, 6786.
- (29) Mahipal Reddy, B.; Padmanabha Reddy, E.; Srinivas, S. T. *J. Catal.* **1992**, *136*, 50.
- (30) Maltha, A.; Favre, T. L. F.; Kist, H. F.; Zuur, A. P.; Ponec, V. *J. Catal.* **1994**, *149*, 364.
- (31) Mentasty, L.; Gorriz, O.; Cadus, L. Chromium Oxide Supported on Different Al₂O₃ Supports. *Ind. Eng. Chem. Res.* **1999**, *38*, 396.
- (32) MacDonald, J. A. F.; Halliop, E.; Evans, M. J. B. The Production of Chemically-Activated Carbons. *Carbon* **1999**, *37*, 269.
- (33) Granite, E. J.; Pennline, H. W.; Hoffman, J. S. Effects of Photochemical Formation of Mercuric Oxide. *Ind. Eng. Chem. Res.* **1999**, *38*, 5034.
- (34) Golightly, D. W., Simon, F. O., Eds. Methods For Sampling and Inorganic Analysis of Coal. *U.S. Geological Survey Bulletin 1823*; USGS: Reston, VA, 1995.
- (35) Reeves, R. D.; Brooks, R. R. *Trace Element Analysis of Geological Materials*; John Wiley: New York, 1978.
- (36) Weast, R. C., Ed. *CRC Handbook of Chemistry and Physics*, 63rd ed.; CRC Press: Boca Raton, FL, 1982.
- (37) *Brochure on Sorbalit*; Dravo Corp.: Pittsburgh, PA, June 1994.
- (38) Teller, A. J.; Hsieh, J. Y. Control of Hospital Incineration Emissions-Case Study. Presented at the 84th Annual Meeting of Air & Waste Management Association, Vancouver, Canada, 1991.
- (39) Hsieh, J. Y.; Confuorto, N. Operation of a Medical Waste Incinerator and the Emission Control System. *Proc. SPIE-Int. Soc. Opt. Eng.* **1993**, *1717* (Industrial, Municipal, and Medical Waste Incineration Diagnostics and Control), 46.
- (40) Tsuji, K.; Shiraishi, I. *Prepr. Pap.-Am. Chem. Soc., Div. Fuel Chem.* **1996**, *41* (1), 404.
- (41) Tsuji, K.; Shiraishi, I. EPRI Report no. TR-101054; EPRI: Palo Alto, CA, 1992; conf-911226, Vol.3, p 8A.1.
- (42) Dunham, G. E.; Miller, S. J. Evaluation of Activated Carbon For Control of Mercury From Coal-Fired Boilers. Presented at the First Joint Power & Fuel Systems Contractors Conference, Pittsburgh, PA, July 1996.
- (43) Livengood, C.D.; Huang, H. S.; Wu, J. M. Experimental Evaluation of Sorbents for the Capture of Mercury in Flue Gases. Presented at the 87th Annual Meeting Air & Waste Management Association, Cincinnati, Ohio, June 1994.
- (44) McNamara, J. D.; Wagner, N. J. *Gas Sep. Purif.* **1996**, *10* (2), 137.
- (45) Roberts, D. L.; Stewart, R. M. Characterization of Sorbents for Removal of Vapor Phase Mercury. Presented at the EPRI Mercury Sorbent Workshop, Grand Forks, ND, July 1996.
- (46) Van Wormer, M. Control of Mercury Emissions From Combustion Applications. Presented at the 1992 AIChE National Meeting, Aug 1992.
- (47) Castilla, C. M.; Marin, F. C.; Hodar, F. J. M.; Utrilla, J. R. Effects Of Non-Oxidant And Oxidant Acid Treatments On The Surface Properties Of An Activated Carbon With Very Low Ash Content. *Carbon* **1998**, *36* (1-2), 145.
- (48) Carrott, P. J. M.; Carrott, M. M. L. R.; Nabais, J. M. V. Influence of Surface Ionization On The Adsorption Of Aqueous Mercury Chlorocomplexes By Activated Carbons. *Carbon* **1998**, *36* (1-2), 11.
- (49) Hargis, R. A.; O'Dowd, W. J.; Pennline, H. W. Mercury Investigations in a Pilot-Scale Unit. Presented at the AIChE National Meeting, Houston, TX, March 1999.
- (50) Mellor, J. W. *A Comprehensive Treatise on Inorganic and Theoretical Chemistry*; Longmans Green and Co.: New York, 1952.
- (51) Angenault, J. *Rev. Chim. Miner.* **1970**, *7*, 651.
- (52) Wessels, A. L.; Jeitschko, W. The Mercury Vanadates with the Empirical Formulas HgVO₃ and Hg₂VO₄. *J. Solid State Chem.* **1996**, *125* (2), 140.
- (53) Golodets, G. I. *Heterogeneous Catalytic Reactions Involving Molecular Oxygen*; Elsevier: New York, 1983.
- (54) Solomons, T. W. G. *Organic Chemistry*; John Wiley: New York, 1980.
- (55) Hargis, R. A.; Pennline, H. W. Trace Element Distribution and Mercury Speciation in A Pilot-Scale Combustor Burning Blacksville Coal. Presented at the 90th AWMA Annual Meeting, Toronto, Canada, June 1997; paper no. 97-WP72B.04.

Received for review October 18, 1999

Revised manuscript received February 5, 2000

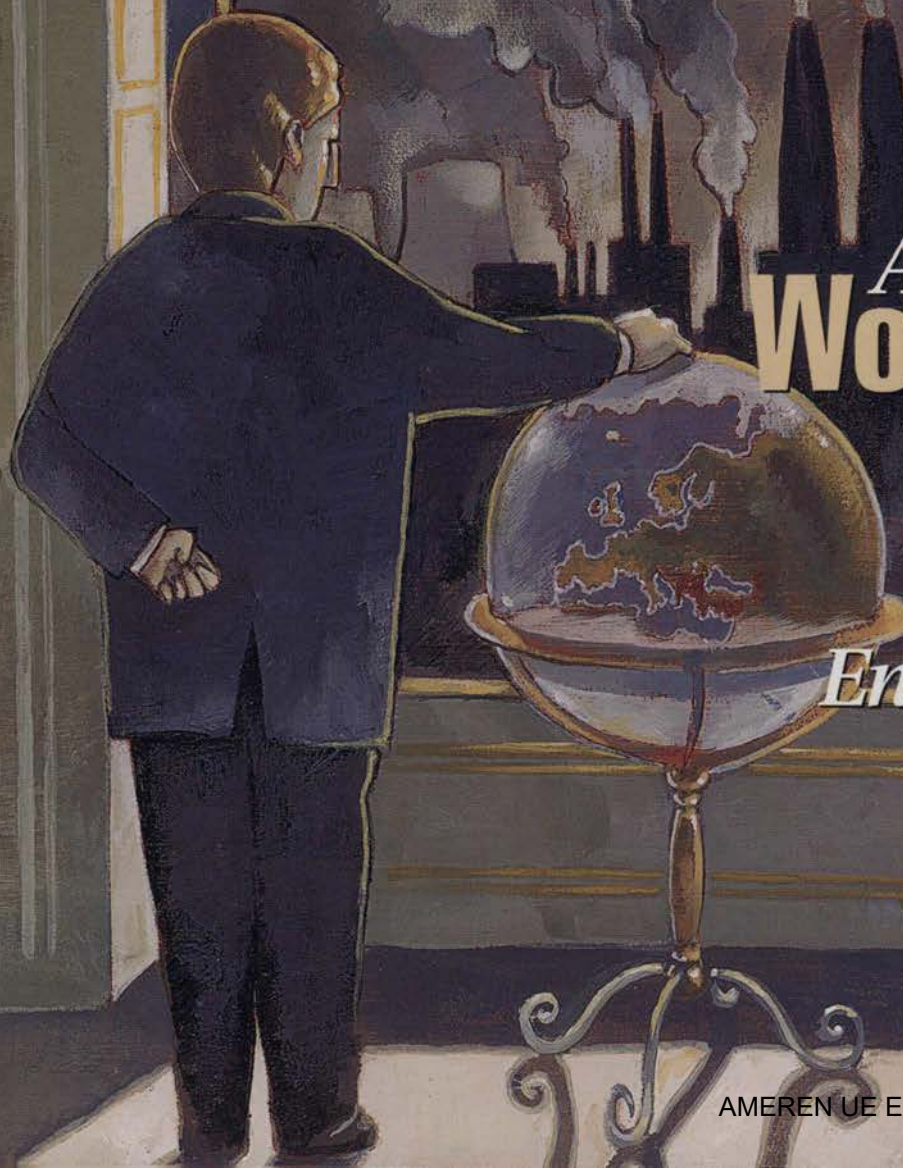
Accepted February 7, 2000

IE990758V

February 1, 2000

ENVIRONMENTAL Science & Technology

<http://pubs.acs.org/est>



A Worrisome Outlook for Europe's Environment?

AMEREN UE EXHIBIT 1082

Page 89

PUBLISHED BY
THE AMERICAN
CHEMICAL SOCIETY

Departments

Comment • 63A

How to thank our reviewers

EPA Watch • 73A

2000 budget includes steady funding; policy orders • PBT releases, including dioxin, will be captured on TRI reports • Confusion over agreement confounds species protection efforts • Proposal to regulate large animal farms still under fire

Technology Update • 75A

Technology costs for arsenic removal

Research Watch • 91A

Huge dioxin emission source • Controlling mercury emissions

Online/In Print • 93A

Web sites and new books

Meeting Calendar • 94A

New events through April 2000

Classifieds • 95A

Environmental career opportunities
• Advertiser index

Research at a Glance

Aminodinitrotoluene, kinetics, 450
Aminodinitrotoluene, oxidation, 497
Atrazine, degradation, 430
Bacterial bioremediation, 535
Biofilters, performance, 461
Chlorobenzene, in sediments, 385
Chloronaphthalenes, in air, 393
Chromium, leaching, 455
Cr(VI), reduction, 438
Diesel fuels, emissions, 349
Haloorganics, FeS, 422
Hydrocarbons, degradation, 489
Iodide, sorption, 399
Mercury, sequestration, 483
MTBE, outboard engines, 368
n-Alkanes, solubilization, 476
Nitroaromatics, reactions, 505
NOM, aromatics, 444
PAHs, in air, 356
PCBs, contamination, 527
PCDD/DFs, source, 377
Pesticides, in air, 393
Phenanthrene, sorption, 406
Phenol, degradation, 509
Pyrene, photochemistry, 415
SOM, composition, 530
Sorption, mechanisms, 468
SVOCs, precipitation, 361
TCE, dechlorination, 514
Trees, pollution damage, 373
Wastewater, treatment, 522

The table of contents of research papers in this issue begins on page 61A.

European ban on use of surfactant alarms U.S. producers • 68A

U.S. chemical producers sharply criticized a draft EU risk assessment that recommends a European ban on many uses of nonylphenol ethoxylates.

Growing conflict over GM trees • 69A

As the number of genetically modified trees being planted in test plots has increased, debate over their pros and cons has grown more heated, concurrent with a rise in vandalism against research laboratories.



European governments urged to consider environmental benchmarks • 70A

The European Environment Bureau hopes that government leaders will base environmental performance on specified targets, timetables, and indicators in 10 key areas.

EPA's diesel health assessment needs tweaking, science advisors say • 71A

EPA's Clean Air Act Scientific Advisory Committee has again declined approval of the Agency's analysis of human health effects from diesel exhaust.

News Briefs • 72A

Market-based pollution control alternatives • Waste reduction • Risks of contaminated underwater sediments • Paper in catalogs • Conservation areas threatened • Chemical accidents • Pollutant-birth defect link • School bus pollution



34(3) 57A-96A/349-540
ISSN 0013 936X



Cover: Maria Burke reviews a new European Environment Agency report, which finds that environmental policies have not achieved desired objectives. (Artwork by Matthew J. Baek)

Optimization of High Temperature Sulfur Impregnation on Activated Carbon for Permanent Sequestration of Elemental Mercury Vapors

WEI LIU AND RADISAV D. VIDIC*

Department of Civil and Environmental Engineering,
943 Benedum Hall, University of Pittsburgh,
Pittsburgh, Pennsylvania 15261-2294

THOMAS D. BROWN

U.S. Department of Energy, Federal Energy Technology Center,
P.O. Box 10940, Pittsburgh, Pennsylvania 15236-0940

Following previous success with the use of activated carbon impregnated with sulfur at elevated temperatures for elemental mercury control, possible improvements in the impregnation procedure were evaluated in this study. Adsorbents prepared by thoroughly mixing sulfur and activated carbon in the furnace at the initial sulfur-to-carbon ratio (SCR) ranging from 4:1 to 1:2 showed similar adsorptive behavior in a fixed-bed system. Maintaining a stagnant inert atmosphere during the impregnation process improves sulfur deposition resulting in the enhanced dynamic capacity of the adsorbent when compared to other sulfur impregnated carbons. The fate of spent adsorbents was assessed using a toxicity characteristics leaching procedure (TCLP). Although mercury concentration in all leachates was below the TCLP limit (0.2 mg/L), virgin activated carbon lost a significant fraction of the adsorbed elemental mercury during storage, while no loss was observed for sulfur-impregnated carbons. This finding suggests that virgin activated carbon may not be appropriate adsorbent for permanent sequestration of anthropogenic elemental mercury emissions.

Introduction

As listed in the Clean Air Act Amendments of 1990, mercury is one of the 189 hazardous air pollutants (HAPs). Although air emissions of mercury occur naturally, major mercury pollution comes from anthropogenic activities. Recent EPA report showed that coal-fired power plants, municipal waste combustors, and medical waste incinerators account for more than 70% of the total anthropogenic mercury emissions (1).

Mercury emission control measures in coal-fired power plants are mainly based on the existing air pollution control devices (APCD). The primary APCDs include multiple cyclones, electrostatic precipitators (ESPs), fabric filters (baghouses), wet scrubbers, and wet and dry flue gas desulfurization (FGD) systems. Several studies revealed that the efficiency of mercury control is a function of a specific device used and flue gas conditions. For example, the oxidized mercury could be trapped to a substantial degree by fabric

filters, while elemental mercury could not be captured due to its small diameter. The average removal efficiency of total mercury for fabric filter was about 30% (2). A series of pilot plants studies on wet scrubbing FGD system has shown that 90% HgCl₂ was removed from flue gas, while essentially no elemental mercury was dissolved in the scrubbing slurry (3).

New technologies are being developed for the control of mercury emissions. Among them, activated carbon adsorption demonstrated potential for capturing both elemental and oxidized mercury species.

Vidic and McLaughlin (4) found that sulfur impregnated carbon performed much better than virgin carbon. Physisorption dominated the capacity of a virgin carbon, while HgS formation controlled the adsorption ability of sulfur-impregnated carbons. Additional study (5) showed that the improved mercury uptake capacity by sulfur-impregnated carbon was also related to the factors such as bonding between sulfur and carbon surface, specific surface area of the carbon, and types of sulfur allotropes impregnated on the carbon surface. Liu et al. (6) further developed this new impregnation protocol to control the parameters (temperature and initial sulfur-to-carbon ratio) that have the major impact on the performance of sulfur-impregnated activated carbons. It was found that the impregnation temperature was the crucial parameter for the performance of sulfur-impregnated carbons, while the amount of sulfur impregnated on the carbon surface had much lower impact. This was explained by the presence of more short chain sulfur allotropes, larger surface area, and larger fraction of meso-pores in the adsorbents prepared at higher temperatures.

One of the major drawbacks of the impregnation procedure used in previous studies (5, 6) was that only 3% of the sulfur used in the procedure was impregnated onto activated carbon. Therefore, one objective of this study was to develop an improved impregnation method that would reduce the sulfur loss while producing equally effective mercury adsorbents. This is done by determining the impact of impregnation process modifications and adsorbent particle size on sulfur deposition and adsorbent performance for elemental mercury uptake.

Current approaches to handling the spent adsorbents include ash pond or landfill disposal or regeneration. Powdered activated carbon injection technology does not allow for the recovery and regeneration of spent adsorbent which is, instead, discharged together with fly ash directly into a pond. For granular activated carbon, both landfilling and regeneration are feasible. Upon disposal of saturated adsorbents, the adsorbed mercury compounds may be dissolved into leachate due to acidic conditions that occur during landfill stabilization. Once mercury compounds are mobilized, their migration could pose significant environmental risk. The second objective of this study was to investigate the environmental impact of mercury-saturated adsorbents after they are removed from the system. Toxicity characteristics leaching procedure (TCLP) (40 CFR 261) was utilized in order to evaluate the fate of the adsorbed mercury compounds once saturated adsorbents are removed from the flue gas.

Experimental Methods

BPL, a commercially available bituminous coal-based activated carbon, was provided by the manufacturer (Calgon Carbon Corporation, Pittsburgh, PA) in 4 × 10 and 12 × 30 U.S. mesh sizes and was used as base adsorbent throughout

* Corresponding author phone: (412)624-1307; fax: (412)624-0135; e-mail: vidic@engr.pitt.edu.

the study. It was ground into 60 × 80, 170 × 230, and minus 400 U.S. mesh size and stored in a desiccator prior to use.

Two sulfur impregnation procedures similar to the method described previously (5, 6) were used in this study. The major difference is that instead of using two ceramic boats, one for sulfur and one for activated carbon, only one boat was used. Sulfur flakes were ground into a fine powder and thoroughly mixed with carbon in a single boat. The initial sulfur-to-carbon ratio (SCR) in the boat was adjusted from 4:1 to 1:5, and the impregnation temperature was set at 600 °C for all tests. The designation of these carbons used a letter M to indicate that the sulfur and carbon were mixed in one ceramic boat. For example, BPL-S-4/1M-600 denotes a BPL carbon impregnated with sulfur at 600 °C with an SCR of 4:1.

The second procedure also used single boat for the impregnation procedure, and the SCR was set at 1:2. However, after an inert atmosphere was created inside the system, nitrogen flow was stopped, the tube furnace was sealed, and a balloon was attached to the furnace exit to compensate for gas expansion. The furnace temperature was raised to 600 °C and held at that level for 2 h. The objective of this method was to further increase the amount of active sulfur molecules on the carbon surface. The designation of this adsorbent was BPL-S-1/2M-600S.

When 170 × 230 and minus 400 U.S. mesh size carbons were used for the preparation of sulfur-impregnated carbons adsorbents, the impregnation conditions were identical to those described previously for BPL-S adsorbents (5, 6) to allow for direct assessment of the impact of carbon particle size on sulfur impregnation process and resulting mercury uptake dynamics.

The sulfur content of all adsorbents was measured using a Leco Model SC 132 sulfur determinator (Leco Corporation, St. Joseph, MI), while surface areas were determined using an Orr Surface-Area Pore-Volume Analyzer Model 2100 (Micromeritics Instrument Corporation, Atlanta, GA) and calculated using the nitrogen BET isotherm method.

Adsorbent samples were subjected to FTIR analysis in an attempt to elucidate predominant sulfur forms resulting from these impregnation procedures. Samples for IR analysis were prepared by grinding a very small amount of adsorbent with KBr salt followed by compression between two stainless steel cylinders to form a thin transparent solid film. This film was subjected to direct scanning in an FTIR spectrophotometer (Mattson IR, Madison Instruments, Inc. Madison, WI) to determine predominant forms of sulfur on the carbon surface.

Mercury uptake by these newly developed sulfur impregnated adsorbents was studied using a fixed-bed adsorber system in order to assess the impact of modifications in sulfur impregnation procedure on their performance. All column tests were conducted using a 1/4 in. (0.635 cm) I.D. stainless steel reactor charged with 100 mg of impregnated carbon and operated at 140 °C in a downflow mode. Pure N₂ at a flow rate of 1.0 L/min was used as the carrier gas in all experiments so that the results can be compared to previous data (5, 6). Unless otherwise noted, influent mercury concentration was 55 µg/m³.

EPA Method 1311 was used to select the proper extraction fluid for TCLP analysis. Based on the tests with various adsorbents, it was found that the extraction fluid 1 (5.7 mL of glacial CH₃CH₂OOH and 64.3 mL of 1 N NaOH in 1.0 L of reagent water, pH = 4.93 ± 0.05, EPA Method 1311) was suitable for the extraction of mercury loaded adsorbents.

Results and Discussion

FTIR Analyses of Virgin and Sulfur Impregnated Carbons. It has long been assumed that the sulfur impregnated on the carbon surface was in the elemental form. However, early research has shown that the actual forms of sulfur on the adsorbent surface could change from simple elemental sulfur

to various sulfur compounds (7). The actual carbon-sulfur complexes were strongly related to the initial structures of carbon. For example, hydrogen sulfide and organic sulfur compounds were found if the carbons contained hydrocarbon compounds (8).

FTIR was used to measure possible sulfur functional groups of on the carbon surface. Figures 1 and 2 depict IR scans of virgin BPL and BPL-S-4/1-600, respectively. As expected, Figure 1 revealed no distinct sulfur-related peaks on virgin BPL because its total sulfur content was below 1%. FTIR analysis of BPL-S-4/1-600 also revealed no distinct sulfur-related peaks (Figure 2) throughout 500–4000 cm⁻¹, where the possible ranges for sulfur-based functional groups are as follows (9):

functional group	possible peaks, cm ⁻¹
S-H	1200–1400, 3700–4000
S-C	1300–1400, 1500–1600
S-O	1100–1300, 1600–1700

The predominant sulfur bonds that are expected in these novel adsorbents are S-C and possibly some S-H and S-O. In addition to the fact that all of these bonds have fairly weak vibrations (9), extremely high background noise in the fingerprint region and overwhelming O-H and C-H vibrations coming from the surface of activated carbon, as evidenced from the spectra of virgin BPL carbon in Figure 1, precluded the observation of such bonds. However, under high impregnation temperature (600 °C), most sulfur-based compounds that could be formed on the carbon surface would evaporate or decompose to simple compounds that would be carried out of the furnace by the purge gas. This is particularly true for the simple sulfur compounds such as H₂S, CS₂, or SO₂ that could easily be volatilized and flushed out of the system. It is reasonable to assume that the major sulfur forms on the carbon surface resulting from sulfur impregnation at elevated temperatures are short linear-chain sulfur allotropes as suggested by Korpiel and Vidic (5).

Performance of BPL-S-M Series. As can be seen from Figure 3, mercury uptakes by BPL-S-1/1M-600 and BPL-S-1/2M-600 are very close to that previously measured for BPL-S-4/1-600 (2300 µg Hg/g carbon) (6). However, the adsorptive capacity for mercury decreased to 1450 µg Hg/g carbon when the initial sulfur-to-carbon ratio was reduced to 1:5.

Sulfur content and specific surface area of these novel adsorbents are shown in Table 1. This table shows that all BPL-S and BPL-S-M adsorbents had very similar surface areas regardless of the impregnation method or SCR used. Furthermore, the sulfur content of BPL-S-M carbons prepared using the SCR of 1:1 and 1:2 is very close to that of BPL-S-4/1-600 (approximately 10%). Hence, all three adsorbents exhibited very similar behavior for the uptake of elemental mercury. Although BPL-S-1/5M-600 had similar BET surface area with other adsorbents, its sulfur content was about 20% lower, which can explain somewhat reduced capacity for elemental mercury.

The key advantage of the new impregnation procedure is that it reduced the amount of sulfur required to maintain sulfur content of about 10%. In our previous study, sulfur and carbon were kept in separate ceramic boats, and the majority of sulfur would be carried out of the furnace by N₂ gas before it had a chance to react with carbon. Furthermore, several mass transfer steps were required before sulfur impregnation onto carbon surface. The initial sulfur loss and mass transfer resistance are reduced for the newly developed methods since sulfur and carbon were thoroughly mixed in a single boat.

Performance of BPL-S-1/2M-600S. Figure 4 shows that the mercury uptake by BPL-S-1/2M-600S was about 10% higher when compared to BPL-S-4/1-600. Table 1 shows that

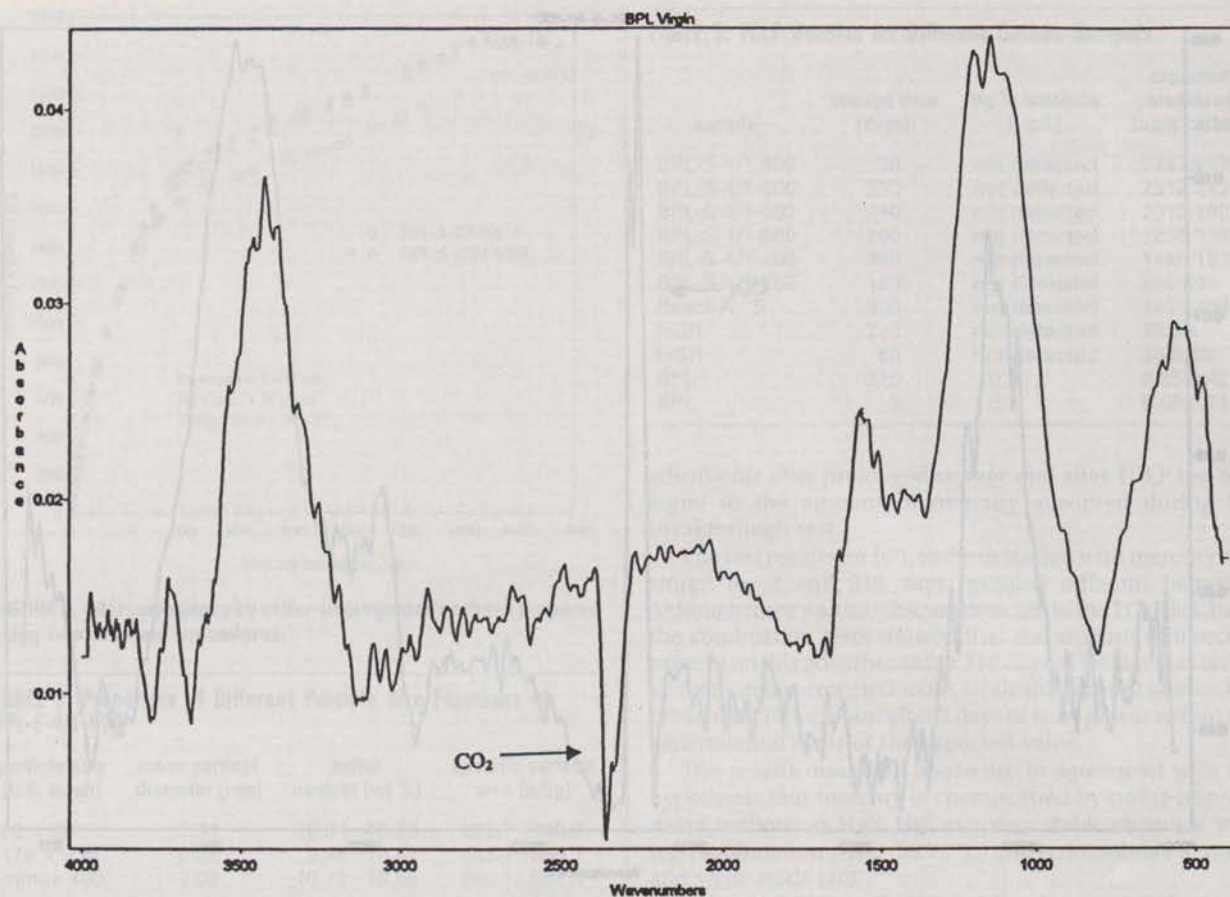


FIGURE 1. IR analysis of BPL surface for possible sulfur structures.

the sulfur content of BPL-S-1/2M-600S was about 20% higher than for the other carbons. Since all the carbons were prepared at same temperature, the predominant forms of sulfur allotropes should be the same (short chain sulfur molecules). Therefore, the amount of active sulfur molecules is proportional to the total sulfur content. Because of the higher sulfur content, BPL-S-21/2M-600S showed slightly better performance. On the other hand, Table 1 also shows that the surface area of this carbon was somewhat lower when compared to other carbons, which was most likely caused by the larger amount of sulfur deposited on the carbon surface. Reduction in surface area would normally offset the effect of having more active sulfur molecules. Furthermore, although the initial SCR used in the production of this carbon was 1:2, only about 20% of the sulfur was deposited on the carbon surface. Significant sulfur loss even in this procedure was probably due to the extreme high impregnation temperature.

The most likely explanation for the incomplete deposition of sulfur on the carbon surface even in a closed system used for the production of BPL-S-21/2M-600S is insufficient reaction time. During a 2-h period when the furnace temperature was maintained at 600 °C only about 20% of the sulfur was deposited on the surface of activated carbon, and, except for the amount that diffused through the balloon, the unreacted sulfur remained in the vapor phase inside the quartz tube. The unreacted sulfur vapor was deposited on the walls of the quartz tube during the cooling phase as evidenced by yellow discoloration. It is possible that longer impregnation time would result in better sulfur utilization and improved economics of the process.

Effect of Adsorbent Particle Size. Data shown in Table 2 indicate that there is no significant difference in sulfur content and specific surface area among the three particle

size fractions used in this study. However, Figure 5 shows that smaller particle size adsorbents exhibited higher dynamic adsorptive capacity when compared to 60 × 80 U.S. mesh size BPL-S-4/1-600. It is clear that Figure 5 does not reflect a true adsorption equilibrium because the adsorbent particle size should not have such a pronounced impact on the adsorption capacity, especially considering that all fractions had very similar surface area and sulfur content. The data shown in Figure 5 reflect a dynamic equilibrium that is established for a given set of fixed-bed operating parameters (e.g., temperature, influent composition, empty bed contact time, adsorbent particle size, etc.) and is defined by the lack of additional measurable mercury uptake. Korpiel and Vidic (5) argued that the dynamic equilibrium established in a single breakthrough test does not reflect the true capacity of sulfur impregnated adsorbents for mercury because the rate of mercuric sulfide formation and subsequent diffusion into the sulfur bulk phase is the rate limiting step in the adsorption dynamics. Rapid formation of large HgS molecules which can block the access to the narrower pores and prevent mercury molecules from accessing the highly reactive S₂ molecules that are present in the microporous region of the BPL-S carbon is responsible for the apparently low sulfur utilization in a single breakthrough test. They also showed that even after 100% breakthrough was observed in a given breakthrough test, additional mercury uptake would occur in subsequent loading steps when HgS formed in the previous loading step was allowed sufficient time to diffuse into the bulk sulfur.

It is obvious that the reduction in the adsorbent particle size from 60 × 80 (0.21 mm) to 170 × 230 (0.08 mm) U.S. mesh size provided sufficient kinetic advantage in a fixed-bed operated at an extremely short empty bed contact time of 0.011 seconds to allow better penetration of mercury

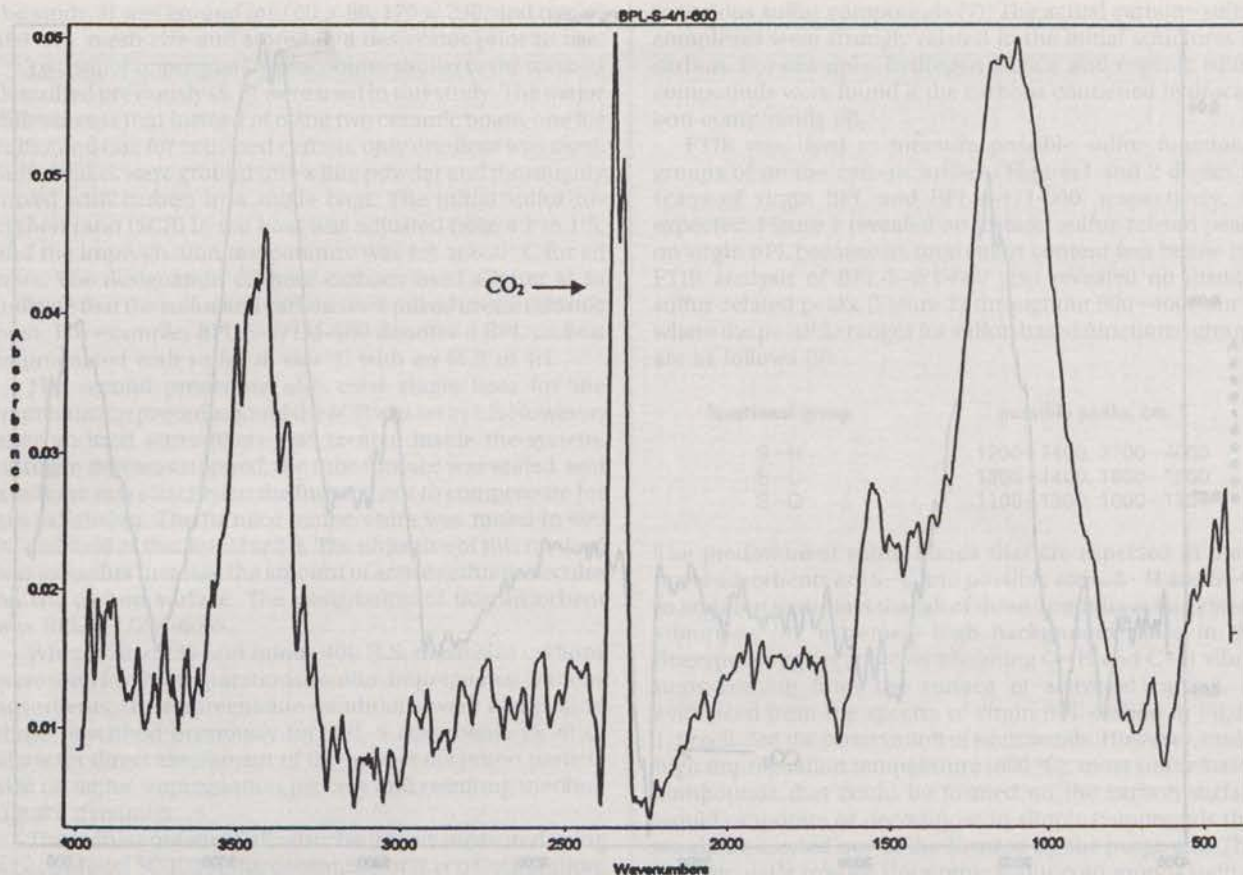


FIGURE 2. IR analysis of BPL-S-4/1-600 surface for possible sulfur structures.

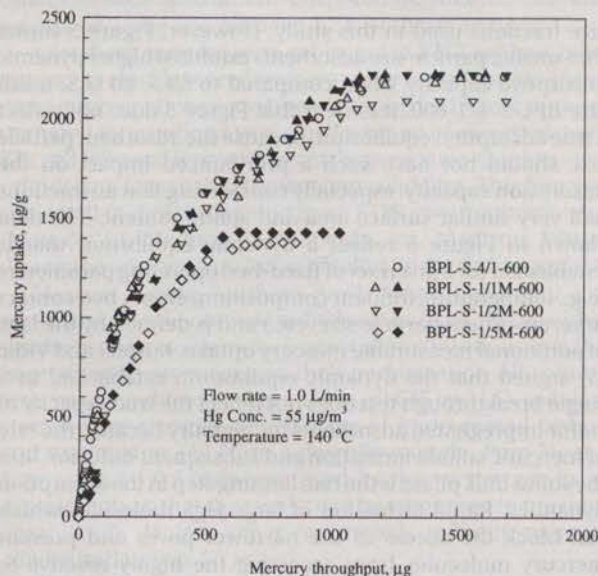


FIGURE 3. Mercury uptake by BPL-S-M adsorbents.

molecules into the microporous region before HgS formation prevented the remaining sulfur molecules to react with mercury. However, no additional increase in capacity was observed as the particle size decreased from 170 × 230 (0.08 mm) to minus 400 (0.03 mm) U.S. mesh size. It is very likely that the kinetic limitations of a short empty bed contact time are fully counterbalanced by the reduction in particle size from 60 × 80 to 170 × 230 and that further particle size reduction brings no benefits to the process of mercury uptake. It is also possible that further reduction in empty bed contact

TABLE 1. Sulfur Content and Surface Area of Sulfur Impregnated Carbons

adsorbent	sulfur content [wt %]	specific surface area [m ² /g]
BPL	0.5–0.7	988–1026
BPL-S-4/1-600	10.0–10.2	824–846
BPL-S-1/1M-600	10.9–11.0	842–871
BPL-S-1/2M-600	9.4–9.8	854–905
BPL-S-1/5M-600	7.9–8.0	857–862
BPL-S-1/2M-600S	12.5–12.9	789–812

time could bring about advantages of using even smaller adsorbent particle size.

Fate of Spent Adsorbents. To determine the fate of mercury adsorbed on activated carbon-based adsorbents, a TCLP test was conducted by placing 0.1 g of spent adsorbent in a glass vial together with 20 mL of extraction fluid 1. The volume of the vial was also 20 mL so that there would be no headspace above the liquid. By doing so, the possibility of losing any mercury into the vapor phase can be eliminated. All the sample vials were capped and sealed tightly by Teflon tapes. Then, the vials were placed in a 30 rpm tumbler for 18–20 h of the extraction process.

The supernatant was separated by pressurized filtration and liquid mercury analysis method (5) was used to measure mercury concentration in the leachate. The solid adsorbent was collected to verify the remaining mercury concentration by combusting the adsorbent in oxygen atmosphere at 800 °C. The combustion off-gas was collected in impingers (15 g of KMnO₄ in 1 L of 10% H₂SO₄) that were analyzed by liquid mercury analysis method.

Table 3 shows the mercury concentrations measured in extracts of different spent adsorbents. It can be seen from

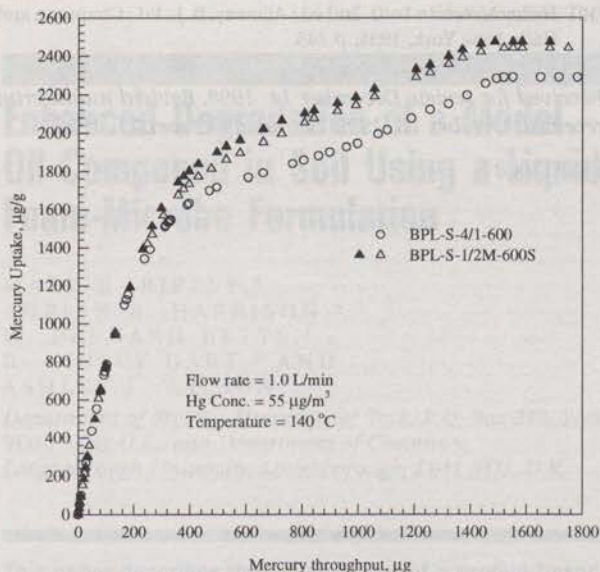


FIGURE 4. Mercury uptake by sulfur-impregnated carbons prepared using two different procedures.

TABLE 2. Properties of Different Particle Size Fractions of BPL-S-4/1-600

particle size [U.S. mesh]	mean particle diameter [mm]	sulfur content [wt %]	specific surface area [m ² /g]
60 × 80	0.21	10.04–10.18	823.7–845.7
170 × 230	0.08	9.88–10.51	833.7–869.2
minus 400	0.03	10.22–10.56	840.1–852.5

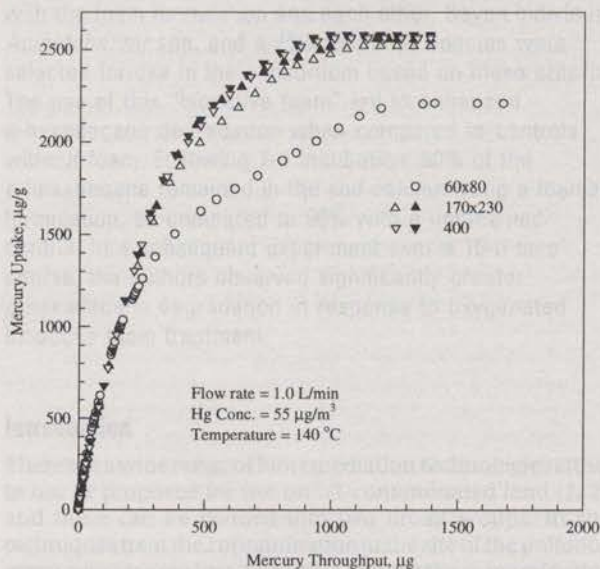


FIGURE 5. Effect of particle size on mercury uptake by BPL-S-4/1-600.

this table that the amount of mercury extracted by acidic solution is below the detection limit of the analytical method used (about 0.1–0.2 µg/L). The sample storage time varied from 2 to 330 days, and the adsorbents included all types of sulfur-impregnated carbons (5, 6) (i.e., HGR, React-A-S, and BPL-S series). The last column in Table 3 shows the ratio of the expected mercury mass on adsorbents after breakthrough tests and the amount of mercury measured by combusting the adsorbents after the TCLP test. These results revealed that the amount of mercury remaining on sulfur-impregnated

TABLE 3. TCLP Results for Different Carbon Samples

sample	storage time [days]	Hg in leachate [µg/L]	expected: measured [µg/g carbon]
BPL-S-4/1-600	30	not detected	2287:2170
BPL-S-4/1-600	330	not detected	2312:2421
BPL-S-2/1-600	240	not detected	2010:1907
BPL-S-1/1-600	200	not detected	1256:1302
BPL-S-4/1-400	260	not detected	1448:1331
BPL-S-4/1-250	180	not detected	550:603
React-A-S	300	not detected	1905:1961
HGR	260	not detected	38:36
HGR	60	not detected	36.9:38
BPL	310	<0.2	0.65:0.42
BPL	2	<0.2	0.68:0.71

adsorbents after prolonged storage and after TCLP test was equal to the amount of mercury adsorbed during the breakthrough test.

The test results for BPL carbons loaded with mercury and stored for 2 and 310 days revealed different behavior. Although there was no mercury detected in the TCLP leachate, the combustion tests showed that the amount of mercury present on this adsorbent after 310 days of storage was much lower than the expected value, while the amount of mercury present on BPL carbon after 2 days of storage was within the experimental error of the expected value.

The results described above are in agreement with the hypothesis that mercury is chemisorbed by sulfur-impregnated carbons as HgS. HgS is a very stable chemical with high sublimation point (583.5 °C) and is not soluble in water and weak acids (10).

Although TCLP results showed that the amount of mercury extracted from carbons were far below the RCRA limit (200 µg/L) (11, 12), the stability of mercury on the adsorbent surface is strongly related to the adsorption mechanism and predominant mercury forms.

Apparently, mercury adsorbed by sulfur-impregnated carbons is more stable than that adsorbed by virgin carbons. It is obvious that converting elemental mercury to HgS would be beneficial in terms of handling the spent adsorbents. Another important conclusion is that although TCLP analysis of spent virgin carbon may pass the regulatory limit, the elemental mercury could re-enter the vapor phase during a long storage time. This will certainly present a threat to the environment, and the spent virgin carbon may have to be treated as hazardous waste regardless of the TCLP results.

Acknowledgments

Funding for this work was provided by the U.S. Department of Energy (Grant No. DE-FG22-96PC96212). The views expressed are entirely those of the authors and do not necessarily reflect the views of the agency. Mention of trade names or commercial products does not constitute endorsement or recommendation for use.

Literature Cited

- (1) Johnson, J. *Environ. Sci. Technol.* **1997**, *31*, 218A.
- (2) Chu, P.; Porcella, D. B. *Water, Air, Soil Pollut.* **1995**, *80*, 135.
- (3) Chang, R.; Owens, D. *EPRI J.* July/August **1994**, 46.
- (4) Vidic, R. D.; McLaughlin, J. B. *J. Air Waste Manage. Assoc.* **1996**, *46*, 241.
- (5) Korpiel, A. J.; Vidic, R. D. *Environ. Sci. Technol.* **1997**, *31*, 2319.
- (6) Liu, W.; Vidic, R. D.; Brown, T. D. *Environ. Sci. Technol.* **1998**, *32*, 531.
- (7) *Chemistry and Physics of Carbon*; Walker, P. L., Jr., Ed.; Vol. 6, Marcel Dekker: New York, 1970; p 264.
- (8) Sykes, K. W.; White, P. *Trans. Faraday Soc.* **1956**, *52*, 660.

- (9) Pouchert, C. J. ed., *The Aldrich Library of FT-IR Spectra Vapor Phase*, 1st ed.; Aldrich Chemical Co.: Milwaukee, WI, 1989; p 343.
- (10) Lide, D. R., ed., *Handbook of Chemistry and Physics*, 73rd ed.; CRC Press: Boca Raton, FL, 1992; pp 4-74.
- (11) U.S. EPA. *Mercury and Arsenic Wastes - - Removal, Recovery, Treatment, and Disposal*; Noyes Data Corporation: Park Ridge, NJ, 1993; p 14.

- (12) *Heavy Metals in Soils*, 2nd ed.; Alloway, B. J., Ed.; Chapman and Hall: New York, 1995; p 245.

Received for review December 14, 1998. Revised manuscript received October 18, 1999. Accepted October 21, 1999.

ES9813008

Wavelength (nm)	Intensity	Wavelength (nm)	Intensity
200	0.00	200	0.00
210	0.00	210	0.00
220	0.00	220	0.00
230	0.00	230	0.00
240	0.00	240	0.00
250	0.00	250	0.00
260	0.00	260	0.00
270	0.00	270	0.00
280	0.00	280	0.00
290	0.00	290	0.00
300	0.00	300	0.00
310	0.00	310	0.00
320	0.00	320	0.00
330	0.00	330	0.00
340	0.00	340	0.00
350	0.00	350	0.00
360	0.00	360	0.00
370	0.00	370	0.00
380	0.00	380	0.00
390	0.00	390	0.00
400	0.00	400	0.00

The test results for BPT carbonates listed with mercury and...
 amount to the amount of mercury absorbed during the...
 through the...

The test results for BPT carbonates listed with mercury and...
 amount to the amount of mercury absorbed during the...
 through the...
 amount to the amount of mercury absorbed during the...
 through the...

The results described above are in agreement with the...
 amount to the amount of mercury absorbed during the...
 through the...
 amount to the amount of mercury absorbed during the...
 through the...

The results described above are in agreement with the...
 amount to the amount of mercury absorbed during the...
 through the...
 amount to the amount of mercury absorbed during the...
 through the...

The results described above are in agreement with the...
 amount to the amount of mercury absorbed during the...
 through the...
 amount to the amount of mercury absorbed during the...
 through the...
 amount to the amount of mercury absorbed during the...
 through the...

The results described above are in agreement with the...
 amount to the amount of mercury absorbed during the...
 through the...
 amount to the amount of mercury absorbed during the...
 through the...
 amount to the amount of mercury absorbed during the...
 through the...

The results described above are in agreement with the...
 amount to the amount of mercury absorbed during the...
 through the...
 amount to the amount of mercury absorbed during the...
 through the...
 amount to the amount of mercury absorbed during the...
 through the...
 amount to the amount of mercury absorbed during the...
 through the...



FIGURE 2. Mercury uptake by soils. Integrated mercury uptake under two different procedures.

Particle size (μm)	Mercury uptake (mg/kg)	Specific surface area (m ² /g)
40 - 60	0.02	18.04 - 19.00
75 - 150	0.02	3.80 - 6.51
400	0.02	10.22 - 10.48



FIGURE 3. Uptake of mercury by soils. Integrated mercury uptake under two different procedures.

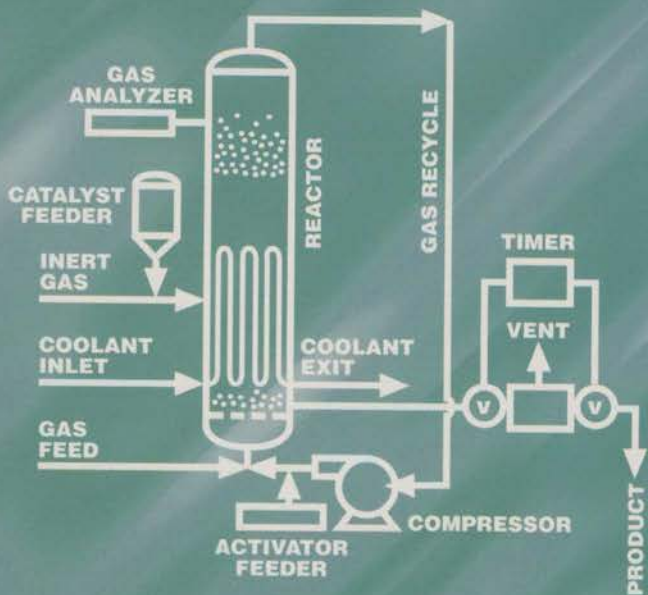
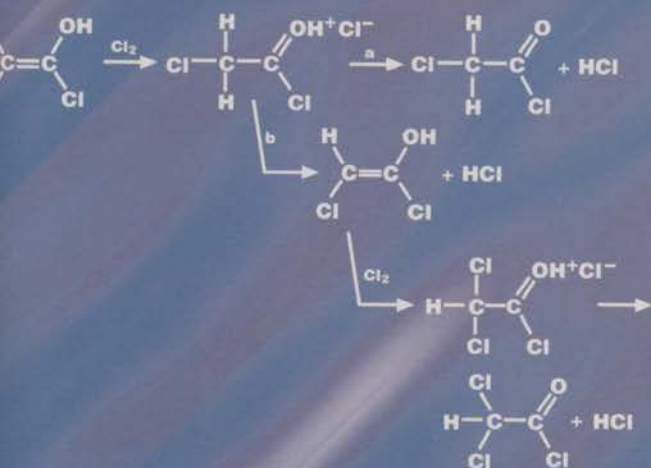
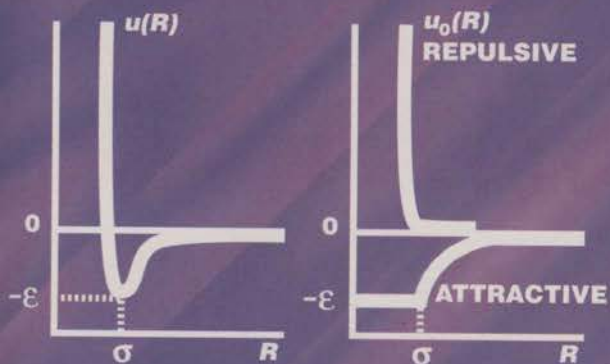
The results described above are in agreement with the...
 amount to the amount of mercury absorbed during the...
 through the...
 amount to the amount of mercury absorbed during the...
 through the...

The results described above are in agreement with the...
 amount to the amount of mercury absorbed during the...
 through the...
 amount to the amount of mercury absorbed during the...
 through the...
 amount to the amount of mercury absorbed during the...
 through the...
 amount to the amount of mercury absorbed during the...
 through the...

EXHIBIT G

INDUSTRIAL & ENGINEERING CHEMISTRY RESEARCH

A PUBLICATION OF THE AMERICAN CHEMICAL SOCIETY FOR APPLIED CHEMISTRY & CHEMICAL ENGINEERING



INDUSTRIAL & ENGINEERING CHEMISTRY RESEARCH

UNIVERSITY OF PITTSBURGH

APR 11 2000

COMPUTER SCIENCE LIBRARY

EDITOR

DONALD R. PAUL

Department of Chemical Engineering, University of Texas at Austin
Austin, Texas 78712-1062

(512) 471-5392; Fax (512) 471-0542

E-mail iecr@che.utexas.edu

ASSOCIATE EDITORS

Spiro D. Alexandratos
University of Tennessee

Lorenz T. Biegler
Carnegie-Mellon University

David T. Allen
University of Texas at Austin

Milorad P. Dudukovic
Washington University

John L. Anderson
Carnegie-Mellon University

Babatunde A. Ogunnaike
DuPont Central Research & Development

ADVISORY BOARD

Joan F. Brennecke
University of Notre Dame

Massimo Morbidelli
ETH Zürich

Joseph M. DeSimone
University of North Carolina—
Chapel Hill

K. J. L. Paciorek
Corona Del Mar, California

Christodoulos A. Floudas
Princeton University

Richard J. Quann
Mobil Technology Company

David S. Hacker
Highland Park, Illinois

G. V. Reklaitis
Purdue University

Bal K. Kaul
ExxonMobil Research &
Engineering Company

Steven F. Rice
Sandia National Laboratories

M. J. Lockett
Praxair, Inc.

Dominique Richon
Ecole des Mines de Paris,
France

William L. Luyben
Lehigh University

Robin D. Rogers
The University of Alabama

Paul Mathias
Aspen Technology, Inc.

Shivaji Sircar
Air Products

Patrick L. Mills
DuPont Company

P. R. Westmoreland
University of Massachusetts

AMERICAN
CHEMICAL SOCIETY

Science That Matters.

Quick...what
alerts you to
ACS Web Edition
Articles ASAP*?

[ASAP Alerts]

It's Free!

Sign up today—it's FREE!

1. Go to <http://pubs.acs.org>
2. Click on the ASAP Alerts icon.
3. Complete the registration form.

*Articles ASAP[™] (As Soon As Publishable) delivers fully accepted articles within 48 hours of final author approval—in both HTML and PDF full-text formats—weeks before appearing in print—only from ACS.

ACS  WEB EDITIONS

Know it Now!

<http://pubs.acs.org>

SEPARATIONS

Novel Sorbents for Mercury Removal from Flue Gas

Evan J. Granite,* Henry W. Pennline, and Richard A. Hargis

National Energy Technology Laboratory, United States Department of Energy, P.O. Box 10940, Pittsburgh, Pennsylvania 15236-0940

A laboratory-scale packed-bed reactor system is used to screen sorbents for their capability to remove elemental mercury from various carrier gases. When the carrier gas is argon, an on-line atomic fluorescence spectrophotometer (AFS), used in a continuous mode, monitors the elemental mercury concentration in the inlet and outlet streams of the packed-bed reactor. The mercury concentration in the reactor inlet gas and the reactor temperature are held constant during a test. For more complex carrier gases, the capacity is determined off-line by analyzing the spent sorbent with either a cold vapor atomic absorption spectrophotometer (CVAAS) or an inductively coupled argon plasma atomic emission spectrophotometer (ICP-AES). The capacities and breakthrough times of several commercially available activated carbons as well as novel sorbents were determined as a function of various parameters. The mechanisms of mercury removal by the sorbents are suggested by combining the results of the packed-bed testing with various analytical results.

Introduction

Over 32% of anthropogenic mercury emissions in the United States are from coal-burning utilities. This percentage will increase over the next few years because of the mandated control of mercury emissions from municipal solid waste and medical waste incinerators. A low concentration of mercury, on the order of 1 ppbv, exists in flue gas when coal is burned. The primary forms in the flue gas are elemental mercury and mercuric chloride.¹

Control technologies for removing mercury from flue gas include scrubbing solutions and activated carbon sorbents. Mercuric chloride is soluble in water; elemental mercury is not. Dry sorbents have the potential to remove both elemental and oxidized forms of mercury. Activated carbons have been successfully applied for the control of mercury emissions from incinerators.^{1,2}

Several sorbents, such as activated carbons, can remove mercury from flue gas produced by the combustion of coal. However, there are problems associated with the use of activated carbons for mercury removal from flue gas. Activated carbons are general adsorbents; most of the components of flue gas will adsorb on carbon, with some in competition with mercury. Carbon sorbents operate effectively over a limited temperature range, typically working best at temperatures well below 300 °F. The projected annual costs for an activated carbon cleanup process are high, not only because of the high cost of the sorbent but also because of its poor utilization/selectivity for mercury. Carbon-to-mercury weight ratios of 3000:1 to 100 000:1 have been projected.^{1,3-5} In addition, activated carbons can only be regenerated a few times before they exhibit unac-

ceptably low activity for mercury removal. Therefore, the development of improved activated carbons as well as novel sorbents merits further research.

A sorbent can capture mercury via amalgamation, physical adsorption, chemical adsorption, and/or chemical reaction. The noble metal sorbents⁶⁻¹⁴ can capture mercury via amalgamation. Unpromoted activated carbons and aluminosilicates¹⁵ physisorb elemental mercury. Both amalgamation and physisorption are low-temperature processes, typically occurring below 300 °F. Chemically promoted (with sulfur, iodine, or chlorine) activated carbons,¹⁶⁻²¹ selenium,^{22,23} and manganese dioxide or hopcalite^{24,25} are examples of sorbents which chemisorb or chemically react with mercury. Chemisorption and chemical reaction can occur over a wider range of temperatures than physical adsorption and amalgamation. The enthalpy and activation energies of chemisorption/chemical reaction are typically larger than those for physical adsorption.

In this work, which is sponsored by the Advanced Research and Environmental Technology Power Subprogram of the U.S. Department of Energy's Fossil Energy Program, various sorbents were examined for the removal of elemental mercury from argon. It was realized that elemental mercury in flue gas would be more difficult to remove than oxidized mercury, and thus the thrust was to initially identify sorbents that could remove the less reactive elemental mercury. Very few techniques can be used to make an on-line and continuous determination of elemental mercury down to ppb levels, and the exact mechanism by which most sorbents remove mercury is unresolved. The atomic fluorescence spectrophotometer can be used to measure the concentration of elemental mercury in argon on a continuous basis²⁶ and was used in determining the breakthrough curves of sorbents in a packed bed. When more complex carrier gases were used, the capacity was

* To whom correspondence should be addressed. Tel.: (412) 386-4607. Fax: (412) 386-6004. E-mail: evan.granite@netl.doe.gov.

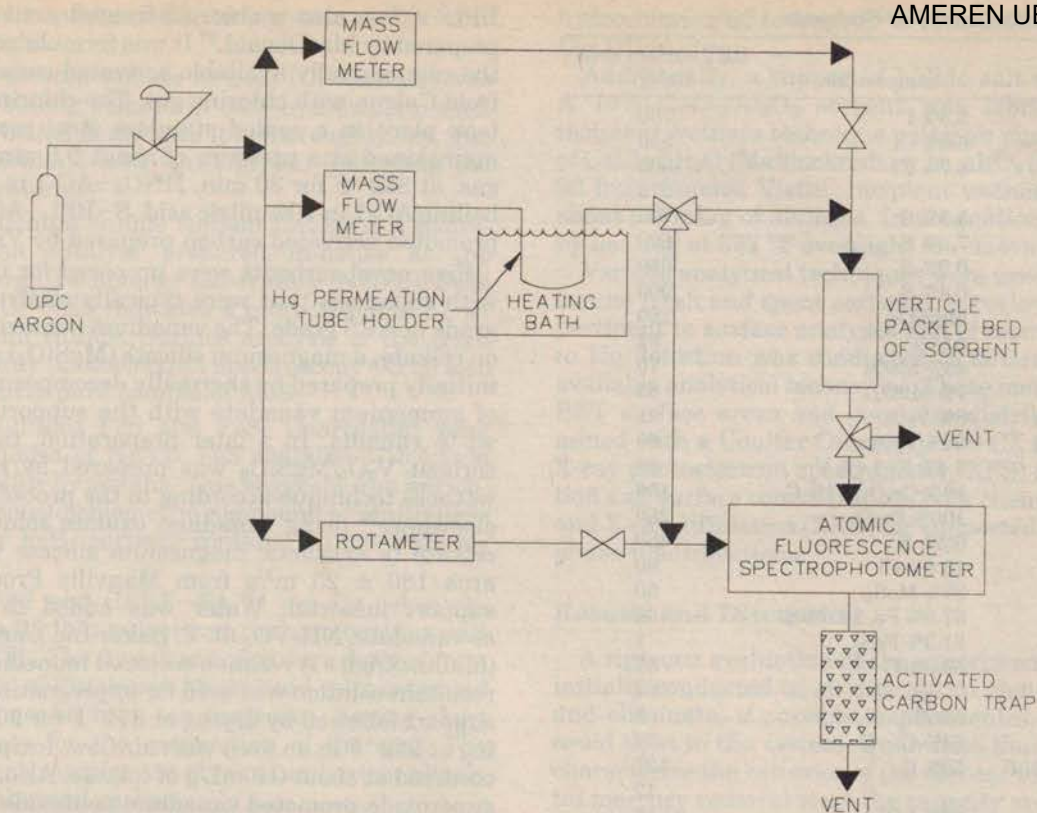


Figure 1. Schematic of sorbent screening unit.

determined off-line via ICP-AES or CVAAS. The capacities of several commercially available activated carbons, metal oxides, a halide salt, metal sulfides, silicates, chlorinated sorbents, a noble metal, and fly ashes were determined.

Experimental Procedures

The assembly used for measuring sorbent capacities consists of an elemental mercury permeation tube, a packed-bed reactor, an on-line atomic fluorescence spectrophotometer, and a data acquisition system. The reactor scheme is shown in Figure 1. A certified Dynacal permeation tube from VICI Metronics is used as the source of elemental mercury. The permeation tube has been certified by the manufacturer to release 144 ng of Hg/min at 212 °F. The permeation tube is located at the bottom of a Dynacal glass U-tube, which is maintained at 212 ± 1.6 °F at all times by immersing it in a Hacke L oil bath. A flow (30 mL/min) of ultra-high-purity carrier-grade (99.999%) argon gas passes over the permeation tube and is maintained at all times with a thermal conductivity mass flow controller. The output of the permeation tube and the flow rate of argon yields a calculated concentration of mercury in argon of 585 ppb. The mercury output of the tube has been verified on a monthly basis via weight loss measurement and has been found to be consistent (155 ng of Hg/min) with the certified release. After a year in service, the output of the permeation tube dropped to 139 ng of Hg/min and was replaced with a second certified tube rated for 119 ng of Hg/min. The output of this tube has also been verified by weight loss measurement and has been found to be consistent (107 ng/min) with the certified release. Sorbent capacities have all been normalized to reflect the output of the original permeation tube.

The reactor (adsorber) is a quartz tube (20 in. in length with an outer diameter of $\frac{1}{4}$ in. and inner

diameter of $\frac{1}{8}$ in.) held in a vertical position. All of the plumbing and valves which come into contact with mercury are constructed from either stainless steel or Teflon. These materials have been demonstrated to have good chemical resistance and inertness toward mercury. The packed bed of sorbent is surrounded by a large clam-shell furnace. A Self-tune Plus 300 PID controller is used to maintain the bed at the desired temperature. The temperature at the top of the bed has been determined to be within 1.8 °F of the temperature at the bottom of the bed.

The detector for elemental mercury is a Brooks Rand CVAFS-2 cold vapor atomic fluorescence spectrophotometer (AFS). When used as a continuous on-line monitor for elemental mercury in argon, the detection limit is below 0.1 ppb. The AFS is an ultraviolet (UV) detector for elemental mercury; mercury atoms absorb 253.7-nm light and re-emit (fluoresce) this wavelength. A mercury bulb serves as the UV source, and a photomultiplier tube serves as the UV fluorescence detector. Any gas can be used as a carrier, although sensitivity varies dramatically with inertness, because of quenching of the excited Hg atoms by collisions with polyatomic species. Maximum sensitivity (ppt) is achieved with high-purity argon or helium carrier gases. When the AFS was used as an on-line detector for elemental mercury, argon was used as the carrier gas. For the more complex carrier gases, the sorbent capacity was determined off-line by analyzing the spent sorbent with ICP-AES or CVAAS. The ICP-AES is a Perkin-Elmer Optima 3000 radial view spectrometer. The CVAAS is a Cetac M-6000A unit dedicated for the analysis of elemental mercury.

Key process parameters were recorded with a data acquisition system. This on-line data acquisition system was used to take and store the various voltage signals

Table 1. Characterization of Sorbents

sorbent	composition	BET surface area (m ² /g)
I-AC	3.5% I	750
Cl-AC-1	6.0% Cl	550
Cl-BPL-AC	6.7% Cl	1000
HNO ₃ -AC-1		575
S-BPL-AC	5.9% S	790
S-AC	7.6% S	690
AC-1	0.9% S	650
AC-2	0.4% S	900
celkate	MgSiO ₃	160
alumina	Al ₂ O ₃	82
MoO ₃ /MgSiO ₃	46% MoO ₃	70
MnO ₂ /Al ₂ O ₃	7% MnO ₂	65
V ₂ O ₅ -MgSiO ₃ -1	8% V ₂ O ₅	91
V ₂ O ₅ -MgSiO ₃ -2	50% V ₂ O ₅	60
KO ₂ -V ₂ O ₅	3.4% K, 1.4% V	85
Cr ₂ O ₃ /Al ₂ O ₃	13% Cr ₂ O ₃ , 11% C	156
Fe ₂ O ₃	100% Fe ₂ O ₃	250
TS-7	3.5% S	450
Cl-celkate	15.0% Cl	80
MoS ₂	87% MoS ₂	50
FeS	57.8% Fe, 22.6% S	32
FeS ₂	81.3% FeS ₂	1
CERF-FA-#2	59.3% C	37
CERF-FA-#4	37% C	24
FA-1	5% C	5
WCFA-1	64% C	32
WCFA-1-air-750F	50% C	127
Cl-WCFA-1		12
DCFA-1	29% LOI	16
DCFA-2	52% LOI	25
DCFA-3	82% LOI	34
CaCl ₂ /Al ₂ O ₃	10% CaCl ₂	41
Pt/wool	40% Pt	20

from the thermocouples, flowmeters, and the atomic fluorescence spectrophotometer. Data logging occurred every 15 s.

Typically, 10 milligram (mg) of 200/325-mesh (45–75- μ m) sorbent is placed in the center of the tube and is supported by about 50 mg of quartz wool. The quartz wool and reactor tube have been demonstrated to be inert toward elemental mercury. Separate argon gas streams flow through the bed and through the permeation tube holder. The latter flow is sent to the AFS to determine a baseline for the mercury concentration. Once thermal stability is reached in the reactor, the mercury/argon mixture is diverted to flow through the reactor. Breakthrough curves were generated by plotting the atomic fluorescence spectrophotometer voltage signal at the reactor exit versus time. Sorbent capacities were determined by integration under the breakthrough curve.

Sorbent Preparation

The sorbents examined in this study and their characterization are listed in Table 1. The sorbents I-AC, S-AC, AC-1, and AC-2 are commercially available activated carbons. I-AC is an iodine-promoted activated carbon, containing both elemental iodine and potassium iodide. S-AC is a sulfur-promoted activated carbon. AC-1 and AC-2 are unpromoted carbons from Calgon and CarboChem, respectively. Some typical mercury control applications for AC-1 include municipal waste combustors, hazardous waste combustors, and hospital waste incinerators.² AC-2 is a food-grade activated carbon used commercially for decolorizing corn syrup.

Cl-AC-1 is a chlorine-promoted activated carbon, prepared by boiling AC-1 in 37% hydrochloric acid. Cl-

BPL-AC is also a chlorine-treated activated carbon prepared by MacDonald.²⁷ It was formulated by treating the commercially available activated carbon BPL-AC from Calgon with chlorine gas. The chlorine treatment took place in a sealed stainless steel reaction vessel maintained at a pressure of about 0.5 atm of chlorine gas, at 330 °F for 30 min. HNO₃-AC-1 is prepared by boiling AC-1 in 70% nitric acid. S-BPL-AC is a sulfur-promoted activated carbon prepared by Vidic.¹⁷

Five novel sorbents were prepared for investigation with chemicals that were typically analytical reagent grade or ACS grade. The vanadium pentoxide dispersed on celkate, a magnesium silicate (MgSiO₃) support, was initially prepared by thermally decomposing a mixture of ammonium vanadate with the support to obtain 8 wt % vanadia. In a later preparation, the supported sorbent V₂O₅/MgSiO₃ was prepared by the incipient wetness technique according to the procedure outlined elsewhere²⁸ using vanadium oxalate solution and the celkate (a synthetic magnesium silicate with surface area 180 \pm 25 m²/g from Manville Products Corp.) support material. Water was added to ammonium *m*-vanadate, NH₄VO₃ (J. T. Baker Inc.), and oxalic acid (Mallinckrodt). A reaction occurred immediately and the resultant solution was used for impregnating the celkate support followed by drying at 572 °F for 2 h and calcining at 932 °F in an oven with air flow. Incipient wetness occurred at about 0.9 mL/g of celkate. Also, a potassium superoxide-promoted vanadium pentoxide (KO₂-V₂O₅) celkate-supported sorbent, whose preparation was similar to the preceding sorbent, was fabricated as well.

The supported sorbent MoO₃/MgSiO₃ was prepared by the incipient wetness technique by dissolution of ammonium molybdate, (NH₄)₆Mo₇O₂₄·4H₂O (Fisher Scientific Co.), with ammonium hydroxide in distilled water, and then contact with the celkate. The solution pH was 8. Impregnation was followed by drying at 248 °F for 24 h and then calcination at 932 °F for 6 h.²⁹

The alumina-supported MnO₂ sorbent was prepared by the incipient wetness technique using an aqueous solution of manganese nitrate, Mn(NO₃)₂·4H₂O (Sigma Chemical Corp.), with alumina, Al₂O₃ (Catalox SCFA 90 with surface area 82 \pm 25 m²/g from Condea Vista). Incipient wetness occurred at about 0.6 mL/g of alumina. Impregnation was followed by the thermal decomposition of manganese nitrate in air at 261 °F as outlined elsewhere.³⁰ Preliminary X-ray diffraction data did not show a MnO₂ diffraction pattern, indicating that the MnO₂ phase was well-dispersed over the alumina and that the crystallite size was below 5 nm.

The chromium oxide sorbent Cr₂O₃/Al₂O₃ that was obtained from Cadus was prepared by impregnation of alumina by chromic acid at room temperature for 30 min.³¹ Immediately after impregnation, the sorbent was dried overnight to 122 °F in a vacuum oven and then calcined at 1202 °F in air for 7 h.

MACH I Inc. supplied the ferric oxide sorbent Fe₂O₃. It was the Nanocat superfine iron oxide, which is a dark brown amorphous powder. The particle size is 3 nm.

The platinum sorbent Pt/wool was prepared by deposition of Engelhard metallo organic platinum ink upon quartz wool. The ink was fired in air at red heat to form a platinum film.

Pacific Northwest National Laboratory provided a novel self-assembled monolayer thiol-promoted aluminosilicate sorbent (TS-7). The sorbent was successfully applied to purify mercury-contaminated water streams.

This sorbent has a high BET surface area and is 3.5% sulfur by weight.

A chlorine-treated celkate sorbent (Cl-celkate) was prepared by boiling celkate in 37% hydrochloric acid. The slurry is boiled in air until it is thoroughly dry. The boiling hydrochloric acid turns green, indicating the evolution of chlorine.

The molybdenum sulfide sorbent (MoS_2) is a hydrodesulfurization catalyst prepared in-house at the National Energy Technology Laboratory (NETL). Bulk analysis by ICP-AES indicates a composition of 87 wt % molybdenum sulfide. Surface analysis of the fresh sorbent by X-ray photoelectron spectroscopy (XPS) also indicates a fairly pure sample of MoS_2 .

The iron sulfides FeS and FeS_2 (marcasite) were prepared in-house at NETL. FeS contains 57.8% iron and 22.6% sulfur by weight. This suggests iron enrichment as in a nonstoichiometric compound or multiphase mixture. The FeS_2 sorbent contains 81.3% FeS_2 by weight.

CERF-FA-#2 and CERF-FA-#4 are fly ashes obtained from a 35 lb/h pulverized coal combustion unit located at NETL. The fly ash samples were derived from the combustion of Pittsburgh #8 coal and were extracted from the furnace at high temperatures, having short residence times for the combustion of the coal. The resulting fly ash samples are atypical and extraordinarily high in unburned carbon.

Sorbents were prepared from fly ash in an effort to utilize unburned carbon from the fly ash. The starting material, FA-1, is fly ash obtained from the combustion of Blacksville coal in the 500 lb/h pilot-scale coal combustion unit located at NETL. FA-1 contains 5% carbon and has a BET surface area of $5 \text{ m}^2/\text{g}$. WCFA-1 is a unburned carbon separated from fly ash obtained from the 500 lb/hr combustion unit. The carbon is concentrated from the fly ash through a wet separation technique. WCFA-1 contains 64% carbon and has a BET surface area of $32 \text{ m}^2/\text{g}$.

Cl-WCFA-1 is a chlorine-treated carbon derived from fly ash. It is prepared by soaking WCFA-1 in aqua regia for 24 h and drying in air. Also, WCFA-1-air-750F is prepared by heating the carbon WCFA-1 in air at 750°F for 2 h. This is done to increase the BET surface area of the carbon.³² Thermal oxidation in air increases the microporosity of carbon resulting from the chemical reaction. WCFA-1 has a BET surface area of $32 \text{ m}^2/\text{g}$, whereas WCFA-1-air-750F has a higher surface area of $127 \text{ m}^2/\text{g}$. The oxidation in air decreases the carbon content from the original 64% down to 50%.

DCFA-1 is a fly ash that is high in carbon content because of poor combustion at a commercial utility; DCFA-2 and DCFA-3 are unburned carbon fractions separated from the DCFA-1 fly ash. The two carbon samples are obtained from the fly ash by a dry separation method (triboelectrostatic) where the first sample is a one-pass separation and the second is a two-pass separation. The elements present in these sorbents were determined via ICP-AES and are silicon, aluminum, iron, titanium, potassium, calcium, magnesium, phosphorus, and sodium. Sulfur, chlorine, and several other elements were not determined by ICP-AES, suggesting that the mass balances obtained (near 90%) are reasonable. Silicon and aluminum accounted for 70–80 wt % of these sorbents (excluding the carbon). These carbons were subsequently treated with chlorine by soaking in

hydrochloric acid to form Cl-DCFA-1, Cl-DCFA-2, and Cl-DCFA-3.

Additionally, a supported halide salt was prepared. A 10% $\text{CaCl}_2/\text{Al}_2\text{O}_3$ sorbent was fabricated by the incipient wetness technique using an aqueous solution of $\text{CaCl}_2 \cdot 2\text{H}_2\text{O}$ (Mallinckrodt) with Al_2O_3 (Catalox SCFA 90 from Condea Vista). Incipient wetness occurred at about 0.6 mL/g of alumina. Impregnation was followed by heating at 392°F overnight to remove the moisture.

Various analytical techniques were used to characterize the fresh and spent sorbents. A review of literature pertinent to surface analyses and of reports pertaining to Hg detection was conducted to determine the best available analytical techniques. These methods included BET surface areas and pore size distributions determined with a Coulter Omnisorp 100 CX apparatus, an X-ray photoelectron spectrometer (XPS) for Hg speciation and surface concentration, bulk chemical analyses, and X-ray diffraction (XRD) for supported oxide sorbent phase identifications.

Results and Discussion

A rigorous evaluation of the experimental setup was initially conducted in an attempt to identify, quantify, and eliminate, if possible, experimental artifacts that could exist in the system. Quantities that were used to characterize the behavior of the sorbent toward elemental mercury removal were the capacity and breakpoint. The capacity was defined as the amount of elemental mercury removed by the sorbent after 350 min on stream. When the continuous on-line AFS monitor for elemental mercury was used, the breakpoint was defined as the time when the outlet concentration of mercury emerging from the reactor bed equaled 10% of the inlet mercury concentration.

The reproducibility of the experimentally determined 350-min capacity and the 10% breakpoint were determined for the baseline sorbent, iodine-promoted activated carbon. Ten milligrams of 200/325-mesh iodine-promoted activated carbon was exposed to 585 ppb of elemental mercury in a $30 \text{ cm}^3/\text{min}$ flow of argon at 350°F in order to generate the breakthrough curves. This sorbent was used in this exercise because it represented the most reactive sorbent to date. The experiment was replicated with good results. The capacity determined via the on-line AFS in argon was reproducible to within $\pm 0.2 \text{ mg/g}$ and the breakpoint time to within $\pm 25\%$.

The capacity determined with the on-line AFS was compared with the results obtained from analyzing the spent sample with cold vapor atomic absorption spectrophotometry (CVAAS) and the inductively coupled argon plasma atomic emission spectrophotometer (ICP-AES). The on-line AFS is the most reliable technique for determining sorbent capacity. Unfortunately, this technique is primarily limited to argon (or other noble gas) or nitrogen carrier gas streams.³³ The AFS also has a detection limit for mercury which is an order of magnitude less than the detection limit for the atomic absorption spectrophotometer (AAS).

CVAAS is the next most reliable method for capacity determination and is the preferred analytical technique for the quantitative determination of trace levels of mercury in solids because of the elimination of the background matrix. Great care is taken to transfer the mercury into a noble carrier gas, providing good reproducibility. In CVAAS, the solid is dissolved into solution. Mercury is reduced from solution with tin chloride,

Table 2. Sorbent Experimental Results: Argon Carrier Gas

sorbent	capacity (mg/g) ^a	breakpoint (min)	temperature (°F)
I-AC	3.1		350
I-AC	4.8	330	350
S-AC	0.4	4	350
S-AC	3.5	7	280
S-BPL-AC	1.9		280
Cl-AC-1	4.0	70	280
Cl-BPL-AC	2.6		280
HNO ₃ -AC-1	1.2	3	280
AC-1	0.37		280
AC-2	0.4	4	280
celkate	0.5	2.5	350
alumina	0.6	2.5	140
MnO ₂ /Al ₂ O ₃	2.2	3	350
MnO ₂ /Al ₂ O ₃	2.4	11	280
MnO ₂ /Al ₂ O ₃	2.4	40	140
V ₂ O ₅ -MgSiO ₃ -1	0.4	3	350
V ₂ O ₅ -MgSiO ₃ -2	0.1	2	350
MoO ₃ /MgSiO ₃	0.2	3	350
Cr ₂ O ₃ /Al ₂ O ₃	1.2	2	140
Cr ₂ O ₃ /Al ₂ O ₃	3.1		280
Cr ₂ O ₃ /Al ₂ O ₃	3.3	9	350
Fe ₂ O ₃	0.1		280
TS-7	0.01 (ICP-AES)		150
Cl-celkate	0.8	0.5	280
MoS ₂	8.8 (ICP-AES)		280
MoS ₂	3.9		280
MoS ₂	3.6	17	280
MoS ₂	4.5	194	140
FeS	cap < 0.01		280
FeS ₂	0.2		280
CERF-FA-#2	1.7	4	280
CERF-FA-#2	1.4		280
CERF-FA-#4	2.2	20	280
CERF-FA-#4	1.7		280
FA-1	0.02		280
WCFA-1	0.1		280
WCFA-1	0.04		350
Cl-WCFA-1	2.5		280
Cl-WCFA-1	0.64		350
DCFA-1	0.03		280
DCFA-2	0.12		280
DCFA-3	0.15		280
Cl-DCFA-1	0.24		280
Cl-DCFA-2	0.30		280
Cl-DCFA-3	0.41		280
Pt/wool	5.0		280
CaCl ₂ /Al ₂ O ₃	0.6	2	140

^a Capacity determined via on-line AFS when a breakpoint time is given; otherwise, the capacity was determined by CVAAS, except as noted.

aerated onto a gold trap, thermally desorbed from the gold trap, and swept into an argon stream to an ultraviolet (AAS) detector. Chemical (tin chloride reduction) and physical (amalgamation) steps are taken to separate the mercury. The detection limit of CVAAS is 10 ng/g.³⁴ The typical precision for measurement of mercury concentrations in solids is 5–10% relative standard deviation.³⁴ A comparison of capacity determinations via the on-line AFS and CVAAS shown in Tables 2 and 3 for I-AC in argon at 350 °F, MoS₂ in argon at 280 °F, CERF-FA #2 in argon at 280 °F, and CERF-FA #4 in argon at 280 °F shows a fair agreement.

The ICP-AES is the least reliable of the three techniques for trace-level mercury determinations. It can be seen from Table 2 that the ICP-AES yields capacities which are high by a factor of 2. The ICP-AES is the most versatile tool for multielement analysis, but it is not the preferred method for trace-level mercury measurements in solids. No steps are taken to separate the mercury from the other elements present in the solid sample.

Table 3. Sorbent Experimental Results: Air Carrier Gas

sorbent	capacity (mg/g)	analysis method	temperature (°F)
KO ₂ -V ₂ O ₅	0.02	CVAAS	280
KO ₂ -V ₂ O ₅	0.04	CVAAS	350
MnO ₂ /Al ₂ O ₃	3.50	CVAAS	280
TS-7	0.00	ICP-AES	140
S-BPL-AC	0.53	ICP-AES	280
S-BPL-AC	0.28	ICP-AES	350
MoS ₂	5.6	ICP-AES	140
MoS ₂	5.2	ICP-AES	280
MoS ₂	1.1	ICP-AES	350
AC-1 ^a	0.04	CVAAS	280
AC-1 ^a	0.19	AFS	280

^a 4% O₂ in N₂ carrier gas.

Other elements could interfere in the detection of mercury. For example, the cobalt emission line at 253.649 nm could interfere in the determination of mercury by the 253.652-nm emission line.³⁵ The concentration of the interfering element (in this case cobalt), monochromator slit width, and relative intensity of the shared emission line are factors in determining the extent of spectral interference. Experiments with the Perkin-Elmer Optima 3000 radial view ICP-AES confirmed that cobalt will interfere in the trace-level determination of mercury in solids. Additionally, because of their emission lines close to 253.7 nm, iron and manganese³⁶ will also interfere in the determination of mercury by ICP-AES.

The effect of intraparticle mass-transfer resistance due to the diffusion of mercury within the pores was determined by carrying out the same experiment but with various size fractions of the baseline iodine-promoted activated carbon. For a sub-400-mesh size fraction of the same carbon, the 350-min capacity was 4.9 mg of Hg/g and the breakpoint was 405 min. This is in good agreement with the data for the larger size fraction (see I-AC in Table 2), suggesting that mass-transfer resistance due to the diffusion of mercury into the sorbent at the sizes used in the testing is negligible. Calculations further indicated that bulk mass-transfer effects, heat-transfer effects, channeling, and pressure drop would not be significant in the experimentation.

Most of the experiments used a gas feed of 585 ppb elemental mercury in argon. This is dramatically different than the composition of a typical flue gas from a coal-fired utility. Most of the components in a typical flue gas (e.g., acid gases, etc.) can adsorb on an activated carbon and could possibly hinder or help the adsorption of mercury on carbon. As pointed out above, the ultra-high-purity argon carrier gas was selected to maximize the sensitivity of the AFS for elemental mercury. However, the capacity of the sorbents in argon can be quite different from the capacity in flue gas. Also, the temperatures at which sorbent capacities were typically determined are 140, 280, and 350 °F. These temperatures were chosen because of their potential relevance to coal-fired utilities. If a sorbent were contacted with the flue gas by injection into the duct work of a coal-fired utility after the air preheater but before the particulate collection device, it would experience temperatures in the range of 350–280 °F. If a sorbent was placed downstream of a wet scrubber, it would encounter a temperature near 140 °F.

The 350 min capacities and the 10% breakpoint times for the sorbents are listed in Table 2. The baseline sorbent—the iodine-promoted activated carbon—exhibited

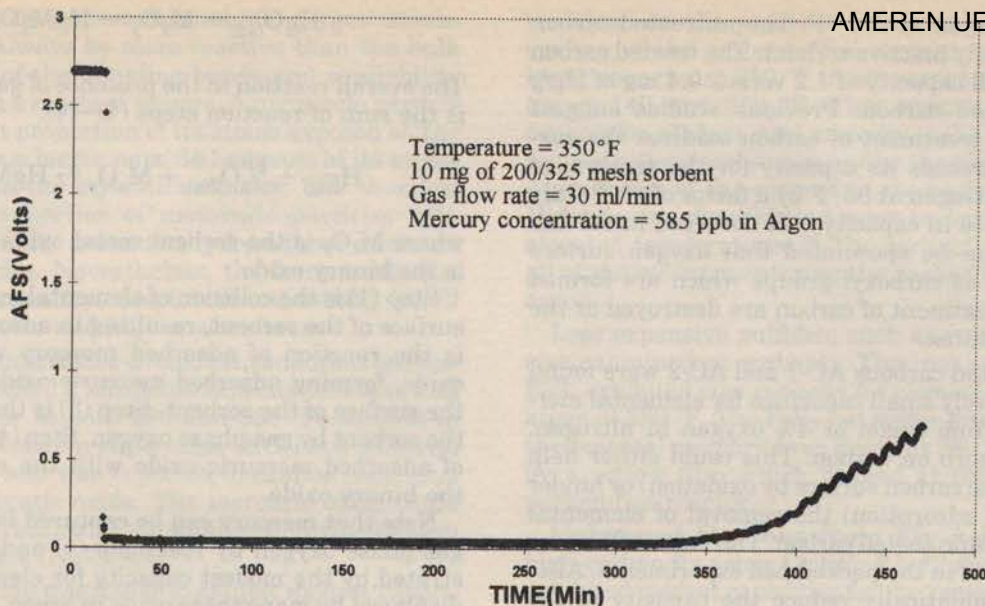


Figure 2. Breakthrough curve for I-AC using the AFS for mercury detection.

both the largest, most reliably determined (on-line AFS) capacity and longest breakpoint time. A typical breakthrough curve for the iodine-promoted activated carbon is shown in Figure 2.

Activated Carbons. With the activated carbons, the effect of the chemical promoter on the capacity for elemental mercury was determined by comparing the capacities of the commercially available unpromoted carbon with the capacities of the sulfur, iodine, chlorine, and nitric acid-treated carbons at the same temperature. The sulfur- and iodine-promoted carbons are available commercially. The carbons, when chemically promoted, exhibited a far greater capacity for elemental mercury. An unpromoted carbon primarily captures elemental mercury via physical adsorption. Chemically promoted carbons capture elemental mercury by both physical adsorption and chemisorption/chemical reaction, where mercuric sulfide, mercuric iodide, and so forth formation enables the promoted carbons to remove more elemental mercury.

Various analyses were performed on the spent baseline iodated carbon sorbent to elucidate the role of the promoter. A 3-day run in the packed bed was performed on 35 mg of iodated activated carbon so that gross differences, if any, between the fresh sorbent and spent sorbent could be differentiated by the BET surface analysis. Results indicate a reduction in surface area from 780 to 300 m²/g. Additionally, after it was determined that the vacuum treatment would not impact the mercury concentration, XPS studies with the spent iodated activated carbon showed that the Hg species on the surface was oxidized and in the form of HgI₂; no elemental Hg was detected. Potassium iodide was also detected. The total iodide concentration was 0.4% atomic and the Hg surface concentration was 0.13% atomic. Also, the capacity of the spent iodine-promoted carbon was confirmed by atomic absorption analysis. The used sorbent was digested in acid, and the concentration of mercury in the solution was measured by an atomic absorption spectrophotometer. The capacity (gaseous determination) of the iodine-promoted carbon found by integration under the breakthrough curve (4.8 mg/g)

was in reasonably good agreement with the capacity (solid determination) established by atomic absorption (3.1 mg/g).

The effect of flue gas temperature was studied by examining the breakthrough curves for the sulfur-promoted carbon S-AC at 280 and 350 °F. The capacity of this carbon at 280 °F was 3.5 versus 0.4 mg of Hg/g at 350 °F. As many studies have demonstrated, activated carbons perform much better at lower temperatures. The temperatures at which activated carbons have been reported to possess good capacities for mercury range from 70 to 500 °F.^{1-6,13,16-19,23,37-46} This suggests that physical adsorption may be the first step in the removal of mercury for both unpromoted and promoted carbons. Physical adsorption, analogous to condensation, is a low-temperature process. For a chemically promoted carbon, such as sulfur-impregnated carbon, chemisorption/reaction between the physically adsorbed mercury and sulfur promoter to form mercuric sulfide could be the second step in the mechanism of mercury removal.

The hydrochloric acid-treated activated carbon Cl-AC-1 exhibited a large capacity of 4.0 mg of Hg/g when tested in argon at 280 °F, making it one of the most active sorbents studied to date. Additionally, the chlorine gas-treated activated carbon, Cl-BPL-AC, exhibited a modest capacity for elemental mercury removal. One previous study suggests that hydrochloric acid treatment yields activated carbons which have chemisorbed chlorine.⁴⁷ Quimby demonstrated that HCl-treated activated carbon will adsorb mercuric chloride from air at 300 °F.²¹ Mercury is known to primarily form the tetrachloromercury complex HgCl₄²⁻ on the surface of activated carbons used for the removal of mercuric chloride from wastewater; little mercuric chloride was found on the surface of these carbons.⁴⁸ Other prior studies have shown that HCl treatment of silica increases its capacity for mercury. It can be speculated that elemental mercury reacts with chemisorbed chlorine to form the tetrachloromercury complex on the surface of the carbon.

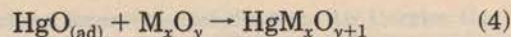
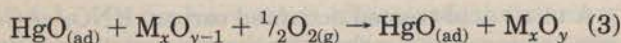
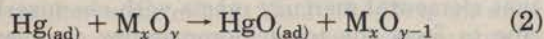
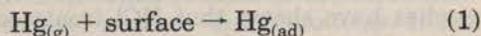
A nitric acid-treated activated carbon, HNO₃-AC-1, was examined as a sorbent for the removal of elemental

mercury from argon at 280 °F. The untreated carbon AC-1 is a relatively inactive sorbent. The treated carbon exhibited a small capacity of 1.2 versus 0.4 mg of Hg/g for the untreated carbon. Previous studies suggest that nitric acid treatment of carbon oxidizes the surface^{20,47} and increases its capacity for the removal of mercury from nitrogen at 86 °F by a factor of 20.²⁰ Only a modest increase in capacity was observed in our lab at 280 °F. It can be speculated that oxygen surface complexes such as carboxyl groups which are formed by nitric acid treatment of carbon are destroyed at the higher temperatures.

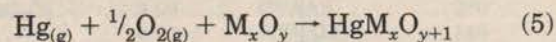
The unpromoted carbons AC-1 and AC-2 were found to possess relatively small capacities for elemental mercury, whether from argon or 4% oxygen in nitrogen. Oxygen will adsorb on carbon. This could either help (by promoting the carbon surface by oxidation) or hinder (by competitive adsorption) the removal of elemental mercury by an unpromoted carbon. The latter effect was probably observed in the packed-bed experiments. Also, oxygen may dramatically reduce the capacity of the sulfur-promoted carbon as the capacity dropped from 3.5 mg/g in argon for S-AC to 0.5 mg/g in air at 280 °F for S-BPL-AC. S-AC and S-BPL-AC both exhibit high capacities for elemental mercury from inert carrier gases.¹⁷ This suggests that oxygen competitively adsorbs on sulfur, reducing the capacity.

The results obtained from the packed-bed unit require judicious interpretation when attempting to extrapolate their relevance to activated carbon sorbent duct injection as a mercury control technique for industrial size combustors. AC-1 was also studied in the NETL 500 lb of coal/h pilot-scale combustor unit for the removal of mercury from the flue gas.⁴⁹ When introduced at a large sorbent-to-mercury ratio of around 5000:1, AC-1 used in the 500 lb/h unit achieved a high level of mercury removal. However, the used AC-1 recovered from the baghouse had mercury levels of less than 300 ppm (0.3 mg of Hg/g), but a high level of mercury removal is achieved. Unpromoted activated carbons sequester elemental mercury via physical adsorption and therefore exhibit small capacities. Duct injection at large sorbent-to-mercury ratios from 5000:1 to 100 000:1 allows them to, nevertheless, achieve high levels of removal of mercury from flue gas.

Metal Oxides. Metal oxides are proposed as novel alternatives to activated carbon sorbents. It is noted that there are many binary oxides of mercury, such as mercury vanadates, mercury molybdates, and mercury manganates.⁵⁰⁻⁵² Vanadium pentoxide, molybdenum trioxide, and manganese dioxide are all partial oxidation oxide catalysts for the oxidation of various hydrocarbons.^{26,53} In the oxidation of various hydrocarbons, lattice oxygen serves as the oxidant in a Mars-Maessen mechanism. This suggests that lattice oxygen of partial oxidation oxides could also serve as the oxidant of mercury. The reaction mechanism for the capture of mercury by oxide catalysts can be written as



The overall reaction in the presence of gas-phase oxygen is the sum of reaction steps (1)–(4):



where M_xO_y is the sorbent metal oxide and $\text{HgM}_x\text{O}_{y+1}$ is the binary oxide.

Step (1) is the collision of elemental mercury with the surface of the sorbent, resulting in adsorption. Step (2) is the reaction of adsorbed mercury with the metal oxide, forming adsorbed mercuric oxide and reducing the surface of the sorbent. Step (3) is the reoxidation of the sorbent by gas-phase oxygen. Step (4) is the reaction of adsorbed mercuric oxide with the sorbent to form the binary oxide.

Note that mercury can be captured in the absence of gas-phase oxygen by reactions (1) and (2), as demonstrated by the modest capacity for elemental mercury displayed by manganese oxide in argon, shown in Table 2. There are many potential rate-limiting factors which can impact oxide capacity for mercury, including surface area, activity of the sorbent as an oxidation catalyst, stability of lower oxides, oxygen partial pressure, and tendency to form the binary oxide. Mercury is a semi-noble metal with a standard reduction potential similar to palladium's. Mercury may not be easily oxidized by the metal oxide sorbent. An oxide's tendency to form sulfates is a critical factor for sorbent performance in flue gas because sulfur dioxide is present at concentrations orders of magnitude greater than mercury's.

Alumina (Al_2O_3) or celkate (MgSiO_3), which were used as supports for some of the novel sorbents, were examined as sorbents for the removal of elemental mercury from argon. Both exhibit small capacities, demonstrating their inertness toward elemental mercury. The role of the alumina or celkate support is to provide a high surface area substrate for maximizing the number of collisions between mercury and the sorbent.

Supported vanadium pentoxide and supported molybdenum trioxide exhibited low capacities for the removal of elemental mercury from argon at 350 °F. Preparation of the V_2O_5 -supported sorbent either via the thermal decomposition of ammonium vanadate or via incipient wetness did not impact the sorbent capacity. Manganese dioxide supported on alumina was examined as a sorbent for the removal of elemental mercury from argon at 350, 280, and 140 °F. Manganese dioxide has been reported to remove elemental mercury from both air and argon at room temperature.^{24,25} MnO_2 exhibited modest 350-min capacities of 2.2 mg of Hg/g at the higher temperature and 2.4 mg of Hg/g, at both 140 and 280 °F.

In the Mars-Maessen mechanism, gas-phase oxygen can serve to reoxidize the reduced oxide. Oxygen was absent from the gas phase in these experiments. Manganese dioxide is the most powerful oxidation catalyst⁵³ of the oxide oxidation catalysts examined and exhibited the largest capacity for mercury. A Mars-Maessen redox mechanism for the removal of mercury has been proposed above for partial oxidation oxide sorbents. The capacity of the manganese dioxide sorbent was observed to be larger in air than in argon at 280 °F (see Table 3).

Nanoscale iron oxide was examined as a sorbent for mercury removal from argon at 280 °F. Each particle

contains about 600 iron atoms and 900 oxygen atoms. A surface will always be more reactive than the bulk lattice because of the dangling bonds and availability for collision with a reactant species. A nanoscale particle has a significant proportion of its atoms exposed on the surface whereas a larger particle has most of its atoms contained within the crystalline lattice. The chemical and physical properties of nanoscale particles will, therefore, often differ dramatically from those exhibited by larger particles. Nevertheless, the ferric oxide displayed a poor capacity, despite the unusually small (3-nm) particle size and high surface area.

A potassium superoxide-promoted vanadium pentoxide sorbent exhibited a miniscule capacity for elemental mercury from air at both 280 and 350 °F, as seen in Table 3. The potassium superoxide (KO_2) is a powerful oxidizing agent and was expected to oxidize elemental mercury to mercuric oxide. The mercuric oxide could then chemisorb/react with vanadium pentoxide to form mercury vanadate (HgV_2O_6).

Chromium oxide was found to exhibit modest capacities for elemental mercury. Cr_2O_3 is a fairly strong oxidation catalyst, with a catalytic activity for the deep oxidation of methane comparable to manganese dioxide.⁵³ A crude correlation was found between the catalytic activity for deep oxidation exhibited by the oxide and the sorbent capacity for elemental mercury removal. Sorbents that are active catalysts for the deep oxidation of methane $\text{Cr}_2\text{O}_3/\text{Al}_2\text{O}_3$ and $\text{MnO}_2/\text{Al}_2\text{O}_3$ exhibit large capacities, whereas the inactive oxide catalysts Fe_2O_3 , $\text{MoO}_3/\text{Al}_2\text{O}_3$, and $\text{V}_2\text{O}_5\text{-MgSiO}_3\text{-1}$ show small capacities.

Promotion of metal oxide supports was also investigated. The chlorine-promoted magnesium silicate Cl-celkate exhibited a small capacity for the removal of elemental mercury from argon at 280 °F. Braman demonstrated that HCl-treated Chromosorb-W, a diatomite chromatographic packing, will adsorb mercuric chloride vapors at 70 °F.⁷ Additionally, the novel thiol-promoted aluminosilicate sorbent (TS-7) exhibited very small capacities for elemental mercury both in argon and in air. Thiols are the sulfur analogues of alcohols. Thiols are also called mercaptans, from the Latin, *mercurium captans*, meaning "capturing mercury".⁵⁴ Mercaptans react with mercuric ions and the ions of other heavy metals to form precipitates. The sorbent was developed for the removal of oxidized mercury from contaminated water. Elemental mercury is insoluble in water. Oxidized forms of mercury are known to react efficiently with thiols. The low decomposition temperatures of thiols as well as the lack of reactivity with elemental mercury suggest that thiols are not practical promoters for the removal of elemental mercury from flue gas.

Metal Sulfides. Molybdenum sulfide (MoS_2) displayed a large capacity for the removal of elemental mercury from argon and air. This sorbent was originally developed as a hydrodesulfurization catalyst for the conversion of thiopene and mercaptans to hydrogen sulfide and alkanes. A possible mechanism of mercury capture is chemisorption/chemical reaction to form mercuric sulfide. XPS analysis of the used sorbent run in argon at 280 °F confirms the presence of mercury on the surface. Elemental mercury was not detected on the surface of the used MoS_2 sorbent. This rules out physical adsorption of elemental mercury as the primary means of sequestration. The X-ray excited photoelectron spec-

tra suggests the presence of mercuric sulfide on the surface of the sorbent. The sorbent exhibits a much lower capacity at 350 °F in air versus the capacities in air at 140 and 280 °F. This suggests that physical adsorption of elemental mercury is the first step in the sequestration mechanism and/or the physical-chemical degradation of the sorbent at the higher temperature. Molybdenum disulfide is known to decompose in air at elevated temperatures.³⁶ The sorbent removed nearly all of the mercury entering the packed bed at 140 °F in argon.

Less expensive sulfides, such as iron sulfides, were also examined as sorbents. The iron sulfides FeS and FeS_2 exhibited poor capacity for elemental mercury from argon at 280 °F. The FeS_2 lost sulfur during the sorption of elemental mercury from argon at 280 °F, as evidenced by a yellow film which formed at the bottom of the packed-bed reactor.

Unburned Carbons from Fly Ash. The atypical high-carbon fly ashes CERF-FA-#2 and CERF-FA-#4 exhibited modest capacities for the removal of elemental mercury from argon at 280 °F. These capacities are, however, significantly higher than those exhibited by the unpromoted carbon and the alumina and celkate supports. Further characterization of these fly ash sorbents is needed to determine the mechanism of mercury capture. These carbons were extracted from the combustor at high temperatures of around 2300 °F. It is speculated that novel forms of carbon present in these samples could positively impact capacity.

The fly ash obtained from the combustion of Blacksville coal, FA-1, exhibited a miniscule capacity for elemental mercury at 280 °F. The carbon separated from this fly ash, WCFA-1, exhibited a small capacity for the removal of elemental mercury from argon at 280 °F. Nevertheless, WCFA-1 does exhibit a larger capacity than the parent fly ash, FA-1. The capacity of WCFA-1 was smaller at 350 °F, as expected. The unpromoted activated carbons show similarly low capacities. The chlorine-promoted carbon extracted from fly ash, Cl-CFA-1, exhibited a much larger capacity for elemental mercury, much like the chlorine-promoted activated carbons. The capacity was lower at the higher temperature, as expected.

DCFA-2 and DCFA-3 are carbons separated from the parent fly ash, DCFA-1, by a dry separation method and exhibit small capacities for elemental mercury. The capacity increases with increasing carbon content. The chlorine-treated materials Cl-DCFA-1, Cl-DCFA-2, and Cl-DCFA-3 showed significantly larger, but still small, capacities. The capacity again increases with increasing carbon content.

Halide salts are also proposed as an alternative to carbon sorbents. There are many binary halides of mercury such as calcium chloromercurate and potassium iodomercurate.⁵⁰ These are double salts of calcium chloride and mercuric chloride and potassium iodide and mercuric iodide, respectively. Potassium iodide is used as a chemical promoter in some of the commercially available activated carbons,^{18,19} such as the baseline sorbent in this study. However, the thermal stability of the binary halides of mercury is poor, as evidenced by their low decomposition temperatures.⁵⁰ Mercuric chloride was absent from the gas phase in these experiments. The absence of mercuric chloride could explain the small capacity exhibited by the calcium chloride sorbent. Mercuric chloride can be present in the flue gas

obtained from the combustion of coal, municipal waste, and medical waste.¹

Noble Metals. The platinum sorbent Pt/wool exhibited a large capacity for elemental mercury from argon at 280 °F. Breakthrough was not observed. After the absorption experiment, the used Pt/wool sorbent was slowly heated in argon to 770 °F over a 70-min period, with the effluent sent directly to the AFS. Over 99.4% of the mercury remained sequestered on the platinum. A minor desorption spike of mercury was observed at 320 °F, likely due to unburned carbon from the organometallic platinum paint precursor. The noble metals are often used for small-scale sampling of gases for mercury, i.e., mercury is often collected on gold, thermally desorbed, and sent to a UV detector for its analytical determination. Thermal desorption of the mercury is accomplished by heating the noble metal to 1470 °F,¹³ greater than the 770 °F maximum temperature in the desorption experiment.

Conclusions

A packed-bed reactor system was used to screen sorbents for the removal of elemental mercury from a carrier gas. An on-line atomic fluorescence spectrophotometer was used to measure elemental mercury in argon on a continuous basis. For more complex carrier gases, sorbent capacities were determined off-line via CVAAS or ICP-AES. Chemically promoted activated carbons exhibit a far greater capacity for mercury than unpromoted carbons. The activated carbons possess higher capacities at lower temperatures. Chlorine could be a cost-effective chemical promoter for carbon sorbents for the removal of mercury.

Metal oxides and sulfides are proposed as a possible alternative to activated carbon sorbents, with MnO₂, Cr₂O₃, and MoS₂ exhibiting moderate capacities for mercury removal among the candidates investigated. Unburned carbon sorbents from fly ash typically showed poor performance toward mercury removal, although promotion of these increases the activity for elemental mercury removal. Future work will concentrate on testing inexpensive chlorine-promoted carbons as well as metal oxides and sulfides in a simulated flue gas matrix which includes acid gases, oxygen, water, and mercuric chloride. Promising sorbent candidates will be further evaluated on a pilot-scale system.^{49,55}

Acknowledgment

Evan Granite acknowledges the support of a post-doctoral fellowship at the U.S. Department of Energy administered by Oak Ridge Institute For Science and Education (ORISE). George Haddad, also through the ORISE program, provided project support. Michael Hilterman, Edward Zagorski, Dennis Stanko, Sheila Hedges, John Baltrus, Mac Gray, Yee Soong, Rod Diehl, Murphy Keller, Mark Freeman, Anthony Cugini, James Hoffman, Karl Schroeder of the Department of Energy, Robert Thompson and Joseph Niedzwicki of Parsons Infrastructure, Donald Floyd of EG&G Technical Services, and Mark Wesolowski of SSI Services, Inc. provided outstanding technical assistance. Several individuals and organizations provided sorbent samples for examination by the DOE. Professor Radisav Vidic of The University of Pittsburgh supplied a sulfur-promoted carbon sorbent. Professor Jayne MacDonald of the Royal Military College of Canada provided a chlorinated carbon sample. CarboChem Inc. donated

an unpromoted activated carbon sorbent. Dr. Shas Mattigod of Pacific Northwest National Laboratory provided the thiol-promoted aluminosilicate. Professor Luis Cadus of INTEQUI Instituto de Investigaciones en Tecnologia Quimica, San Luis, Argentina supplied the chromium oxide sorbent. Dr. John Stencil of the Kentucky Center For Applied Energy Research provided carbons derived from fly ash. MACH I Inc. of King of Prussia Pennsylvania contributed the iron oxide sample.

Disclaimer

Reference in this paper to any specific commercial product, process, or service is to facilitate understanding and does not necessarily imply its endorsement by the U.S. Department of Energy.

Literature Cited

- (1) *Mercury Study Report to Congress*; EPA 452/R-97-003; U. S. Environmental Protection Agency, Office of Air Quality Planning and Standards: Washington, DC, Dec 1997.
- (2) *Flue Gas Treatment Reference Bulletin*; Calgon Carbon Corporation: Pittsburgh, PA, Nov 1994.
- (3) Ghorishi, B.; Jozewicz, W.; Gullet, B. K.; Sedman, C. B. Mercury Control: Overview of Bench-Scale Research at EPA/APPCC. Presented at the First Joint Power & Fuel Systems Contractors Conference, Pittsburgh, PA, July 1996.
- (4) Waugh, E. G.; Jensen, B. K.; Lapatnick, L. N.; Gibbons, F. X.; Haythornthwate, S.; Sjostrom, S.; Ruhl, J.; Slye, R.; Chang, R. Mercury Control on Coal-Fired Flue Gas Using Dry Carbon-Based Sorbent Injection: Pilot-Scale Demonstration. Presented at the Fourth International Conference on Managing Hazardous Air Pollutants, Washington, DC, Nov 1997.
- (5) Brown, T. D.; Smith, D. N.; Hargis, R. A.; O'Dowd, W. J. Mercury Measurement and Its Control: What We Know, Have Learned, and Need to Further Investigate. *J. Air Waste Manage. Assoc.* **1999**, *6*, 1.
- (6) Attari, A.; Chao, S. Trace Constituents in Natural Gas; Sampling and Analysis. *Oper. Sect. Proc. Am. Gas Assoc.* **1994**, *28-32*.
- (7) Braman, R. S.; Johnson, D. L. Selective Absorption Tubes and Emission Technique for Determination of Ambient Forms of Mercury in Air. *Environ. Sci. Technol.* **1974**, *8* (12), 996.
- (8) Williston, S. H. Mercury in the Atmosphere. *J. Geophys. Res.* **1968**, *73* (22), 7051.
- (9) Henriques, A.; Isberg, J.; Kjellgren, D. Collection and Separation of Metallic Mercury and Organo-mercury Compounds in Air. *Chem. Scr.* **1973**, *4* (3), 139.
- (10) Henriques, A.; Isberg, J. A New Method for Collection and Separation of Metallic Mercury and Organomercury Compounds in Air. *Chem. Scr.* **1975**, *8* (4), 173.
- (11) Roberts, D. L.; Stewart, R. M. Novel Process for Removal and Recovery of Vapor Phase Mercury. Presented at the First Joint Power & Fuel Systems Contractors Conference, Pittsburgh, PA, July 1996.
- (12) Yan, T. Y. A Novel Process for Hg Removal from Gases. *Ind. Eng. Chem. Res.* **1994**, *33*, 3010.
- (13) Dumarey, R.; Dams, R.; Hoste, J. Comparison of the Collection and Desorption Efficiency of Activated Charcoal, Silver, and Gold for the Determination of Vapor-Phase Atmospheric Mercury. *Anal. Chem.* **1985**, *57*, 2638.
- (14) Roberts, D. Novel Process for Removal and Recovery of Vapor-Phase Mercury. Presented at the Advanced Coal-Based Power and Environmental Systems '97 Conference, Pittsburgh, PA, July 1997.
- (15) Livengood, C. D.; Huang, H. S.; Mendelsohn, M. H.; Wu, J. M. Enhancement of Mercury Control in Flue Gas Cleanup Systems. Presented at the First Joint Power & Fuel Systems Contractors Conference, Pittsburgh, PA, July 1996.
- (16) Walker, P. L.; Sinha, R. K. Removal of Mercury by Sulfurized Carbons. *Carbon* **1972**, *10*, 754.
- (17) Korpel, J.; Vidic, R. Effect of Sulfur Impregnation Method on Activated Carbon Uptake of Gas-Phase Mercury. *Environ. Sci. Technol.* **1997**, *31* (8), 2319.
- (18) *Material Safety Data Sheet for Activated Carbon 717*; Barnebey & Sutcliffe: Columbus, OH, Sept 1996.

- (19) Carbon Product Bulletin HGR-LH; Calgon Carbon Corp.: Pittsburgh, PA, Feb 1994.
- (20) Matsumura, Y. Adsorption of Mercury Vapor on the Surface of Activated Carbons Modified by Oxidation or Iodization. *Atmos. Environ.* **1974**, *8*, 1321.
- (21) Quimby, J. M. Mercury Emissions Control From Combustion Systems. Proceedings of Annual Meeting, Air Waste Management Association: Pittsburgh, PA, 1993.
- (22) Hogland, W. K. H. Usefulness of Selenium for the Reduction of Mercury Emissions From Crematoria. *J. Environ. Qual.* **1994**, *23*, 1364.
- (23) Tsuji, K.; Shiraishi, I.; Olson, D. G. EPRI Report no. TR-105258; EPRI: Palo Alto, CA, 1995; conf-950332, Vol. 3, pp 66.1-66.15.
- (24) Janssen, J.; Van Den Enk, J.; De Groot, D. Determination of Total Mercury in Air by Atomic Absorption Spectrometry After Collection on Manganese Dioxide. *Anal. Chim. Acta* **1977**, *92*, 71.
- (25) Rathje, A.; Marcero, D.; Dattilo, D. Personal Monitoring Technique for Mercury Vapor in Air and Determination by Flameless Atomic Absorption. *J. Am. Ind. Hyg. Assoc.* **1974**, *35*, 571.
- (26) Granite, E. J.; Pennline, H. W.; Hargis, R. A. Sorbents For Mercury Removal From Flue Gas. *Topical Report DOE/FETC/TR-98-01*; National Energy Technology Laboratory: Pittsburgh, PA, Jan 1998.
- (27) MacDonald, J.; Evans, M.; Halliop, E.; Liang, S. The Effect of Chlorination On Surface Properties Of Activated Carbon. *Carbon* **1998**, *36*, 6 (11), 1677.
- (28) Oyama, S. T.; Went, G. T.; Lewis, K. B.; Bell, A. T.; Somarjai, G. A. *J. Phys. Chem.* **1989**, *93*, 6786.
- (29) Mahipal Reddy, B.; Padmanabha Reddy, E.; Srinivas, S. T. *J. Catal.* **1992**, *136*, 50.
- (30) Maltha, A.; Favre, T. L. F.; Kist, H. F.; Zuur, A. P.; Ponec, V. *J. Catal.* **1994**, *149*, 364.
- (31) Mentasty, L.; Gorriz, O.; Cadus, L. Chromium Oxide Supported on Different Al₂O₃ Supports. *Ind. Eng. Chem. Res.* **1999**, *38*, 396.
- (32) MacDonald, J. A. F.; Halliop, E.; Evans, M. J. B. The Production of Chemically-Activated Carbons. *Carbon* **1999**, *37*, 269.
- (33) Granite, E. J.; Pennline, H. W.; Hoffman, J. S. Effects of Photochemical Formation of Mercuric Oxide. *Ind. Eng. Chem. Res.* **1999**, *38*, 5034.
- (34) Golightly, D. W., Simon, F. O., Eds. Methods For Sampling and Inorganic Analysis of Coal. *U.S. Geological Survey Bulletin 1823*; USGS: Reston, VA, 1995.
- (35) Reeves, R. D.; Brooks, R. R. *Trace Element Analysis of Geological Materials*; John Wiley: New York, 1978.
- (36) Weast, R. C., Ed. *CRC Handbook of Chemistry and Physics*, 63rd ed.; CRC Press: Boca Raton, FL, 1982.
- (37) *Brochure on Sorbalit*; Dravo Corp.: Pittsburgh, PA, June 1994.
- (38) Teller, A. J.; Hsieh, J. Y. Control of Hospital Incineration Emissions-Case Study. Presented at the 84th Annual Meeting of Air & Waste Management Association, Vancouver, Canada, 1991.
- (39) Hsieh, J. Y.; Confuorto, N. Operation of a Medical Waste Incinerator and the Emission Control System. *Proc. SPIE-Int. Soc. Opt. Eng.* **1993**, *1717* (Industrial, Municipal, and Medical Waste Incineration Diagnostics and Control), 46.
- (40) Tsuji, K.; Shiraishi, I. *Prepr. Pap.-Am. Chem. Soc., Div. Fuel Chem.* **1996**, *41* (1), 404.
- (41) Tsuji, K.; Shiraishi, I. EPRI Report no. TR-101054; EPRI: Palo Alto, CA, 1992; conf-911226, Vol.3, p 8A.1.
- (42) Dunham, G. E.; Miller, S. J. Evaluation of Activated Carbon For Control of Mercury From Coal-Fired Boilers. Presented at the First Joint Power & Fuel Systems Contractors Conference, Pittsburgh, PA, July 1996.
- (43) Livengood, C.D.; Huang, H. S.; Wu, J. M. Experimental Evaluation of Sorbents for the Capture of Mercury in Flue Gases. Presented at the 87th Annual Meeting Air & Waste Management Association, Cincinnati, Ohio, June 1994.
- (44) McNamara, J. D.; Wagner, N. J. *Gas Sep. Purif.* **1996**, *10* (2), 137.
- (45) Roberts, D. L.; Stewart, R. M. Characterization of Sorbents for Removal of Vapor Phase Mercury. Presented at the EPRI Mercury Sorbent Workshop, Grand Forks, ND, July 1996.
- (46) Van Wormer, M. Control of Mercury Emissions From Combustion Applications. Presented at the 1992 AIChE National Meeting, Aug 1992.
- (47) Castilla, C. M.; Marin, F. C.; Hodar, F. J. M.; Utrilla, J. R. Effects Of Non-Oxidant And Oxidant Acid Treatments On The Surface Properties Of An Activated Carbon With Very Low Ash Content. *Carbon* **1998**, *36* (1-2), 145.
- (48) Carrott, P. J. M.; Carrott, M. M. L. R.; Nabais, J. M. V. Influence of Surface Ionization On The Adsorption Of Aqueous Mercury Chlorocomplexes By Activated Carbons. *Carbon* **1998**, *36* (1-2), 11.
- (49) Hargis, R. A.; O'Dowd, W. J.; Pennline, H. W. Mercury Investigations in a Pilot-Scale Unit. Presented at the AIChE National Meeting, Houston, TX, March 1999.
- (50) Mellor, J. W. *A Comprehensive Treatise on Inorganic and Theoretical Chemistry*; Longmans Green and Co.: New York, 1952.
- (51) Angenault, J. *Rev. Chim. Miner.* **1970**, *7*, 651.
- (52) Wessels, A. L.; Jeitschko, W. The Mercury Vanadates with the Empirical Formulas HgVO₃ and Hg₂VO₄. *J. Solid State Chem.* **1996**, *125* (2), 140.
- (53) Golodets, G. I. *Heterogeneous Catalytic Reactions Involving Molecular Oxygen*; Elsevier: New York, 1983.
- (54) Solomons, T. W. G. *Organic Chemistry*; John Wiley: New York, 1980.
- (55) Hargis, R. A.; Pennline, H. W. Trace Element Distribution and Mercury Speciation in A Pilot-Scale Combustor Burning Blacksville Coal. Presented at the 90th AWMA Annual Meeting, Toronto, Canada, June 1997; paper no. 97-WP72B.04.

Received for review October 18, 1999

Revised manuscript received February 5, 2000

Accepted February 7, 2000

IE990758V